Université de Montréal

Quantification of Ventricular Mechanical Dyssynchrony under Stress

Par
Samaneh Salimian

Sciences biomédicales
Faculté de médecine

Thèse présentée en vue de l'obtention du grade de doctorat
en sciences biomédicales
Option général

Juillet, 2016

Résumé

L'évaluation de l'asynchronisme mécanique ventriculaire sous stress a soulevé une attention importante en tant que facteur prédictif de la réponse au traitement de resynchronisation cardiaque (CRT). De plus, il semble exister une relation significative entre le devenir du patient et la présence d'asynchronisme au repos. Plusieurs méthodes échocardiographiques peuvent être utilisées pour évaluer l'asynchronisme. Cependant, parmi toutes les différentes méthodologies ou index existant dans ce domaine, aucun critère ne fait l'unanimité. Cette thèse étudie l'importance des techniques d'imagerie nucléaire dans le cadre de l'évaluation de l'asynchronisme cardiaque induit par le stress en utilisant trois différents modèles canins expérimentaux.

Le premier chapitre vise à examiner les effets du stress sur le synchronisme de la contraction du ventricule gauche (VG) en utilisant l'imagerie synchronisée de perfusion myocardique dans une cohorte canine normale. Le stress a été induit par différents niveaux d'infusion de dobutamine sur six sujets sains. Les paramètres hémodynamiques et l'asynchronisme ont été évalués par des mesures de pressions ventriculaires. L'analyse de phase sur l'imagerie s'est effectuée en utilisant un logiciel commercialement disponible (*QGS*) et un logiciel interne (*MHI$_4$MPI*), basée sur le déplacement et l'épaississement des parois ventriculaires. L'augmentation de la concentration de dobutamine a démontré une amélioration de la capacité fonctionnelle et une réduction de l'asynchronisme ventriculaire. L'analyse de l'asynchronisme calculée à partir de l'épaississement de la paroi semble plus robuste et plus sensible que l'utilisation du déplacement des parois. *(Salimian et. al., J Nucl Cardiol., 2014)*

Le second chapitre étudie les différents paramètres d'asynchronisme au repos et à différents niveaux de stress dans un modèle de cardiomyopathie dilatée et à QRS étroit. Ce modèle a été créé sur dix chiens par tachycardie via stimulation de l'apex du ventricule droit pendant 3-4 semaines, permettant d'atteindre une fraction d'éjection cible de 35% ou moins. Le stress a ensuite été induit par une perfusion de dobutamine jusqu'à un maximum de 20

μg/kg/min. Les données hémodynamiques et l'asynchronisme ont été analysés par des mesures de pression ventriculaire et l'analyse de l'imagerie dynamique du compartiment sanguin. L'importante variabilité individuelle des sujets inclus dans notre cohorte empêche toute conclusion définitive sur la mesure de l'asynchronisme interventriculaire. Cependant, les différents niveaux de stress, même dans des intervalles rapprochés, ont démontré un effet significatif sur les paramètres hémodynamiques et l'asynchronisme. *(Salimian et. al., J Nucl Cardiol., 2015)*

La troisième section vise à déterminer si l'estimation du mode de stimulation optimal effectuée au repos demeure le choix optimal lorsque le niveau d'activité cardiaque s'intensifie pour des sujets avec bloc auriculo-ventriculaire (AV) et fonction ventriculaire normale. Cinq chiens ont été soumis à une ablation du nœud AV et des sondes de stimulation ont été insérées dans l'oreillette droite pour la détection, l'apex du ventricule droit (VD) et une veine postérolatérale du VG pour la stimulation. Cinq modes de stimulation ont été utilisés : LV pur, biventriculaire (BiV) avec pré-activation de 20 ms du LV (LVRV20), BiV pur, BiV avec pré-activation de 20 ms du VD (RVLV20), VD pur. Des niveaux jusqu'à 20 μg/kg/min de dobutamine ont été atteints. Le stress a modifié l'étendue de l'asynchronisme de base et ce, pour tous les modes de stimulation. De plus, les effets physiologiques intrinsèques du stress permettent une évaluation plus précise de l'asynchronisme ventriculaire, diminuant la variabilité inter-sujet. Le mode de stimulation LVRV20 semble le mode optimal dans ce modèle, supportant l'utilisation de la stimulation bi-ventriculaire.

Mots-clés: Asynchronisme ventriculaire mécanique, SPECT synchronisée de la perfusion myocardique, le stress de la dobutamine, SPECT synchronisée du compartiment sanguin, cardiomyopathie dilatée avec QRS étroit, thérapie de resynchronisation cardiaque, contraction homogénéité, bloc auriculo-ventriculaire et la fonction normale.

Abstract

Assessment of ventricular mechanical dyssynchrony (MD) under stress has attracted a large amount of attention as a stronger predictor of response to cardiac resynchronization therapy (CRT) and as a parameter whose variation bears a greater relationship to clinical outcomes than resting-MD either in CRT candidates or another subset of patients. Several echocardiographic methods can be used to assess stress-MD. However, no standardized approach is currently used to explore stress-induced variations in inter- and intraventricular MD. This dissertation studies the importance of nuclear imaging techniques in assessing stress-induced MD variations by providing three different experimental canine models.

The first chapter sought to examine the impacts of stress on the left ventricular (LV) synchrony with phase analysis of gated SPECT myocardial perfusion imaging (GMPS) within a normal canine cohort. Stress was induced by different levels of dobutamine infusion in six healthy subjects. Hemodynamic and LV MD parameters were assessed by LV pressure measurements and phase analysis of GMPS using commercially available QGS software and in-house MHI_4MPI software with thickening- and displacement-based methodology. The increase of dobutamine level was shown to be in accordance with the improvement of LV functional capacity and reduction of MD parameters. MD analysis based on wall thickening was more robust and sensitive than the global wall displacement. *(Salimian et. al., J Nucl Cardiol., 2014)*

The second chapter investigated the range of difference in inter- and intraventricular MD parameters from rest to various levels of stress in a dilated cardiomyopathy (DCM) and narrow QRS complex model. Ten large dogs were submitted to tachycardia-induced DCM by pacing the right ventricular apex for 3-4 weeks to reach a target ejection fraction of 35% or less. Stress was then induced by infusion of dobutamine up to a maximum of 20 μg/kg/min. Hemodynamic and MD data were analyzed by LV pressure measurements and gated-blood pool SPECT (GBPS) imaging. Individual differences in the magnitude and pattern of change in the various levels of stress precluded any definitive conclusion about interventricular MD. However, different levels of stress, even in close intervals, showed a significant positive

impact on hemodynamic and intraventricular MD parameters. *(Salimian et. al., J Nucl Cardiol., 2015)*

The third chapter sought to examine if the optimal pacing mode at rest could be the best one during the maximum stress level in terms of MD parameters in subjects with an atrioventricular (AV) block and normal function. Five dogs were submitted to AV node ablation and pacing leads were placed in the right atrium for sensing, in right ventricular (RV) apex, and in posterolateral LV vein for pacing in five modes of LV, biventricular (BiV) with 20 ms of LV pre-activation (LVRV20), BiV, BiV with 20 ms of RV pre-activation (RVLV20) and RV pacing. Stress was induced by dobutamine infusion up to a maximum of 20 μg/kg/min. Data analyses were the same as chapter one. Dobutamine stress changed the extent of resting-LV MD at all pacing modes. Intrinsic physiologic effects of stress resulted in more accurate MD assessment with lesser variability in subjects who underwent pacing. LVRV20 was the preferred site of stimulation in this model rather than single-site pacing.

Keywords: Ventricular mechanical dyssynchrony, gated myocardial perfusion SPECT, dobutamine stress, gated blood pool SPECT, dilated cardiomyopathy with narrow QRS, cardiac resynchronization therapy, contraction homogeneity, atrioventricular block and normal function.

Table of Contents

List of Tables

List of Figures

List of Abbreviations

AV: Atrioventricular

RV: Right ventricle

LV: Left ventricle

HF: Heart failure

LBBB: Left bundle branch block

CRT: Cardiac resynchronization therapy

MD: Mechanical dyssynchrony

MRI: Magnetic Resonance Imaging

SPECT: Single-photon emission computed tomography

GBPS: Gated blood pool SPECT

GMPS: Gated myocardial perfusion SPECT

PET: Positron emission tomography

MHI: Montreal Heart Institute

CAD: Coronary artery disease

FBP: Filtered backprojection

ML: Maximum likelihood

OSEM: Ordered-subsets expectation maximization

CHI: Contraction homogeneity index

TSLD: Thickening-based septal-to-lateral wall delay

THI: Thickening homogeneity index

DSLD: Displacement-based septal-to-lateral wall delay

DHI: Displacement homogeneity index

LVEF: Left ventricular ejection fraction

LVESV: Left ventricular end-systolic volume

LVEDV: Left ventricular end-diastolic volume

SV: Stroke volume

HR: Heart rate

CI: Contractility index

CO: Cardiac output

P_{max}: Maximum pressure of left ventricle

dP/dt_{max}: Maximum rate of left ventricular pressure change

TAC: Time-activity curve

ROI: Region of interest

SD: Standard deviation

E: Efficiency

DCM: Dilated cardiomyopathy

RVA: Right ventricular pacing

AVB: Atrioventricular block

BiV: Biventricular pacing

LVRV20: Biventricular pacing with 20 ms of LV pre-activation

RVLV20: Biventricular pacing with 20 ms of RV pre-activation

FDG: ^{18}F- fludeoxyglucose

CT: Computed tomography

ICC: Intra-class correlation

APD: Action potential duration

AT: Activation time

RT: Repolarization time

To my beloved parents for their endless love,

support and encouragement

Acknowledgements

First, I would like to express my sincere appreciation to my supervisor Dr. François Harel for the continuous support of my PhD study, for his patience, motivation, and helpful guidance during the last years. I could not have imagined having a better supervisor for my PhD study.

Second, I would like to thank the members of my thesis committee, Dr. Raymond Lambert, Dr. Éric Thorin, Dr. Raymond Taillefer, and Dr. Marcio Sturmer for their insightful comments and helpful questions on my thesis.

Besides, I would like to express my sincere thanks to Dr. Bernard Thibault who provided me an opportunity to join his research team, and who gave me access to the Electrophysiology Service and research facilities. I have learned a lot from his insightful comments. As well, I wish to thank his team: Marc-Antoine Gillis, Evelyn Landry, and Marie-Pierre Mathieu. All in all, without their precious support it would not be possible to conduct this work.

My sincere thanks also go to the nuclear medicine research team in particular Sophie Marcil and Vincent Finnerty who enlightened the first assets of research to me; for the stimulating discussions, and for all the fun we have had in the last few years.

I would also like to extend my appreciation to Dr. Jean Grégoire and the staff at Montreal Heart Institute for their guidance and patience during my research.

Last but not the least; I would like to thank my family: my parents and my two sisters for supporting me spiritually throughout my studies and my life in general and to my husband for his love, patience, motivational thoughts, and encouragement.

Introduction

In this chapter, the clinical motivation and a detailed background to mechanical dyssynchrony (MD), its applications and methods of assessment are provided. First, the main clinical motivation for the current thesis is identified in order to have a global view about the importance of the pacing and MD assessment. Next, the cardiac normal electrical activation sequence as an opening window to the ventricular pacing and cardiac resynchronization therapy is reviewed. Then, a detailed description is provided for better understanding of the MD concept, its applications, dynamic nature as well as quantification techniques. In the following, nuclear imaging techniques are overviewed both with the theory and practice vision. This section is helpful for the understanding of the overall methods used in this thesis. Next, the stress-induced modalities and the overview of the literature on dynamic left ventricular MD discourse are provided to add to the background knowledge of the stress-MD concept. Finally, the summary, objectives, and outline of remaining parts of the thesis are presented.

Clinical motivation

There are more than 200,000 Canadians and nearly 3 million individuals in North America living with permanent pacemakers or, cardiac rhythm devices.[1] Also, more than 250,000 new devices are implanted each year in North America because of an aging population and increased recommended indications for these devices.[1] The first pacemaker was implanted in 1960 with the hope to save the life of a patient with atrioventricular (AV) conduction block.[2] Since then, not only it was served as a life saver in patients with bradycardia due to sinus or AV node dysfunction, but also since 2000, as a treatment option for increasing the patients'

quality of life and expanding the survival rate in specific disorders (e.g. after cardiac transplantation or neuromuscular diseases) and cardiomyopathies (dilated or hypertrophic).[3] In the latter case, instead of treating or preventing the abnormal rhythms, pacing alters the activation sequence of the ventricles and influences the central hemodynamics in severe systolic heart failure (HF) and dilated cardiomyopathies.[3] Pacemaker implantation in these indications has been emphasized in previous guideline statements[3] since first, the indication for patients with sinus node dysfunction and AV block is inevitable thus it has been deemphasized and second, large number of new cases are diagnosed with HF each year (50,000 Canadians[4] and 915,000 Americans[5]). Despite major efforts have been made to identify the HF patients most likely to benefit from pacing therapy, still about 30% of recipients do not show any beneficial responses and ongoing efforts continue to develop more robust predictors.[6] One of the suggested predictors since 2000 has been the MD or timing disparity in ventricular regional contraction. However, it is not clear why the past efforts for optimizing the candidates by improving the characterization and quantification of MD have not resulted in substantial improvement in non-responders' percentage. As it might be due to the lack of understanding about dynamic nature of MD and somehow the limitation of the previous MD assessment methods, the aim of this work is to apply the nuclear imaging techniques to understand how stress can modify the mechanics of the ventricles and how pacing affects the left ventricular contraction at stress condition.

Normal electrical activation, a window to the artificial pacing

Since having knowledge about normal cardiac electrical activation is of special importance in the context of cardiac mechanics and resynchronization, a quick review of the sequence of normal activation is provided here.[7] Cardiac conduction system consists of a group of cardiac

muscle cells within the cardiac walls which produce the action potential and conduct it throughout the cardiac chambers, causing the heart to depolarize and eventually contracts and pumps the blood out to the other organs. Under normal sinus rhythm, the action potential starts from the sinus node (first component of the system) in the atria and after activating the whole atria which take approximately 100 ms, by the inter-cellular conductions, reaches to the AV node (the second component of the system). In the normal heart, the AV node is the only electrical connection between the atria and ventricles. The impulse spends about 80 ms waiting to travel from the atrial side to the ventricular side in order to allow optimal ventricular filling before the ventricular contraction. Given the high resistivity (low conductivity) of the AV node tissue, it is susceptible to conduction impairments even a complete conduction block. In the following, the impulse reaches the His bundle of the Purkinje system (specialized conduction system of the ventricles) and then is conducted to the ventricles by the right and left bundle branches and eventually exits from both the anterolateral wall of the right ventricle (RV) and inferolateral wall of the left ventricle (LV). Electrical stimulation develops the action potential processes in the myocardial cells which are the sequence of ion fluxes through specific channels in the cell membrane. Myocytes exit the resting potential by depolarization wavefront and return the resting voltage after a short time by repolarization wavefront (for more information see reference (8)). Hence repolarization time is the sum of activation time (AT), the time between the earliest QRS deflection to the action potential upstroke, and the action potential duration (APD) or the action potential upstroke to 90% repolarization.[9]

Based on the observations in the isolated human hearts,[10] excitation synchronously happens in three LV endocardial areas, 0 to 5 ms after the start of the LV action potential: on

the anterior paraseptal wall just below the attachment of the mitral valve; central on the left surface of the interventricular septum and on posterior paraseptal about one-third of the distance from apex to base. These areas grow rapidly and merge in 15 to 20 ms, while the pattern of activation is mostly from the apex to the base through both the septum and free walls of the LV and RV, and transmurally from the endocardium to the epicardium.[10] Interestingly, endocardial cells are able to conduct the electrical impulses faster than the rest of the LV myocardium.[7] For the RV, endocardial activation starts near the insertion of the anterior papillary muscle 10 ms after the onset of LV activation.[7] The last parts of the RV and LV that become activated are the AV sulcus and the posterobasal area respectively.[7,10] In fact, the activation of the entire ventricles happens in a few ms (about 80 ms) in a homogenous and simultaneous way with the help of specialized Purkinje system; making the mechanical activation of the myocardium very coordinate.[7]

The aforementioned extraordinary valuable information on the excitation and activation of a normal heart and many other physiologic investigations opened the window into the use of artificial pacing which can mimic the AV activation sequence in patients with bradycardia and conduction disorders. In fact, if for any reason one of the components of the conduction system becomes dysfunctional, electric signals confront with functional block in their way through the system, finding new pathways through the working myocardium which makes the signal propagation to flow more slowly throughout the myocardium. This condition may create further structural and functional alterations which may ultimately result in the HF, a condition that impairs the ability of the ventricle to fill with or eject blood according to the needs of the body.[11] Thus, artificial pacing, as an inevitable therapy helps to improve the

function and the status of the HF patients and even may play a role as a life saver in patients with complete AV block.

Ventricular pacing

From more than 40 years ago, the ventricular pacing was introduced as a life saver in patients with complete AV block.[12] The site of the stimulation was first chosen to be the RV apex, given the ease of access, good fixation and a low capture threshold that RV pacing could provide.[12] However, after so many investigations on the long-term effects of the RV apical pacing, serious detrimental effects were proven to LV function[13,14] and structure.[15] These effects were mostly attributed to the late activation of the LV free wall.[12] Thus, less effective ventricular contraction by RV apical pacing and its long-term effects which were similar to the left bundle branch block (LBBB) status[12] shifted the interest toward finding alternative pacing sites (biventricular pacing) that induce a more physiologic activation sequence and ventricular performance. However, as Arenas et al.[12] recently suggested, it is not basically correct to fully extrapolate the detrimental effects of LBBB and the benefits of biventricular pacing, that will be explained in the next section to all patients who need RV pacing. Since, as they mentioned, the activation pathway, electromechanical delay, and the LV synchrony is completely different between these two conditions. But how could we determine whether a patient with AV block would benefit from an alternative pacing site? This problem has been further discussed and investigated in the third chapter. Hence, although ventricular pacing in the mode of RV apical pacing was first introduced only for AV block patients, several years later new pacing devices were also developed for further conduction disorders.

Cardiac resynchronization therapy

In the mid-1990s, biventricular pacing device namely cardiac resynchronization therapy (CRT) was developed and found to be a clinically significant treatment in patients with end-stage HF and intrinsic conduction delay.[16] CRT consists of the electric pre-excitation of two opposing sites of the heart: the RV apex or septum and the LV free wall which can be stimulated simultaneously or with a phase delay while the atrial electric activation is sensed or artificially paced and a programmed shorter AV delay time is used to achieve the ventricular capture.[6] Not only acute improvement was seen in hemodynamics after CRT implantation, but also chronic benefits such as improved LV function, symptoms, exercise capacity, and quality of life were proven at longer follow-ups.[17-20]

As it was apparently logic, CRT was first only targeted to a subset of patients who had a wide QRS duration[16] (e.g., LBBB); since simultaneous electrical stimulation of both ventricles in this treatment nearly compensated the later activation of the LV free wall relative to the RV and led to a practically synchronous ventricular contraction and therefore an efficient ventricular performance. However, using the QRS duration as an inclusion criterion in most of the early large clinical trials[17-20] for evaluation of response to CRT yielded some disappointed results.[16] Indeed, QRS duration poorly predicted the acute and chronic responses to CRT and about one-third of selected patients failed to show the expected clinical benefits.[16,21] Though, the interest was shifted toward other parameters that might better identify the CRT beneficiaries; since the CRT was (and still is) an expensive therapeutic option and so many procedural and follow-up complaints might occur from the patient side.

Mechanical dyssynchrony (MD)

Ventricular MD is the timing delay in ventricular regional contraction and was proposed as an alternative for QRS duration in CRT patient selection.[16] The first documented use of MD as a parameter for prediction of response to CRT dates back to the early 2000s.[22] Primary studies found that MD better correlated with the acute[22] and chronic[23,24] CRT benefits and that it was an independent predictor of clinical events and survival in HF patients.[25,26] These findings, representing the assumption that mechanical rather than electrical dyssynchrony would better identify the CRT responders, initiated a cascade of research beyond the characteristics of MD, how prevalent it is, whether the method of its measurement is reliable and accurate, and if HF patients without a wide QRS duration are also appropriate for CRT.

A true attempt toward understanding of MD

Based on the results of studies including a variety of classified HF patients, MD seems to be quite common in HF patients neglecting the QRS duration. In another hand, as suggested by Kass in 2008, there is almost an epidemic of MD, which a majority of HF patients suffer from.[16] At this step, it is important to consider what exactly results in MD developing? As mentioned previously, homogenous, diffused and rapid electrical activation in the ventricles through the Purkinje system makes a coordinate and homogenous mechanical activation. But if there is a conduction disorder whether specific (e.g. LBBB) or non-specific, demonstrable in the ECG, it will cause a phase delay in the contraction of early and late activated regions. The electrical dyssynchrony is not always the reason of MD; there are still about 30% to 50% of HF patients, based on different studies, with a substantial amount of MD but without any widening or change in the QRS duration.[16,27,28] Kass [16] listed three logical reasons in his excellent MD review for this case:

1) RV activation is so quick that in spite of LV dyssynchrony still a narrow QRS complex is recorded.
2) Abnormal excitation-contraction coupling alters the kinetics of force development in one part of the heart compared with another.
3) Ischemic damage, fibrosis, etc. make regional disparity in the myocardial contractility.

Based on the fact that which mechanism is involved in HF patients with a narrow QRS duration, they might benefit (e.g. if the first reason is true) or otherwise be non-responders to CRT.

In spite of small studies[29] on a subset of patients with narrow QRS complex and some promising CRT results, overall, a recent multi-center randomized trial "Echocardiography-Guided Cardiac Resynchronization Therapy" (EchoCRT)[30] reported no benefit in terms of number of HF hospitalization or death in patients with a QRS interval of < 120 ms. Thus, it seems that electrical resynchronization is not an effective therapy when the MD is not resulted from the electrical dyssynchrony.[31,32] However, it is not clear why the past efforts for optimizing the CRT candidates by improving the characterization and quantification of LV MD have not resulted in any substantial improvement in clinical outcomes (still 30% non-responders) even when further refining based on the ECG morphology (excluding no-LBBB patients) has been performed.[33] As it has been pointed out in literature, it might be due to the limitations of the MD assessment methods.[33] Also, the dynamic nature of MD may play a role per se. These two important constraints must be further investigated; since the MD not only has a critical role in the prediction of response to CRT but also has several other applications in today's clinical practice that are discussed in the next section.

As a note, although the current guidelines still recommend the CRT in patients with New York Hear Association (NYHA) class III or IV symptoms, LV ejection fraction (EF) ≤ 35% and QRS duration ≥ 150 ms, the CRT indications have been expanded to include NYHA I-II, LVEF < 40%, QRS > 120 ms, and chronic RV pacing secondary to AV block via randomized controlled trials in recent years.[34]

MD applications

The utility of the MD was shown to not being circumscribed to CRT optimization. Other potential clinical applications have been examined from about last 5 years. These applications include MD utility in prognostication and risk stratification of different subsets of patients[35] with ischemic[36] or non-ischemic cardiomyopathy,[37] implantable defibrillators,[38] and end-stage renal disease.[39,40]

A classic parameter used to predict the future cardiovascular events or survival has been the LVEF which is a measure of global systolic function.[41] However, because of getting influenced by ventricular geometry and hemodynamic conditions, it could not be a sensitive indicator of ventricular function.[41] Among various parameters identified for better risk-stratification, LV MD has been proposed as a unique indicator not only capable of determining the clinical outcomes in HF patients but also predicting major adverse cardiovascular events in asymptomatic individuals without evidence of heart disease.[41] The quantification of LV MD accordingly helps to identify the risk of HF progression in individuals who do not have the symptoms of any recognized heart disease and have a preserved EF.[42] This is of significant value since the optimal intervention period is always at early stages of the cardiac disease.

As previously studied, the age, increased LV mass, and lower regional myocardial perfusion are related to the superior extent of myocardial dyssynchrony in asymptomatic

individuals.[43] Also, LV MD was found to be closely linked to presence of coronary artery disease (CAD) risk factors (hypertension, diabetes, dyslipidemia, and obesity), QRS interval ≥ 120 ms, history of CAD (primarily acute myocardial infarction), LV dysfunction (LVEF < 45 %), male sex, and presence of myocardial perfusion defects, especially of the fixed type in a retrospective study of 1000 patients with or suspected to have myocardial disease who underwent myocardial perfusion imaging.[42]

Dynamic nature of MD

MD is not a stable phenomenon; since the mechanical contraction is affected by different conditions and factors such as exercise, drug administration, inducible ischemia, pacing-induced tachycardia and so forth; thus MD would change from time to time.[44] Dynamic LV MD has been assessed in different subset of patients, mostly in HF patients amenable to CRT,[45-47] and is thought to be a potential interfering mechanism for the lack of predictive value of resting MD.[44] Rocchi et al. was the first one that assessed this hypothesis and showed that exercise-MD is a stronger predictor of response to CRT than resting-MD.[48] Also, stress-induced variation in MD, whether positive or negative, has been shown to bear a greater relationship to clinical outcomes (death, heart transplant, assist device implantation, etc.) than resting-MD as assessed either in CRT candidates[49] or patients with dilated cardiomyopathy.[50] In fact, increased myocardial contractility during the exercise or pharmacological-induced stress (e.g. dobutamine infusion) may bring regional differences in myocardial contraction that is easily detectable at stress levels.[44,51]

Imaging techniques for quantification of MD

Echocardiography

So far, the echocardiography has been the most useful tool in cardiology for assessment of cardiac function and contraction abnormalities, since it is inexpensive and largely available.[52] Thus, it was also mostly used in the case of CRT patient selection, optimization of lead placement and device configuration as well.[52] Despite promising preliminary data from single-center studies in the value of CRT patient selection by echocardiography,[24,53,54] the PROSPECT trial (with a multi-center setting) announced that echocardiographic parameters assessing MD do not have enough predicting value to be recommended in routine clinical assessments.[55] This fact was more highlighted in EchoCRT[30] trial; since using even modern echocardiographic tools (speckle-tracking strain) in this trial could not change the belief stimulated by PROSPECT trial. Indeed, these methods are highly subject-dependent both in the case of image acquisition and analysis and because of limited repeatability and reproducibility cannot be reliable.[16,55] Probably, besides dynamic nature of MD, using echocardiography for quantification of MD has been resulted in a lack of a significant improvement in clinical outcomes (or reducing the number of non-responders).[33] As Van Everdingen et al. suggested, echocardiography is a friend of CRT but with known limitations and not in the patient selection but in other aspects like optimization of lead placement.[52]

Cardiac magnetic resonance imaging

Cardiac magnetic resonance imaging (MRI) as a non-invasive imaging modality provides excellent image spatial resolution and soft tissue contrast and does not have any ionizing radiation.[56] MRI as a gold standard for volumetric functional analysis, can also track the myocardial surfaces in 3-D space and analyze longitudinal, radial and circumferential strains

(i.e. myocardial deformation or length differences in the direction of long axis of the ventricles, across the wall (transmurally), and in the direction of ventricular circumference respectively) in a quite reproducible way using tagging techniques.[57] Thus, it seems to be quite functional for prediction of CRT response. However, MRI is not widely used in the measurement of MD because of high equipment cost, image acquisition complication, and lack of automated algorithms for image quantification.[51]

Nuclear imaging modalities

Nuclear cardiology techniques have been reliable alternatives to echocardiography for assessment of cardiac function since 1980.[51,58] First, planar radionuclide ventriculography[59] in 2-D, and then single-photon emission computed tomography gated blood pool (SPECT; GBPS)[60] in 3-D space were applied for better functional analysis and MD quantification. In both methods, the MD associated with endocardial motion can be analyzed by the variation of counts within the region of interest over the cardiac cycle.[51] Both planar and GBPS are promising in the assessment of not only LV intra- but also interventricular MD (phase delay between RV and LV contraction); because blood pool rather than myocardial wall imaging allows to a reliable volumetric estimation.[61] However, they cannot provide further information on the myocardial infarction, ischemia, and scar which has been shown to be a key determinant of response to CRT.[62] To make all this information in one session imaging, as Zhou et al.[63] so-called "one-stop shop", gated myocardial perfusion SPECT (GMPS), over 10 years ago,[64] and later positron emission tomography (PET) have been proposed for the purpose of CRT response prediction. Phase analyses of GMPS or PET assess the LV function, scar burden and location, LV site of the latest contraction, and MD from a single scan.[63]

Thus, depend on what information is needed based on each application and in which level of accuracy, the technique should be chosen.

Given the automated nature of phase analysis,[65] mostly determined by GMPS, it has shown excellent repeatability and reproducibility for quantification of ventricular MD.[66] This property facilitates the use of phase analysis for CRT patient selection process. In fact, the accuracy of predicting value of MD by phase analysis has been shown in previous single-center acute[33] and chronic[58] studies in HF patients considering the current CRT inclusion criteria. However, prospective multicenter studies are warranted in this regard.

Overall, compared to other assessment methods, nuclear imaging is very promising for widespread clinical use in the CRT application; since it is routinely practiced, well standardized, and inexpensive.[63] Information about myocardial scar burden, viability, MD and global function in one-stop shop, automatic and highly reproducible fashion can be provided by these techniques.[63]

SPECT imaging techniques for MD assessment

The use of computer techniques in today's nuclear medicine from the acquisition to processing, display, and data analysis has standardized the imaging and final image interpretation. It is the reason of an upward increase in utilization of nuclear medicine modalities (SPECT and PET) in today's busy and demanding clinical environment.[67] The focus of the current thesis is on the SPECT imaging and techniques. In the following sections, two main cardiac SPECT techniques and the steps through which a 3D cardiac image is obtained will be described.

Gated SPECT myocardial perfusion imaging

One of the most common methods for simultaneous evaluation of myocardial perfusion, function, and synchrony of contraction is GMPS. In this method, a radioactive-labeled substance which is mostly the Technetium-99m (^{99m}Tc) agents (sestamibi or tetrofosmin) is intravenously injected into a patient. After intravenous injection, the ^{99m}Tc agent is rapidly cleared from blood and uptakes by the myocardium. First-pass extraction and percentage of cardiac uptake for tetrofosmin and sestamibi are 50% and 1.2% versus 60% and 1.5% respectively.(68)

^{99m}Tc is a radionuclide with a half-life of 6 hours which emits the gamma rays in the range of 140.5 keV.(69) The energy is high enough not to be that much attenuated and low enough to be well detected by gamma cameras in nuclear medicine. The purpose of this radionuclide imaging is to obtain a 3-D image of the distribution of ^{99m}Tc within the LV myocardium.(70) In addition, the high counting statistics of ^{99m}Tc agents beside the use of the electrocardiographic gating makes a tomographic image set which allows for the visual and quantitative assessment of functional parameters such as myocardial motion and thickening.(70) To reach this aim, several steps are needed as gated SPECT acquisition, image reconstruction, filtering, image reorientation, segmentation, and final quantitative analysis. The following has described each of the steps respectively.

Gated SPECT acquisition

After the injection of a ^{99m}Tc-labeled agent to the patient and its uptake by the myocardium, gamma rays are emitted at the energy level that is high enough to be detected by the gamma camera without increasing the patient dose (there must be a balance between attenuation and detection). Although some of these photons undergo scatter or attenuation in the body, a

considerable amount can reach to the detectors of gamma camera consist of a scintillation crystal and an array of photomultiplier tubes (PMTs) and could be detected.[69,70] The collision of gamma photons to the scintillation crystal which is commonly the thallium-activated sodium iodide or NaI(Tl) crystal, leads to their conversion into the light photons (scintillation).[69] In the next step, light photons reach to the PMTs to be transformed into the electric signal and to be amplified and produce a strong electric current. The ultimate current is proportional to the energy of incident gamma ray and the amount of light from the scintillation process that reaches the PMT surface.[69] The final electric signals contain the acquisition data which is acquired in the form of tomography because the gamma camera head rotates around the patient in an orbital path and gathers several projection images[70] (in this thesis a dual-head gamma camera was used with 64 projections dispatched on a 360˚ configuration). Using more than one camera head provides more counts for the image acquisition in the same acquisition time since at least 2 projections could be acquired simultaneously. Typically the procedure of the scan takes about 15–20 minutes in which the projections are acquired every 3–6 degrees.[71]

If the signal gating is used for the acquisition, each R wave of electrocardiogram plays a role as a trigger which provides a time window (R-R interval) for selected set of projections from among many during the data collection. Then, R-R interval could be divided into 8 or 16 equal segments and thus 8 or 16 projection images could be acquired corresponding to each portion of the cardiac cycle. Gating in several time frames helps to have a 4-D (3-D plus time) image which allows for the dynamic cardiac function assessments.[70] Also before reconstruction, summing all the projection images from different time intervals at each angle produces an ungated or static SPECT image from which perfusion can be assessed.[70]

Image reconstruction

As mentioned in acquisition section, a 2-D projection image at each angle includes a series of counts or a projection profile related to the activities detected in the body. All the profiles known as sinogram are used to reconstruct a 2-D cross-sectional image of activity from the myocardium. For instance, all the profiles related to the apex section must be used to reconstruct the apex transaxial slice which is then stored in the first row of a 2-D matrix. Thus, if 16 frames per cardiac cycle and 64 projection angles at one complete patient rotation are used, data could be collected in 16 matrices of 64 × 64 pixels. Each matrix represents the maximal count in each myocardial segment from apex to base (row of the matrix) for each projection angle (column of the matrix).[67] In fact, collecting data at 64 different angular positions and summing all projection profiles, can provide enough information for reconstruction of a 2-D cross-sectional image at each time interval. To exclude extra-cardiac activity for the reconstruction process, the cardiac region can be manually selected. There are several approaches to reconstruct an image from the projection profiles as are discussed in the following.

Simple Backprojection

As it is apparent from its name, this approach is a basic and simple approach to image reconstruction. Projecting (or distributing) the data or counts recorded in a particular projection profile back uniformly on the pixels of an image matrix along its projection angle helps to have an approximate source distribution.[69] One of the drawbacks of this approach is the blurriness of the final image that even using an infinite number of views does not make the image completely clear.

Filtered Backprojection

To improve the image quality in simple back-projection approach, filtering was suggested to be applied on the count profiles before the reconstruction.[69] Filtering process will be discussed in the next section in detail. However, what is important here is that to apply a filter in filtered back projection (FBP), the data are preferred to be in the frequency domain rather than the spatial domain. In this method, a ramp filter is used so as to selectively amplify high-frequency components relative to low-frequency components.[70] Although filtering besides the back-projection process can eliminate the disadvantage of the previous approach, it still has some constraints. Filtering process in datasets with poor counting statistics can produce specific artifacts in the image. Once more, if the filtering in high spatial frequencies is used to eliminate those artifacts, it would further decrease the image resolution.[69] Also, the FBP algorithm requires additional data processing to compensate for some physical aspects of the imaging system and data acquisition, such as the limited spatial resolution of the detector and scattered radiation.[69] To consider these aspects directly into the algorithm and to decrease the probability of producing artifacts, iterative reconstruction approach came into the routine clinic with the support of higher computer speeds.

Iterative Reconstruction Algorithms

This approach uses several steps of estimation and comparison with the actual image to reach a successful true estimation of the image. A simple initial estimation could be even a blank or uniform image from which the intensities along each angle are summed up to yield a projection profile (inverse to the back-projection).[69] Doing so for all projections through the estimated image yields an estimated sinogram which will be compared with the actually recorded sinogram. If the convergence has not been achieved in comparison process, it can be

adjusted based on the difference between the estimated and actual projections.[69] The update and compare process is repeated until the estimate approaches the maximum likelihood (ML) (usually in 10 – 15 iterations).[69] All the projection profiles or a complete sinogram must be produced at each iteration, and compared to the actual sinogram which is a long procedure. A method called ordered-subsets expectation maximization (OSEM) has been used to reduce the time of the conventional ML algorithm so that only a small number (or subset) of projection angles are used in the initial iterations and a larger number of projection angles are included in further refinements.[69,72] Iterative reconstruction can provide a more accurate image of the radioactive distribution within the body relative to the FBP.

Filtering

Even after iterative reconstruction, the quality of the image is not as good as expected; since there are several restrictions during the acquisition of gamma rays that lead to have generally poor statistics and high noise levels. These factors are the attenuation and scatter of gamma ray photons, the detection efficiency and the spatial resolution of the collimator-detector system.[71] Hence, post-processing or filtering is an important part of SPECT imaging to obtain a high-quality image. The choice of a filter for a reconstruction technique is always a trade-off between the extent of noise reduction and detail preserving.[71] In order to filter an image, it must be transformed from the spatial domain to the frequency domain or K-space (the coordinate system in the frequency domain) so that each 1-D projection profile from the object domain at each angle must be transformed into the 1-D K-space profile by Fourier function.[69] The Fourier analysis will be discussed in the following sections. In fact, it seems quite logical to filter the images based on the frequencies to highlight certain features or remove others.

To reduce the statistical noise of a SPECT image, the smoothing or low-pass filters are commonly used, the inverse of high-pass filters such as ramp filters, which block the high frequencies and allow the low frequencies to remain constant in the image.[71] A number of low-pass filters are available for SPECT reconstruction but the most usual choice in nuclear medicine is the Butterworth filter. Given the ability to change not only the critical frequency, the frequency above which the filter starts to roll-off, but also the steepness of the cut-off, Butterworth filters are able to smooth the noise while preserving the image resolution.[71] Comparing Butterworth filter with Gaussian filter (a band-pass filter which allows certain range of frequencies to pass, more in the origin and less in the edges) and several other low-pass filters in a study by cardiac phantom indicated that Gaussian filter was the best for contrast and signal-to-noise ratio while, Butterworth filter was the best for trade-off between contrast, signal-to-noise ratio, and defect size accuracy.[71,73] As a result, for qualitative analysis requiring high contrast and signal-to-noise ratio, Gaussian filter was suggested whereas for quantitative analysis requiring both image quality and defect size accuracy Butterworth filter was proposed.[71,73]

During the present thesis, quality of the cardiac images was important for the final segmentation processes and 4-D functional tracking and further analysis. Consequently, a ramp and a Gaussian function were multiplied to form the Fourier spatial frequency filter used in the FBP reconstruction process, when applicable, and only the symmetric Gaussian function was applied when the OSEM reconstruction was used.

Reorientation

Reconstruction of the image with either of the above methods provides a set of transaxial images (images perpendicular to the long axis of the patient). In this thesis, Siemens e-soft

auto-cardiac processor is used as camera software to provide the vertical and horizontal long axis views from stacking the short axis images after reconstruction and cutting them along the sagittal and coronal planes respectively. This step is always automatically done within the camera software which can be seen in Figure 1.

The orientation of the heart in chest is oblique and the angle varies from patient to patient. To be able to have a standard view and orientation in all the patients, it is important to reorient the transaxial images perpendicularly to the long axis of the LV[70] (Figure1). Most of the time, the tomographic image reorientation is performed manually. However, the software is available today for automatic reorientation which can greatly improve the accuracy and reproducibility of the process. [70]

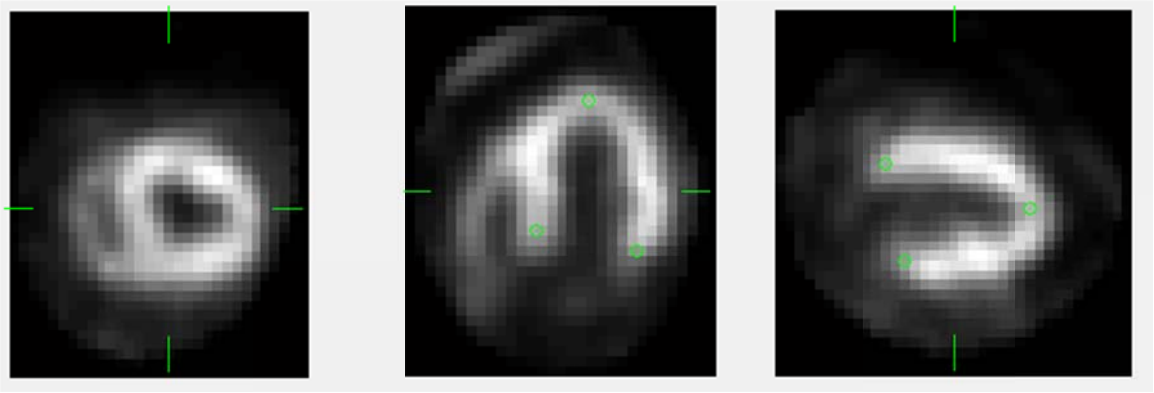

Short axis view Horizontal long axis view Vertical long axis view

Figure 1. Different views of the distribution of the tracer in the left ventricle by cutting through the center of the stacked reconstructed short axis images from different planes.

Left ventricular segmentation

Short axis image slices produced from the reconstruction step is used for the segmentation or the process of separation of LV from the rest of the cardiac portions. Segmentation is one of

the most important parts of the imaging for quantitative analysis such as perfusion or EF assessments and its precision is based on the precision of previous steps. There is a number of commercially available software for automatic segmentation of the LV which can produce a 3-D LV image with the myocardial boundaries for further motion and functional analysis. Some of the well-known software in this regard include the Quantitative Gated SPECT (QGS; Cedars-Sinai Medical Centre), Emory Cardiac Toolbox (Emory University), and Corridor4DM (Michigan University). The details of each software method for segmentation and analysis are beyond the focus of the present thesis. However, I briefly remark some important points about the QGS software that is used throughout this thesis along with our in-house software in the following section.

Generally, if the aim is to assess the function or to calculate the volume and EF, the correctness of the estimated myocardial boundaries is of special importance. However, if the aim is only to evaluate the synchronicity (the coincidence of the motion or thickening) of the LV walls, it is not essential to find the actual positioning of the myocardial edges.[70]

Quantitative Gated SPECT (QGS) software

The QGS software uses the gated short-axis data sets after stacking them together to form a 3-D image volume.[70] The first step involves the automatic segmentation of the LV myocardium based on several segmentation methods which are performed simultaneously in an iterative process to obtain a mask consistent with the expected size, shape, and location of the LV.[74] In fact, segmentation subdivides the image into its subsequent regions and the process is stopped when the LV is isolated. Various and complicated algorithms of segmentation are commonly used by engineers in the field of biomedical imaging based on the properties of intensity values either discontinuity or similarity. However, two main categories can be defined for

these techniques: 1) abrupt changes in intensity (or edges) 2) partitioning of regions that are dissimilar according to a set of predefined criteria; e.g. thresholding, region growing, region splitting, and merging.[75] The details of these methods are beyond the focus of our discussion but the interested readers can find good information in the following references.[76,77] The QGS uses several methods in both mentioned categories to obtain the expected LV mask.[70,74]

Germano et al. first introduced the QGS software in 1995 for accurate EF measurements where precise myocardial surface generation was important.[74] To accurately estimate the mid-myocardium as well as endocardial and epicardial surfaces, the QGS performs the following procedures. Once the LV is isolated, its center of mass (within the cavity) is automatically determined as the origin of the sampling coordinate system. Then, radial count profiles are drawn from the origin both longitudinally and latitudinally, every 10º at each direction, according to a spherical sampling model[74] (Figure 2). The local maxima along all rays identify the maximal count in the myocardium or the estimated mid-myocardial surface.

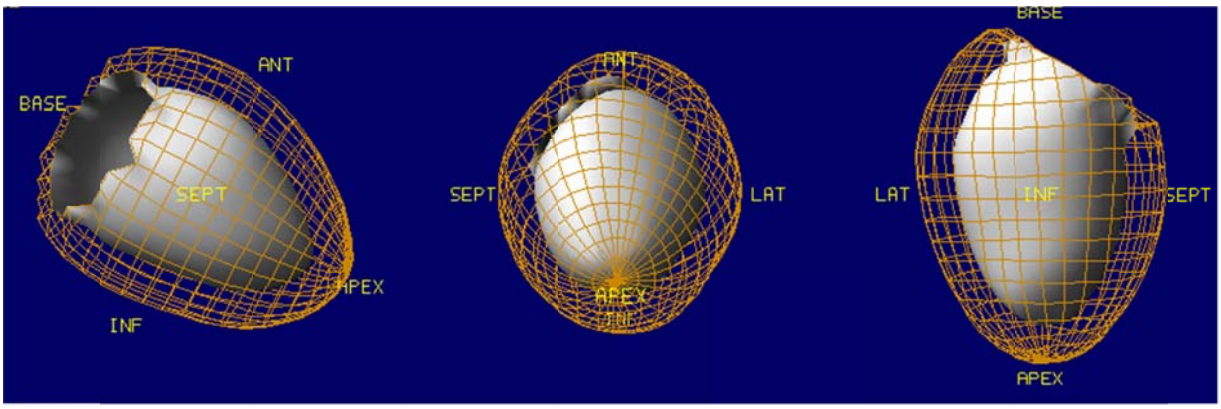

Figure 2. Three-dimensional display of the endocardial (solid) and epicardial (grid) surfaces calculated by the QGS automatic algorithm (Cedars-Sinai) for a patient at end diastole in septal, apex and inferior views. Retrieved from http://cedars-sinai.edu/Patients/Programs-and-Services/Medicine-Department/Artificial-Intelligence-in-Medicine-AIM/Projects/Quantitative-Gated-SPECT-QGS.aspx. Copyright (2016) by Cedars-Sinai[78]

To be sure of the first estimated mid-myocardial surface, it is fitted to an ellipsoid and previous procedure of placing the original coordinate system or center of mass along the ellipsoid's long-axis and sampling is iteratively performed until the long-axis angular variation is less than 0.5 degree.[74] The count profiles from sampling the center of the final ellipsoid then are fitted to asymmetric Gaussian curves. The peak of Gaussian curves represent mid-myocardial surface, while the endocardial and epicardial surfaces are determined by the calculation of Gaussian standard deviations, and the valve plane is determined by fitting a plane to the most basal myocardial points.[70]

The important matter at this point is the preservation of myocardial mass throughout the cardiac cycle which is imposed to the algorithm as a constraint. Once all the myocardial surfaces are calculated for each gating interval, quantitative analysis for LV cavity volumes can be performed. Multiplying the individual voxel volume by the number of voxels contained in the 3-D space between the endocardium and the valve plane yields the LV volume.[70] Based on calculating at end-diastole or end-systole, the volume would be the largest or smallest one from which the LVEF is derived as following:

$$LVEF = \frac{EDV - ESV}{EDV} \times 100 \quad (1)$$

Where, the EDV and ESV stand for end-diastolic and end-systolic volumes respectively.

Left ventricular synchrony parameters (QGS)

QGS software added a phase analysis plug-in option in 2008 and introduced several parameters for ventricular synchrony measurements. All of these parameters are used in synchrony assessments throughout the present thesis.

The QGS considers several spatial sampling points along the mid-myocardial surface and tracks the local maximum myocardial counts at each time interval. This creates a unidimensional array that represents a time-varying or periodic function. The number of counts varies with time, meaning that the counts increase at end-systole and decrease at end diastole and this happens cyclically. The QGS takes advantage of this periodic function by transforming it into the frequency domain to be able to work easier and more efficient with the sinusoidal signal in this domain. Using 8 or 16 frames per cardiac cycle is insufficient to have a continuous sinusoidal curve. QGS uses the first harmonic of Fourier function to increase the temporal resolution and to replace the discrete curves by the continuous ones.

The characteristics of a continuous sinusoidal signal during a cardiac cycle in the frequency domain can be determined by first, the phase angle which is the timing of mechanical contraction, the basis of all synchrony parameters, and second, the amplitude which is the magnitude of contraction or representative of regional stroke volume. In fact, the amplitude is only used by the algorithm to eliminate phase measurements that their corresponding amplitudes are considered too low to yield accurate measurements.[65] As it has been reported, around 5% of the samples with lowest amplitudes across the sampling region are automatically removed from the QGS analysis; since phase measurements are inaccurate for signals with low temporal variations.[65]

Once the phase signals are calculated for all the sampling points, a histogram of the distribution of those phase angles can be displayed in the software (Figure 3). On the basis of the whole-ventricle, wall-based, vessel-based, and segment-based statistics, phase histograms can be displayed and multiple global and regional LV synchrony parameters can be extracted from these histograms.[65] The mean and standard deviation are calculated as a routine part of

histogram distribution measurements in the software. Also, the bandwidth of the histogram which is the width of the phase band or range that contains 95% of the histogram samples is calculated. Moreover, the entropy or the randomness of the phase distribution within the whole region of interest is also defined in the QGS software as a part of phase parameters.

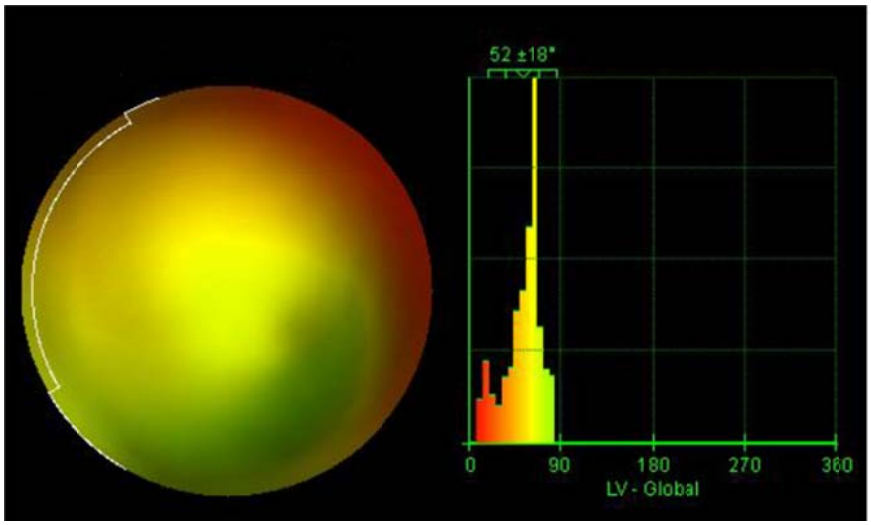

Figure 3. The phase histogram and polarmap display of the GMPS assessed by QGS software.

The entropy is a familiar term in various science and engineering applications to estimate the randomness within a system or process. In fact, the entropy here is an estimate of how random and uncoordinated the sample points contract within the entire ventricular myocardium. The use of entropy in cardiac mechanical synchrony analysis first was proposed by the O'Connell et al. [79] in 2005 to distinguish between two forms of ventricular contraction when the synchrony supposed to be zero. In this case, first assumption is to think that the contraction is completely random and nonhomogeneous in the region of interest. The second assumption is to consider the region of interest be made of two sub-regions, one 180° out of synchrony with the other, where each sub-region is highly synchronous, yet their sum is

not.[79] Using the entropy hence, the actual randomness of the contraction could be determined within the region when the synchrony of contraction is diminished. The simplest and most common approach for entropy measurement is the histogram-based estimation via the following formula:[79]

$$\varepsilon = \frac{-\sum_{i=1}^{M} P_i \times \log_2(P_i)}{\log_2(M)} \quad (2)$$

in which M represents the number of histogram bins and P_i is the frequency of the occurrence of phase angle i. Thus, the entropy is the number of measured phase angles that fall within bin i divided by the total number of bins or phase measurements in the histogram in a logarithmic form ranging from 0 to 1. In the ventricular synchrony assessments, if only one phase value exists in the histogram, entropy would be equal to zero and synchrony of contraction would be at maximum level.[65] We take benefits of all mentioned QGS synchrony parameters to assess ventricular mechanical synchrony under stress in our experimental models.

MHI_4MPI software

The MHI_4MPI is a fully automated in-house algorithm that assists in the diagnostic evaluation of mechanical synchrony in gated myocardial perfusion SPECT by segmentation of the LV and computation of the synchrony of wall contractions.[80] Although the QGS software is valuable on its own in segmentation and phase analysis, it does not consider the amplitude of contraction in its computations. However, besides the phase of contraction, the amplitude or the magnitude of wall contraction is important in wall thickening or motion abnormalities, since a dyssynchronous wall contraction with greater magnitude can more affect the entire contraction efficiency.[81] MHI_4MPI algorithm takes both the phase and amplitude of contraction into account in its wall contraction synchrony analysis.[80]

The algorithm first starts with segmentation of the LV by identifying the basal plane with automatic tracking points throughout the systolic and diastolic frames in a cardiac cycle using intensity and gradient values.[80] Afterward, the initial static mid-myocardial surface is defined by searching for maximal intensity points in ungated image. A deformable surface algorithm (3D-Snake) is then used to segment the LV volume. A deformable model is a geometric structure whose shape evolves following an iterative process.[82] Hence, the algorithm starts from a simple 3-D structure like a polyhedron with some faces and vertices and evolves with applying some external and internal forces in an iterative process (64 times) till the shape fits the ventricle volume. The external forces are submitted on each of the vertices along the direction normal to the myocardial surface, towards pixel intensity greater than the current position (Figure 4). In order to keep the surface smooth, internal forces are exercised to keep each vertex near the average of its neighbors, while conserving the global surface dimensions.

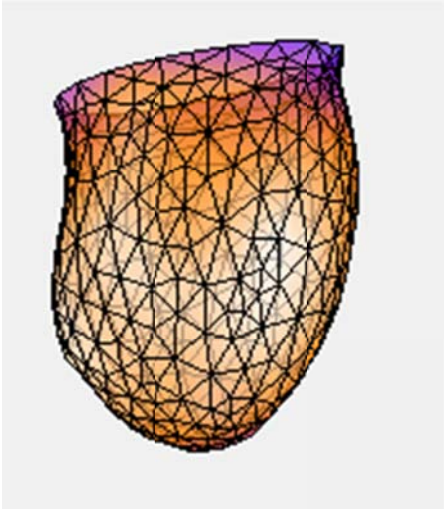

Figure 4. The dynamic mid-myocardial surface of approximately 360 vertices which are linked together making triangular shapes and surface tetrahedrons.

The second step consists of creating the surfaces for the myocardial limits (endocardial and pericardial surfaces) and applying a deformable dynamic surface algorithm (4D-Snake) in the gated images. Again external and internal forces are carried out sequentially in an iterative process on the mid-myocardium and two other surfaces. The algorithm will search along the normal to the endocardial and pericardial surfaces to find the zero crossing of the Laplacian at each frame.

The Laplacian technique is the most common approach for the edge-detection in nuclear medicine which is suitable for the objects with clear or sharp boundaries in radiotracer uptake.[69] Laplacian is defined by the second partial derivative of the function or pixel value with respect to the spatial coordinate x, y, and z in 3-D.[69] The point at which the Laplacian crosses zero reflects an edge, since it represents a high rate of change between neighboring pixel values.[69] Despite the fact that with limited SPECT resolution, this technique does not permit to an exact estimate of the wall thickness, it is good enough to correctly position the myocardial walls which are coherent in the structure. The actual positioning of the edges is not necessary since the goal is only to obtain the phase analysis of wall contractions, not the volumetric analysis.

Besides the previously described smoothing internal forces and the basal plane restrictions, the three surfaces are kept close to one another and a unique basal ring is forced on all three surfaces (Figure 5). Finally, to make sure that the movements are smooth and continuous, temporal forces are used to remove high-frequency harmonics on each vertex.

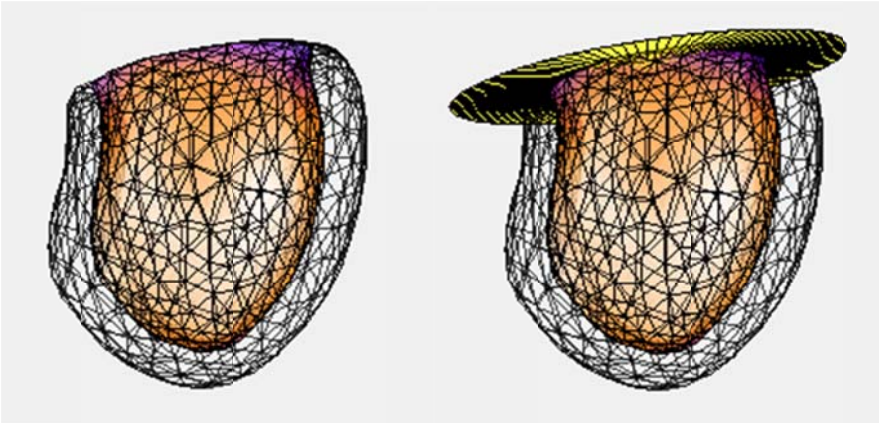

Figure 5. Dynamic surfaces for the myocardial limits. In left side figure, the mid-myocardium, endocardium, and epicardium are shown as the yellow surface, the white shadow within the yellow surface and the exterior netted surface respectively. The right side figure shows the basal plane fitting.

Once the myocardial wall edges are constructed, phase analyses are performed with either the thickening or the displacement methods. In order to have an estimate of the change in myocardial thickness, the algorithm uses the partial-volume effect. As a note, when the size of an object, in our case the thickness of the myocardial wall, becomes smaller than the resolution of the SPECT system, it partially fills a pixel volume (partial-volume effect) in the image matrix. Thus, the individual pixels do not accurately reflect the concentration of activity within them (showing a lower number of counts).[69] This leads to a greater decrease in maximum counts when the myocardium becomes thinner. As a result, the amount of intensity or change in the maximal count for each vertex on the maximal surface could be used as a local thickening estimation for each frame throughout the cardiac cycle. The software averages relative intensification thickening in the septal and lateral wall (Figure 6).

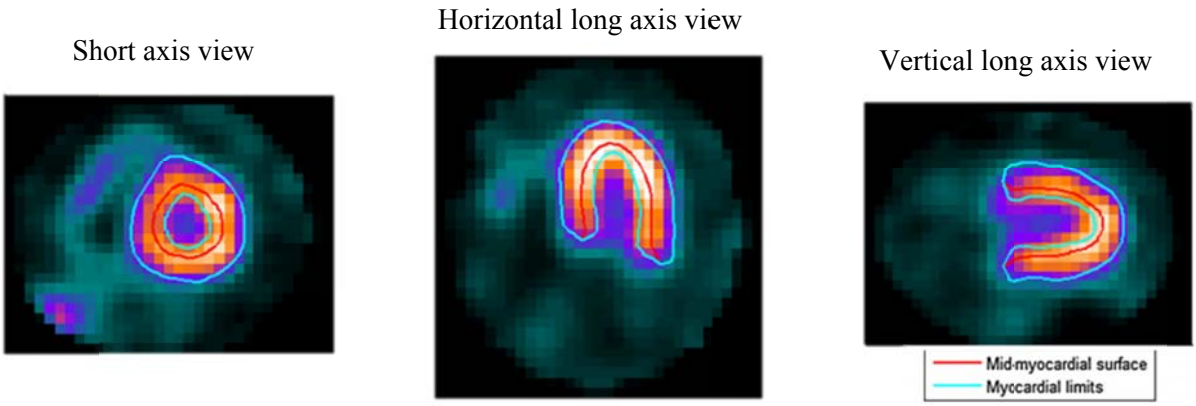

Figure 6. An example of the segmentation process by MHI4MPI algorithm during systole at different views.

Again as previously mentioned for QGS phase analysis, transforming a periodic function (maximum myocardial count change at each time interval during systole and diastole) into a sinusoidal function in frequency domain makes it easier to find the synchrony of mechanical contraction based on the phase (timing) and amplitude of sinusoidal curves for each mid-myocardial vertex. MHI_4MPI uses a three harmonics Fourier analysis to estimate the phase and amplitude of the contraction, in both thickening and displacement methods. In the following sections, first the Fourier function and then the MHI_4MPI synchrony parameters are described.

Fourier analysis

As discussed before, the product of SPECT imaging would be the time-activity curves related to each of the individual vertices along the mid-myocardial surface at a cardiac cycle. This time-based continuous waveform can be used by a mathematical tool called Fourier transform to be converted into its sinusoidal components. In fact, transforming a time-domain function into the frequency-domain with sinusoidal waveforms helps us better show the characteristics of the signal. A sinusoidal signal path can be shown as a circular path by walking through the

circumference with a specific size (radius), speed, and starting angle; then the combined position of all the cycles yields the final signal with amplitude, frequency and phase characteristics respectively (Figure 7).[83] Circular statistics help us understand the sinusoidal (time-activity) signals and final parameters that will derive from the Fourier transform. For this reason, some detail has been discussed here on the subject.

If you imagine the starting point to be the x-coordinate in a polar coordinate system, regular exponential growth continuously from the x-coordinate along the circumference with a certain rate closely simulates the movement of a signal in a cyclic way with a specific phase (starting point), amplitude (the radius of the circle) and frequency (how fast spins around the circle) (Figure 7). Therefore, a signal (maximum count change at a vertex of mid-myocardium), appearing as a point in the circle, moves x radians towards the imaginary dimension in an exponential mode to get to -1 (half of the cycle) and then continue to finish the cycle. This is exactly what Euler's formula $e^{i\pi} = -1$ means[83] and the Fourier transform is all about these to transform the time-activity curves as discrete curves containing maximal counts at different time frames (points at different places in circle circumference) into continuous sinusoidal curves. The formula is as following:

$$F_k = \sum_{t=1}^{N} f_t \, e^{-i2\pi k \frac{t}{N}} \tag{3}$$

Which means: to find the signal (maximum count change for a vertex in the mid-myocardium) in a particular frequency (F_k), spin (e^{-i}) the signal backwards (f_t) around the circle (2π) at that frequency (k) and average ($\sum_{t=1}^{N} \frac{t}{N}$) a bunch ($N$) of points (number of gates, t) along that path (a cardiac cycle). This is a simple and informative interpretation of Fourier transform proposed by Stuart Riffle[84] which has been linked to our discourse.

As it has been shown in Figure 7, spinning around the cycle ($e^{i\theta}$) in degree from the x-coordinate for each signal point gives exactly the same result as to adding up the real and imaginary parts ($\cos\theta + isin\,\theta$) of the x-y coordinates for that specific signal point. [83]

$$e^{i\theta} = \cos\theta + isin\,\theta \tag{4}$$

Hence, the Fourier transform can be rewritten and simplified as the sum of cosine (R: real) and sine (I: imaginary) functions: [85]

$$R_k = \sum_{t=1}^{N} f_t \cos 2\pi k \frac{t}{N} \tag{5}$$

$$I_k = \sum_{t=1}^{N} f_t \sin 2\pi k \frac{t}{N} \tag{6}$$

$$F_k = \sum_{t=1}^{N} (R_k - iI_k) \tag{7}$$

Again as it has been shown in Figure 7, with having the real and imaginary components of the right angle triangle, the hypotenuse or the amplitude (A) and the angle from the positive real coordinate or the phase (θ) of signal point at each time interval can be measured as following:

$$A = \sqrt{R^2 + I^2} \tag{8}$$

$$\theta = \tan^{-1}\frac{I}{R} \tag{9}$$

Hence, the phase and amplitude which can be described by complex numbers made of real and imaginary components are the bases of all ventricular synchrony parameters produced by any software in this field.

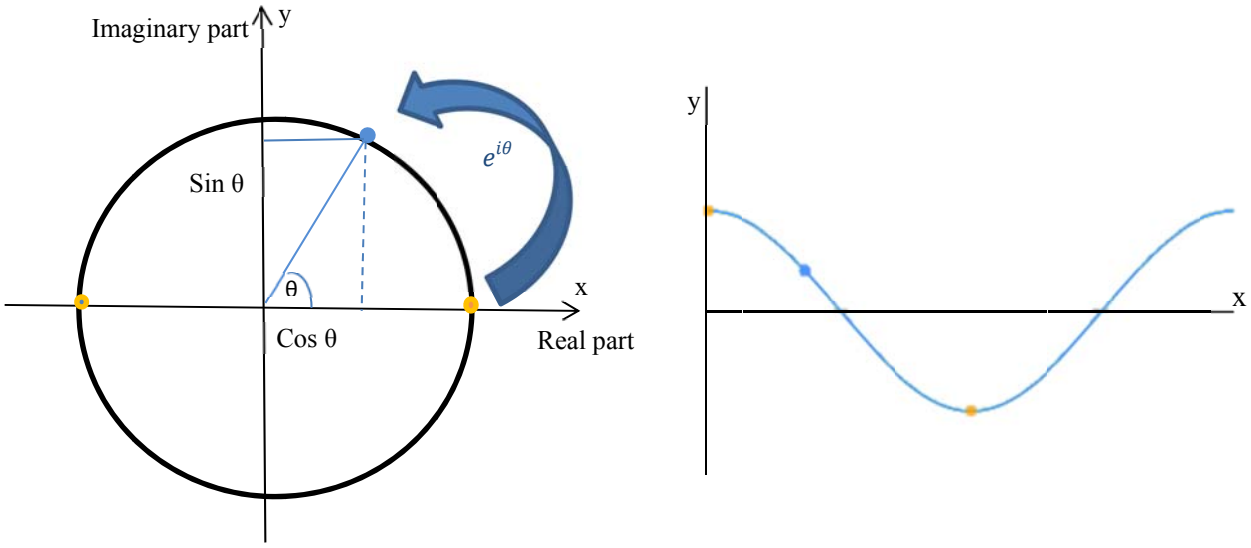

Figure 7. The simulation of the movement of a sinusoidal signal in a circular path. The left side figure shows a polar coordinate system and a signal point swirling around the circle counter clockwise from the x-coordinate (real part). The spinning of the signal vector about θ° in the circumstance (Euler's formula) is equal to sum of cosine (real) and sine (imaginary) of θ in the coordinate. The right side figure shows the place of the mentioned vector in a sinusoidal wavefront.

Left ventricular synchrony parameters

Similar circular math concepts mentioned above is applied by MHI_4MPI to calculate and show the phase and amplitude of different vertices relative to the mean phase and amplitude in a circle. As shown in figure 8, big white circle, white line, and small circle each represents the mean amplitude, phase, and the efficiency of the activity signal during a bunch of cardiac cycles respectively.

But what is the efficiency? In order to find the magnitude of effective contraction or efficiency (E) of the contraction, each individual signal point, as a complex harmonic

including phase and amplitude should be evaluated relative to the average phase (or should be projected onto the mean phase) as following:

$$E = \frac{A_1 e^{i\theta_1}}{e^{i\bar{\theta}}} \tag{10}$$

If the phase difference between the point and mean phase ($e^{i\theta_1 - \bar{\theta}}$) is zero, the point is exactly in line with the mean phase thus efficiency would be equal to (A_1) but if the difference is 180º, the result will be equal to ($-A_1$). As it has been shown in the Figure 9, in the case of having two points with same amplitude, the one that is in line with the mean phase direction is more efficient (having larger magnitude) within the entire system (ventricular contraction) than the point farther away from the mean phase.

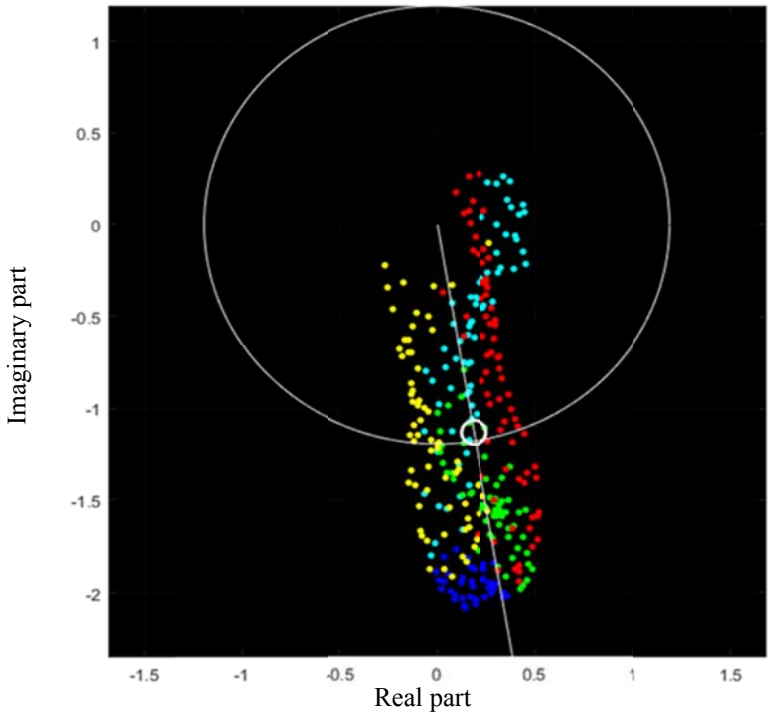

Figure 8. Fourier phase analyses of left ventricular thickening signals. Each point is an actual vertex on the surface in different regions of the left ventricle. The big circle, white line, and small circle each represents the mean amplitude, phase and the efficiency of contraction respectively

The efficiency is of amplitude domain, it thus represents the portion of amplitude that is in the direction of the mean phase in a complex plane. Therefore, evaluating the average efficiency relative to the average amplitude gives us the magnitude of positive or efficient contraction that contributes to the stroke volume and ejection of blood out of the chamber. The latter concept is called contraction homogeneity index (CHI) as following:

$$CHI = \frac{\bar{E}}{\bar{A}} \tag{11}$$

Based on the type of signal used for CHI calculation, it could be defined as thickening homogeneity index (THI) or displacement homogeneity index (DHI) (the proportion of wall thickening or displacement that is in synchrony with the average signal). Overall, efficiency lets us know what is happening locally while CHI gives us a global idea of how much synchrony or efficiency there is in the LV myocardium. In our point of view, evaluation of the amplitude is significantly important in mechanical dyssynchrony assessments; since looking only at the phase of contraction does not respond to the question that how much a region contributes to the stroke volume or total thickening. Also, as previously mentioned, a dyssynchronous wall contraction with greater magnitude can more affect the entire contraction efficiency. The amplitude will be even more functional in predicting the response to CRT. In our opinion, if a region is off-phase but it has the amplitude even negative, it might be possible to be resynchronized. However, an off-phase region with no amplitude or movement and thus no contribution to the contraction may not answer to the resynchronization therapy.

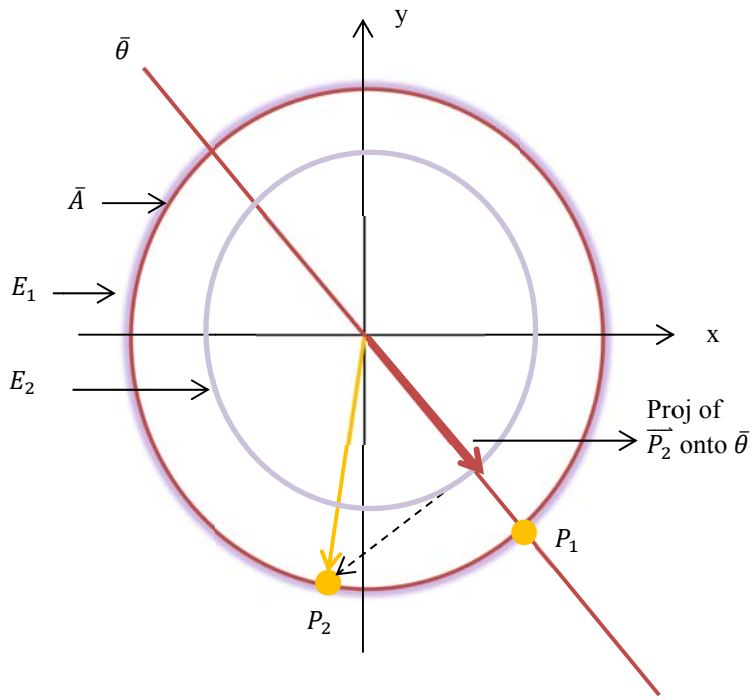

Figure 9. Efficiency concept for signals in a circular path. Each signal point (P_1 *or* P_2) is like a vector which starts to spin around the circular path (cycle) from the x-coordinate or real part of the system. The phase and amplitude of the P_1 signal is the same as the mean phase ($\bar{\theta}$) and amplitude ($\bar{A}$) shown as the circle and the line in cherry color. Thus, the efficiency(E_1) of P_1 is equal to the value of the amplitude (shown as a purple circle overlapped with ($\bar{A}$)). While, the P_2 signal vector has exactly the same amplitude as P_1, it has a phase difference with $\bar{\theta}$. The efficiency (E_2) of its movement though is estimated (through the projection of the P_2 vector onto $\bar{\theta}$) to be lower than ($\bar{A}$).

Besides the CHI, septal-to-lateral delay (SLD) is another index for intra-ventricular mechanical synchrony measurement by MHI4MPI. The cross-correlation of the septal and lateral mean signals (either thickening or displacement) is used to obtain the SLD which based on the applied signals is called the thickening SLD (TSLD) or the displacement SLD (DSLD). As a note, to estimate the myocardial displacement, principle component analysis is used to find the direction of the largest possible variance for each vertex of the mid-myocardial

surface. The motion is analyzed by projecting the 3-D displacement vector along the variance vector with the positive direction defined as pointing outside of the mid-myocardium.[80] With these displacement signals, the DSLD and DHI can be calculated.

Gated blood pool SPECT

As previously mentioned, the most convenient way to assess the LV function, dynamics, and dyssynchrony in 3-D format is to use GMPS imaging with the administration of ^{99m}Tc labeled radiopharmaceuticals. However, in the case of having many defects in myocardial walls, evaluation of LV function and dyssynchrony may be interrupted. Also, the appraisal of RV function and inter-ventricular dyssynchrony is sometimes of special interest in the ventricular analysis; but perfusion images do not represent this information. Instead, gated blood pool SPECT (GBPS) can provide a more accurate estimation of right and left ventricular function without any geometric assumption for volumetric analysis.[70] Also, either intra or inter-ventricular dyssynchrony parameters could be performed in GBPS based on wall motion analysis.

The radiotracer in GBPS is yet again ^{99m}Tc that should be labeled with red blood cells of the patient. Thus, as it is apparent from the name of the imaging, the blood pool within the cardiac chambers can be imaged in this technique. All the procedures for the perfusion imaging such as acquisition, image reconstruction, filtering, reorientation, segmentation, and phase analysis could be performed in an identical manner for the GBPS imaging. The only difference is the segmentation of the region of interest which in the case of perfusion imaging is the myocardial wall and in the case of blood pool imaging is the endocardial-blood interface for both the right and left ventricles. Then in phase analysis section, a 3-harmonic inter-

correlation of the RV and LV time-activity curves is used to compute the phase differences between ventricular chambers (inter-ventricular delay).

Overall, all the final synchrony quantifications in both techniques depend on the quality of the raw projection data. Therefore, some factors during acquisition such as an inadequate number of counts, improper gating or positioning of the rotating camera and excessive motion of the patient can affect the final quantification process.[70] Also, the final quantifications depend on proper processing of the raw data during the image reconstruction and reorientation.[70]

Cut-off values for phase analysis parameters

As mentioned previously, the MD assessment is of special importance in the prognostication of a variety of cardiac dysfunctions mostly in the field of CRT. The GMPS as an automatic and reproducible imaging technique provides not only the MD parameters but also as a "one-stop shop" technique, the perfusion, function and the presence, extent, and location of scar tissue. While these advantages have led to the growing use of GMPS in routine clinical practice once the MD assessment is essential, some questions have raised about the cut-off values of GMPS phase analysis parameters for normal versus electrical and/or mechanical cardiac dysfunctions. There are number of studies including control groups that have compared different parameters of phase analysis. However, no cut-off values have been provided in those studies.[66,86-89]

In a recent study by Romero-Farina et al.,[90] the cut-off values for a control group versus patients with electrical and mechanical dysfunctions were proposed that are summarized in Table 1. This valuable study was performed prospectively with the recruitment of 150 normal subjects and 305 patients of whom 121 patients had mechanical cardiac

dysfunction such as dilated cardiomyopathy and myocardial infarction and 63 patients had electrical conduction disorders. The criteria of being normal were as following: having no history of CAD, normal resting electrocardiogram (sinus rhythm, QRS < 120 ms), no perfusion defect, and gated-SPECT EF > 50% which was the same criteria used in the previous studies including control groups for phase comparisons as cited in Table 2. As a note, the normal values of the phase parameters in different published studies are not exactly the same, maybe because of using different methodologies.

In the study performed by Romero-Farina et al.,[90] a linear trend was seen between the extent of myocardial disturbance and the value of mechanical dyssynchrony parameters so that the amount of MD significantly increased from the normal to the electrical conduction diseases, mechanical cardiac diseases and both the electrical and mechanical diseases respectively. Although this study could provide an idea of group differentiation between different patients' categories, as authors believe, a prospective clinical trial is needed to assess the cut-off values for MD parameters especially in the case of response to CRT.

Table 1. Different cut-off values of phase parameters between normal subjects and patients with conduction and mechanical disorders (Romero-Farina et al. 2015).

Group differentiation	Cut-off for phase SD	Cut-off for bandwidth
Patient/normal	>18.4	>51
Mechanical/electrical disorder	>26.1	>70
With/without criteria of CRT	>40.2	>132

Table 2. Mean standard deviation and bandwidth in different control groups derived in different studies

Authors	Subject Number (F/M)	Post stress/rest	If categorized	Standard deviation	Bandwidth
Trimble et al.[87] 2007	157(75/82)	Post stress	-	15.7 ± 11.8	42 ± 28.4
Chen et al.[86] 2008	90 (45/45)	Post stress	F (45)	11.8 ± 5.2	30.6 ± 9.6
			M (45)	14.2 ± 5.1	38.7 ± 11.8
Trimble et al.[66] 2008	50 (10/40)	-	-	8.6 ± 2.9	27.9 ± 8.9
Atchley et al.[88] 2009	75 (50/25)	Post stress	-	8.8 ± 3.1	28.7 ± 9.3
Chen et al.[89] 2011	30 (19/11)	Rest	-	7.6 ± 2	26.1 ± 7
Romero-Farina et al.[90] 2015	150 (75/75)	Rest	All	12.2 ± 4.9	36.5 ± 12
			F	11.4 ± 4.6	34.2 ± 10.7
			M	12.9 ± 4.9	38.7 ± 12.9

Stress-induced modalities

Exercise stress

Dynamic stress testing has been an established clinical test mostly in the diagnosis, treatment, and prognosis of CAD.[91] However, it is also used for risk stratification after myocardial infarction and before non-cardiac surgical procedures, identification of viable myocardium in patients with LV dysfunction, predicting the recovery of LV function after coronary revascularization,[92] and assessment of MD for using in a number of applications as previously mentioned. Since the exercise stress testing is widely available and is less expensive than the pharmacologic stress, it is more preferable and if applicable, it can help to draw a link between the physical activity and inducing abnormalities.[92] The hemodynamic changes over the peak exercise have been well explained by Rallidis et al.,[93] as following: during exercise, heart rate increases as a result of sympathetic stimulation and parasympathetic withdrawal, to a lesser extent. Thus, increased venous return as a result of sympathetic vasoconstriction of the large capacity veins and also the pumping effect of muscular contraction generate an increase in stroke volume as the results of concomitant Frank-Starling effect. Also, an increase in systolic blood pressure can be seen with much greater cardiac output in spite of the decrease in peripheral resistance.

Pharmacological stress: dobutamine

Dobutamine is a catecholamine with a potent $beta_1$-adrenoreceptor agonist activity and mild action on $alpha_1$- and $beta_2$-adrenoreceptors.[94] As a note, binding of a catecholamine to an adrenergic receptor or adrenoceptor stimulates the sympathetic nervous system. Hence, dobutamine induces a progressive increase in heart rate and myocardial contractility; therefore

produces an increase in the stroke volume and cardiac output as the results of both chronotropic (increase in heart rate) and inotropic (increase in EF) responses mediated by $beta_1$-receptor.[93] A decrease in systemic vascular resistance mediated by $beta_2$-receptor induces a mild increase in blood pressure.[95-97] Decline in central venous, pulmonary artery and capillary wedge pressures by dobutamine effect, in turn, results in a decrease in LV filling pressures and volume.[93] Also, myocardial oxygen demand will be increased in the response of the increase in both heart rate and contractility.[93] $Beta_2$-mediated coronary vasodilation as a primary neural effect of sympathetic beta stimulation along with a $beta_1$-mediated increase in heart rate, contractility and oxygen demand as a secondary metabolic effect of sympathetic beta stimulation, leads to an increase in coronary blood flow and increased perfusion in the regional myocardium.[98] It is the cause of using dobutamine stress test for diagnosing the CAD; since in the case of having an occlusion in one of the arteries, lack of regional blood flow can be seen in the myocardial image. High levels of dobutamine stress may induce ischemic wall motion abnormalities by increasing the myocardial oxygen demand in the case of any coronary stenosis. Whereas, low levels of dobutamine may improve the contractile response of the myocardial regions where show abnormal motion at rest, illustrating the contractile reserve.[99]

Dobutamine as an inotropic agent is also used as a treatment option in dilated cardiomyopathy patients with acute decompensated HF and low LVEF to improve the myocardial contractility and function until the acute causing problem is resolved or an ultimate therapy such as coronary revascularization or heart transplantation is performed.[51] Also, dobutamine has been used as a stress-induced agent in the assessment of MD either in CRT candidates for predicting the response to therapy[48] or in patients with dilated cardiomyopathy

without baseline electrical dyssynchrony for predicting the future outcomes.[50] The use of dobutamine in these circumstances helps to precisely identify the regional differences in the onset of myocardial contraction since stress-MD variations have been proven to correlate more with clinical outcomes.[48,50]

Exercise versus dobutamine stress

Comparing the treadmill exercise and dobutamine stress echocardiography, Rallidis et al.[93] demonstrated that the average heart rate as well as the systolic blood pressure thus workload in the exercise was greater than that obtained with peak dobutamine stress. Also, a greater ischemic burden was seen with exercise which was explained to be resulted from higher oxygen demand as an outcome of increased systolic blood pressure, heart rate, and myocardial contractility.[93] In another comparison study of the exercise and dobutamine stress echocardiography, Mehrotra et al.[100] reported that the degree of stress produced by dobutamine is considerably different than the exercise. In fact, exercise not only increases the cardiac myocardial contraction but also the skeletal muscle contraction that results in constriction of large capacitance veins and in consequence an increase in venous return. Since dobutamine does not increase the peripheral venous tone, it has been observed that it produces greater reductions in LV EDV and ESV than exercise and along with lower systolic blood pressure, results in a lower wall tension and peak systolic stress.[100]

Owing to the hemodynamic differences between the exercise and pharmacological (dobutamine) stress and to be more realistic, it is recommended to use the exercise stress testing for examining the patients suspected to have a CAD.[100] There are several patient subsets in whom the exercise cannot be used or should be substituted with dobutamine or pharmacological stress such as the elderly patients (many of patients with HF), patients with

inadequate amount of exercise thus leading to inconclusive test results, and the patients in whom dynamic exercise might be absolutely (e.g. sever aortic stenosis or LV dysfunction) or relatively (e.g. tachyarrhythmias or bradyarrhythmias) contraindicated.[91] It is worth mentioning that patients undergoing dobutamine stress testing usually experience less angina, ST-segment depressions, and wall motion abnormalities relative to exercise stress testing.[100]

Assessment of dynamic left ventricular dyssynchrony

From 2005 to 2009, many types of research were performed to assess the feasibility of LV MD quantification under stress and also the MD variations and its relationship with other hemodynamic results and clinical outcomes.[46,48,101-104] Most of these studies reviewed by Lancellotti et al.[44] applied echocardiographic methods on patients with and without ischemic heart disease. The first precise study was performed by Lancellotti et al.[102] who showed a noticeable MD variation during exercise in patients with HF as a result of CAD. MD increased in about half of the patients (from 35 patients) and decreased or remained unchanged in others. A remarkable result in their study was the strong correlation between the exercise-induced variation in LV MD and the change in stroke volume, mitral regurgitation and brain natriuretic peptide release (a secreted hormone from ventricles during excessive stress that rises in several cardiac diseases[105]).

In a greater number of HF patients (n = 65) with QRS ≥ 120 in about 2/3 of patients, Lafitte et al.[46] demonstrated that HF patients showed either exercise induction or normalization of MD, of whom LV MD increased in 34% by at least 20%, remained stable in 37%, and decreased in 29% by at least 20%. However, exercise did not modify the extent of dyssynchrony parameters in patients with normal LV function. Also, a significant correlation was found between exercise-induced changes in MD and the presence of ischemic

cardiomyopathy; since 80% of ischemic patients showed more than 20% of changes in MD during exercise as a result of abnormal regional wall motion. Lafitte et al. also confirmed the previous results based on the correlation between the stress-induced variation in LV MD and changes in cardiac output and mitral regurgitation.

In a different subset of patients, either with HF or normal ventricular function, researchers studied the effect of exercise or dobutamine stress on LV MD and confirmed the dynamic nature of dyssynchrony. In 60 patients with idiopathic dilated cardiomyopathy and narrow QRS, D'Andrea et al.[106] found that exercise unmasked the MD in more than half of the patients. Moreover, exercise-induced MD was independently associated with increased functional mitral regurgitation, reduced exercise capacity, and impairment of LV exercise stroke volume. Six years later in 2013, the same group reported the potential prognostic power of dynamic dyssynchrony in patients with dilated cardiomyopathy and narrow QRS.[50] In a cohort of 180 patients, they observed that the increase in echocardiographic dyssynchrony during exercise was the strongest predictor of cardiac events during a 4-year follow-up. Based on the results, they believe that assessment of LV MD during exercise can further improve the understanding of the pathophysiology of some functional and mechanical cardiac changes during the exercise, such as stroke volume impairment and an increase in mitral regurgitation severity.[50] Also, they emphasized on the use of stress-MD test besides the routine echocardiography not only for prognostication but also for better identification of patients who might benefit from CRT (if applicable as previously discussed).

Exercise dyssynchrony was also used by Rocchi et al.[48] to select the CRT responders. Sixty-four patients scheduled for CRT implantation performed exercise echocardiography before and 6 months after CRT implantation. Based on the results, exercise intra-ventricular

MD was a stronger predictor of CRT response than resting MD. Also, they noticed that exercise-induced a spatial change in the electromechanical activation of the LV, the lateral wall was the most delayed at rest but during exercise, the posterior wall became more delayed. Since more delayed site of activation is preferred to be stimulated during the CRT, the site of the LV lead might be better selected based on exercise rather than resting MD assessments.[48] Overall, dynamic dyssynchrony assessment is of special importance in CRT field based on many authors as they believe that neglecting the QRS duration at rest, HF patients who show significant dynamic dyssynchrony might benefit from CRT. In contrast, patients in whom ventricular MD disappears with exercise might not have a desire response to CRT.[48,50]

Using modern real-time 3-D echocardiography, Izumo et al.[107] studied the changes in LV shape and dyssynchrony during exercise and found a close relationship between the exercise dyssynchrony and the exercise-induced changes in LV shape and mitral regurgitation in HF patients. In fact, exercise-induced LV dyssynchrony and spherical remodeling resulted in mitral valve tethering and worsened mitral regurgitation in those patients.[107]

As previously mentioned, dobutamine can also be used as a stress agent instead of exercise for assessing dynamic LV MD. Using dobutamine infusion, Chattopadhyay et al.[101] showed that both the prevalence and severity of intra-ventricular LV MD increase in HF patients during stress no matter what the QRS duration is. Seventy-seven patients (47 with QRS < 120 ms and 30 with QRS ≥ 120 ms) with HF due to LV systolic dysfunction and 22 normal subjects underwent dobutamine stress echocardiography in this study. Although, dobutamine stress shortened the LV MD (time to peak systolic velocity in 12 segments) in healthy subjects, both the prevalence and severity of dyssynchrony increased in patients with systolic dysfunction irrespective of QRS duration. The reason why the QRS does not matter at

peak pharmacological stress is that the prevalence of MD at rest is lower in patients with QRS < 120 ms; hence the stress-induced increase in MD was most visible in this population and approached that of patients with QRS ≥ 120 ms during dobutamine stress.[101] LV MD can also be unmasked and easily detected during low-dose dobutamine infusion in patients receiving CRT and its extent was shown to be related to the extent of reverse remodeling after CRT implantation.[45]

Feasibility of dynamic dyssynchrony quantification was evaluated by stress echocardiographic methods in most of the previous studies. However, during stress echocardiography, changes in heart rate, the type of stress-induced method, the absence of standard criteria by which to identify the dyssynchrony, and measurement errors due to procedural complications result in some intra- or inter-observational differences in identifying the dyssynchrony in HF patients. Phase analysis of nuclear imaging methods can solve the associated problems.

Summary

Both the proven importance of assessing stress MD in prediction of response to CRT and correlation with adverse outcomes, together with the appearance of more automated and reproducible techniques such as nuclear imaging have contributed to new clues for accurate MD assessment, while raising new questions: Which nuclear methodology is more accurate and robust in stress-MD assessments? What is the range of difference in inter- and intraventricular dyssynchrony parameters when the patient is submitted to various levels of functional stress? What is the range of difference in stress LV synchrony when different modes of electrical stimulation are applied? In another word, is the optimal pacing mode at rest, in terms of synchrony of contraction, also the best one during the exercise and increased

heart rates? The goal of current research is to answer these questions by providing three different experimental canine models and using the promising nuclear imaging techniques.

Organization of thesis: objectives and approaches

Under-stress ventricular mechanical dyssynchrony in this thesis is assessed by canine models in three different studies. In order to fully characterize the relation between cardiac stress and synchrony of contraction, multiple stress levels are required which is a long procedure and difficult to be performed on human subjects. In addition, invasive hemodynamic measurements are unbearable in a clinical subset. Therefore, experimental models are used to follow the procedures accurately and more flexibly in the current thesis.

Chapter 1: The effects of dobutamine stress on cardiac mechanical synchrony determined by phase analysis of gated SPECT myocardial perfusion imaging in a canine model.

Rational

Stress-MD assessment is of special interest since it is a better predictor of response to CRT than QRS width or resting MD and its variations have been proven to correlate more with clinical outcomes. However, it is not known to what extent stress can modify the mechanics of the left ventricle. In addition, although the excellent repeatability and reproducibility of phase analysis of GMPS have been proven for LV MD measurements over echocardiography modalities, it is not well-known that which methodology in phase analysis is more accurate and robust in stress-MD assessments. Hence, a control study is needed to help better

understand the hemodynamic and mechanical characteristics of LV under various stress levels and to identify the best phase analysis methodology for stress-MD assessments.

Hypotheses

Dobutamine as a stress-induced factor modifies the synchrony of LV mechanical contraction and these synchrony variations can be shown more robustly through the thickening-based phase analysis than the displacement-based analysis.

Specific objectives

The primary objective of this study was to evaluate the effects of different levels of dobutamine on LV synchrony of contraction. The secondary objectives were to define 1) the feasibility and efficacy of our experiment protocol in this basic study, 2) the normal values of phase parameters either at rest or stress levels, and 3) the accuracy of two different methods of acquiring the phase dyssynchrony parameters (thickening or displacement) in GMPS imaging. The results of this study are discussed in detail in chapter 1 of the current thesis.

Chapter 2: Phase analysis of gated blood pool SPECT for multiple stress testing assessments of ventricular mechanical dyssynchrony in a tachycardia-induced dilated cardiomyopathy canine model.

Rational

In the first study, we defined the mechanical characteristics of LV contraction under stress in the normal canine hearts. However, we were also interested in how dobutamine stress affects the mechanics of the ventricles in the presence of a systolic dysfunction. Few studies[46,50,101,108] have investigated the effect of stress on MD either in CRT candidates or in

patients with dilated cardiomyopathy and narrow QRS complex. However, none have examined the range of difference in inter- and intraventricular dyssynchrony parameters when the patients are submitted to various levels of stress. The quantification of stress dyssynchrony in those studies has been performed by different echocardiography-based methods. However, an intrinsic property of these methods lies in their limited reproducibility, since they are largely subject-dependent, both in the case of image acquisition and analysis.[55] Also, there is no standardized methodology with accurate and robust parameters for detecting mechanical dyssynchrony using echocardiographic imaging tools.[44] Hence, phase analysis of SPECT imaging specifically the GBPS can help to better understand the mechanical characteristics of LV contraction under stress both in the level of inter- and intraventricular dyssynchrony in an experimental model of non-ischemic cardiomyopathy and systolic dysfunction.

Hypothesis

Different levels of dobutamine stress even in close intervals can change the extent of inter- and intraventricular dyssynchrony in non-ischemic HF subjects.

Specific objectives

We aimed to examine the range of difference in inter- and intraventricular dyssynchrony parameters when the subjects were submitted to various levels of stress. The results of this study are discussed in chapter 2 of the thesis.

Chapter 3: Effects of various modes of ventricular pacing on left ventricular mechanical synchrony under stress as assessed by phase analysis of gated myocardial perfusion SPECT in a canine model of atrioventricular block and normal function.

Rational

After achieving the results of two previous studies with the focus of LV MD either in normal or in HF subjects, we attempted to further explore the relationship between the MD and pacing therapy. Until now, it is not well-known to what extent stress affects the synchrony of mechanical activation of a paced heart. During the period of stress, patients need to a more synchronous ventricular contraction and a better pumping function than the resting condition. Hence, whether the optimal pacing solution in terms of synchrony of contraction which is usually identified at rest can be the optimal one at stress condition is still a question. Considering the fact that previous evidence shows the superiority of stress-MD in predicting the response to CRT than resting-MD,[48] a detailed knowledge about mechanical characteristics of the pacing-induced LV contraction under stress condition is of special interest.

Hypothesis

BiV pacing with pre-activation of LV more resembles the intrinsic ventricular activation in developing normal contraction at stress.

Specific objectives

Our objective was to quantify the acute variations in LV function and MD during single, simultaneous, and sequential BiV pacing modes, under both rest and dobutamine stress levels in a canine model with normal function. The results are shown and discussed in chapter 3 of the current thesis.

Contribution statement

The present thesis describes the author's research accomplished at the Montreal Heart Institute (MHI) under the supervision of Dr. François Harel as part of the Ph.D. program at Université de Montréal.

The research was conducted with the collaboration of Dr. Bernard Thibault in the Electrophysiology Service of the MHI. The thesis author had no involvement in the study design, study protocol, and animal experimental procedures. Acquisitions were reconstructed following standard protocol by MHI technician, Sophie Marcil. Manual reorientation of the images, segmentations and functional and mechanical dyssynchrony (MD) assessments were performed by the thesis author. The current research used two different techniques for the assessment of MD: GBPS and GMPS. Besides using already available QGS software for the functional and MD assessments in GMPS, two other in-house MHI software packages, written by Vincent Finnerty the physicist, were used for the segmentation and data analysis in the current thesis for both aforementioned techniques. First, MHI segmentation software for GBPS which was formerly developed in 2007 for the volumetric analysis, then used for MD analysis in 2008, and validated in 2010 as an accurate measurement tool for volumetric analysis. It eventually was used during the current thesis for a complete assessment of functional and MD parameters with minor improvements in the case of MD analysis. Next, MHI_4MPI segmentation software which was developed during this thesis used to assist in the diagnostic evaluation of under-stress ventricular MD in GMPS using the thickening- and displacement-based methodologies. Although the thesis author had no involvement in the software programming, she used these intuitively appealing software packages to analyze different aspects of under-stress ventricular contraction and when applicable, bring new idea

for further improvement in the case of analyzed parameters to better interpret the findings and to link the real-time hemodynamic outcomes with the MD results. The thesis author analyzed all the SPECT data referred to the current thesis from the segmentation to the subsequent phase analysis and ultimately the statistical data throughout all three subsets of animal studies.

Some of the findings of the current research were published as an abstract in Canadian Journal of Cardiology which was presented in Canadian Cardiovascular Congress and Canadian Association of Nuclear Medicine annual meeting and as journal articles in the Journal of Nuclear Cardiology which is outlined further in next section.

The thesis author prepared the manuscripts for publication and presented the abstract in oral and poster format in both conferences. Also, she responded to the reviewer's comments for both the manuscripts which were published. Dr. François Harel, Dr. Bernard Thibault, Dr. Jean Grégoire, and Vincent Finnerty all helped to have intellectually vigorous discussions in the manuscripts and also all revised the manuscripts as well.

Except the software interfaces, all the thesis content including the literature reviews, tables and graphs were performed and produced by the author.

Proposed Articles

- The effects of dobutamine stress on cardiac mechanical synchrony determined by phase analysis of gated SPECT myocardial perfusion imaging in a canine model; *Journal of Nuclear Cardiology 21.2 (2014): 375-383.*

- Phase analysis of gated blood pool SPECT for multiple stress testing assessments of ventricular mechanical dyssynchrony in a tachycardia-induced dilated cardiomyopathy canine model; *Journal of Nuclear Cardiology (2016): in press*

- Effects of various modes of ventricular pacing on left ventricular mechanical synchrony under stress as assessed by phase analysis of gated myocardial perfusion SPECT in a canine model of atrioventricular block and normal function; *working manuscript*

Chapter 1

The effects of dobutamine stress on cardiac mechanical synchrony determined by phase analysis of gated SPECT myocardial perfusion imaging in a canine model

Samaneh Salimian, MSc,[a] Bernard Thibault, MD,[b] Vincent Finnerty, MSc,[a] Jean Grégoire, MD,[a] and François Harel, MD, PhD,[a]

[a]Department of Nuclear Medicine, Montreal Heart Institute and Université de Montréal, Montreal, QC, Canada

[b]Department of Medicine, Montreal Heart Institute and Université de Montréal, Montreal, QC, Canada

Received Oct 16, 2013; accepted Dec 2, 2013

J Nucl Cardiol. 21.2 (2014): 375-383

doi:10.1007/s12350-013-9847-3

Abstract

Background: Precise identification of left ventricular (LV) systolic mechanical dyssynchrony may be useful in optimizing the response to cardiac resynchronization therapy in heart failure (HF) patients. However, LV dyssynchrony is mostly measured at rest; patients often suffer from the HF symptoms during exercise.

Objectives: Our objective was to examine the impacts of stress on LV synchrony with phase analysis of gated SPECT myocardial perfusion imaging (GMPS) within a normal animal cohort.

Methods: Stress was induced with different levels of dobutamine infusion in 6 healthy canine subjects. Hemodynamic properties were assessed by LV pressure measurements. Also, LV mechanical synchrony (coordination of LV septal and lateral wall at the time of contraction) was determined by phase analysis of GMPS using commercially available QGS software and in-house MHI_4MPI software, with thickening- and displacement-based method. Synchrony indexes in MHI_4MPI included the septum-to-lateral delay and homogeneity index, derived from each of the two methods. Also, bandwidth, SD and entropy (synchrony indexes) of the QGS software were assessed.

Results: LVEF increased from 36.7 ± 8.7% at rest to 53.67 ± 12.34% at 20 μg/kg/min (P<0.001). Also, cardiac output increased from 3.67 ± 1.0 L/min at rest to 8.4 ± 2.6 L/min at 10 μg/kg/min (P<0.001). The same trend was observed for dP/dt_{max} which increased from 1,247 ± 382.7 at rest to 5,062 ± 1800 mmHg/s at 10 μg/kg/min (P<0.01). Entropy decreased from 55.2 ± 8% at baseline to 43.5 ± 8.5% at 5 and 43.0 ± 3.7% at 10 μg/kg/min dobutamine (P<0.01). Thickening homogeneity index showed a difference from 91.7 ± 5.53% at rest to 98.2 ± 0.75% at 20 μg/kg/min (P<0.05).

Conclusion: Dobutamine stimulation could amplify the ventricular synchrony, and the thickening-based approach is more accurate than wall displacement for assessment of mechanical dyssynchrony in GMPS. (J Nucl Cardiol 2013)

Keywords: Cardiac resynchronization therapy ▪ contraction homogeneity ▪ gated-SPECT myocardium perfusion imaging

Introduction

Left ventricular (LV) mechanical dyssynchrony has become as an important clinical parameter for optimizing the response to cardiac resynchronization therapy (CRT) in heart failure (HF) patients.[1] There are many lines of evidence that the magnitude of mechanical dyssynchrony would increase the CRT efficacy in HF patients.[1-5] Most of the studies concerning the measurements on ventricular dyssynchrony have been accomplished at rest. However, patients often suffer from the HF-related symptoms during exercise.

Echocardiography has extensively been used up to now for diagnosing the LV dyssynchrony.[6-8] During exercise echocardiography, changes in heart rate, the type of stress-induced method, the absence of standard criteria by which to identify the dyssynchrony and measurement errors because of procedural complications result in some intra- or inter-observational differences in identifying the dyssynchrony in HF patients.[9]

Currently, assessment of cardiac dyssynchrony with phase analysis of gated single-photon emission computed tomography (SPECT) myocardial perfusion imaging (GMPS)[10] has provided valuable diagnostic information on LV function and volumes incorporated with the information about myocardium viability, ischemia, and prognostic information on cardiac dyssynchrony.[11-13] Repeatability and reproducibility of phase analysis of GMPS have been shown to be excellent for measuring LV dyssynchrony.[14]

Previously, we developed and validated new segmentation software (MHI) for accurate and reproducible analysis of radionuclide-gated blood-pool SPECT (GBPS) imaging. The accuracy of volumetric estimates, as well as LV ejection fraction was yielded in comparison with the planar isotopic ventriculography and cardiac magnetic resonance imaging as a gold standard for volumetric measurements.[15] Moreover, we previously described and validated a

novel Contraction Homogeneity Index (CHI) as a single parameter for evaluating the ventricular dyssynchrony in 3D GBPS imaging.[16] We improved the MHI software to analyze under-stress mechanical dyssynchrony in GMPS that, to our knowledge, there have been no reports concerning this issue.

Accordingly, the aim of this study was to evaluate the effects of different levels of dobutamine, as a stress-induced factor, on LV synchrony of contraction with phase analyses of GMPS using our in-house software (MHI_4MPI) in comparison with already available QGS software, within a normal cohort.

Methods

General Preparation

The protocol was approved by the local Animal Ethics Committee and all procedures followed the guidelines of the Canadian Council on Animal Care. Six adult male dogs (mixed races; mean weight 36.73 ± 3 kg) underwent a general anesthesia with isoflurane 1.5% after induction with doses of 5 mg kg^{-1} ketamine/0.25 mg kg^{-1} diazepam. Venous access and arterial access were initially obtained in carotid and femoral arteries as well as the jugular and femoral veins. A Swan-Ganz catheter (931HF75, Edward Life Sciences, Mississauga, ON, Canada) was introduced in a segmental pulmonary artery in order to perform cardiac output measurements using the thermodilution method. This method was followed by bolus injections of 10 ml of sterile physiological solution cooled to 4 ºC to increase the signal stability which was monitored using a standard biomedical recording device (Eagle 4000,

Marquette Medical System, Milwaukee, WI, US). Surface ECGs were recorded using a standard three-lead configuration (Cardiac Trigger Monitor 3000, Ivy Biomedical Systems inc., Branford, CT, USA).

Additional peripheral venous access was positioned in the left leg for the dobutamine infusion. A pressure catheter (Ventri-cath 507S, 5F, straight tip, Millar) was installed in the left ventricle via the left carotid artery. Signals were conditioned (MPVS Ultra 753-2083, Millar), digitized (ITF156, Emka Technologies, Falls Church, VA, USA), and subsequently analyzed with a dedicated software (Iox2, ver. 2.5.1.6, Emka). At the end of experiments, dogs were euthanized with the administration of isoflurane 5% and then using 149 mg kg^{-1} potassium chloride which was injected into the dogs intravenously.

Dobutamine GMPS Image Acquisition and Data Processing

A standard gated SPECT myocardial perfusion scan with ^{99m}Tc-tetrofosmin (Myoview, GE Healthcare) protocol was performed using a dual-head gamma camera (e.cam; Siemens PA, USA), low-energy and high-resolution collimators, and 64 projections over a 360° arc with a 64 × 64 matrix. Myocardial perfusion gating was performed at 16 frames per R-R interval per projection. Immediately after the completion of baseline imaging with ^{99m}Tc-tetrofosmin (dose adjusted to dogs' weight), dobutamine which was prepared in 500 μg/ml in saline solution was infused at different levels of 2.5, 5, 10 and 20 μg/kg/min over, in average, 31 minutes in continuous infusion at each level. Standard gated image acquisition was acquired for each level, so that dobutamine increased to the expected level and stress image acquisition started without any rest period; that was the same over the entire experiments.

Transaxial slices were generated by 2D-OSEM (10 iterations, 8 subsets) reconstruction and a Gaussian filtering of 8.4 mm with a reconstructed pixel size of 4.8 mm. After manually reorienting images, cardiac gated short-axis images were produced with a provided camera software package (Siemens Autocardiac 8.5.10.1).

Assessment of Phase Analysis in QGS

Short-axis images were submitted to automatic segmentation QGS® 2009 software including the phase analysis plug-in (Cedars-Sinai Medical Center, Los Angeles, CA). QGS phase analysis indicates the value of myocardial wall contraction synchrony using a phase distribution histogram and several parameters calculated for this distribution throughout a cardiac cycle[17] such as phase histogram bandwidth (the width of the band with 95% of the samples over the entire LV), mean phase, SD (standard deviation) and entropy (a degree of variability in histogram phase angle). In fact, in the assessment of cardiac synchrony, the number of phase angle measurements in the histogram would identify the entropy value. If only one phase value exists in the histogram, entropy would be equal to zero and synchrony of contraction would be in the maximum level.[17] In addition, LV functional volumes and ejection fractions were obtained from this software.

Assessment of Phase Analysis in MHI_4MPI

MHI_4MPI segmentation

The MHI_4MPI segmentation software is a fully automated algorithm which assists in the diagnostic evaluation of mechanical dyssynchrony in GMPS by segmentation of the LV and

computation of phase analysis of wall contractions. The first step to performing the segmentation was identifying the basal plane with automatic tracking points throughout the systolic and diastolic frames in a cardiac cycle using intensity and gradient values. Afterward, a deformable surface iterative algorithm (3D-Snake) was applied on the static mid-myocardium surface, where external forces pushed towards maximal intensity in the image while internal forces kept the surface smooth.

The second step consists of creating endocardium and pericardium surfaces and applying a deformable dynamic surface algorithm (4D-Snake) in the gated images. In each frame, the external forces would track along the normal of each surface to find the maximum intensity for the mid-myocardium and the zero crossing of the Laplacian for the endocardium and pericardium. On top of the smoothing internal force, the three surfaces were kept close to one another and a unique basal ring was forced on all three surfaces. Finally, to insure that the movements were smooth and continuous, temporal forces were used to remove high-frequency harmonics on each vertex; Figure 1-1.

Once the myocardium wall edges were constructed, phase analyses were performed with either the thickening or the displacement methods. The always present partial volume effect leads to a greater decrease in maximum counts when the myocardium is thinner; Figure 1-2. Therefore, the intensification for each vertex on the maximal surface was used as a local thickening estimation for each frame. The software averages relative intensification in septal and lateral wall; Figure 1-3. Then, a three-harmonic Fourier analysis was used to estimate the phase (timing) and amplitude of the contraction, in both thickening and displacement methods; Figure 1-4. Indeed, the phase, measured as an angle, is the base of all dyssynchrony parameters. Subsequently, cross-correlation of the septal and lateral mean thickening signals

was used to obtain the thickening-based septal-to-lateral wall delay (TSLD) as an index of intraventricular mechanical dyssynchrony. In fact, the septum-to-lateral delay is frequently used in almost all modalities in order to predict the response to CRT.[3,18,19] We adapted the CHI, as previously introduced in our group for GBPS,[16] to quantify another thickening-based synchrony index. CHI is a transformation of the ratio between wall motion contribution in stroke volume and total wall movement. The thickening homogeneity index (THI), computed using the same equations, now represents the proportion of wall thickening that is in synchrony with the average thickening. In fact, the average efficiency is the projection along the direction of the mean phase and is negative if the vertex phase differs from the mean phase for more than a quarter of the cardiac cycle. THI, though, is measured by the average efficiency divided by average amplitude; Figure 1-4.

Also, to estimate the myocardium displacement, principle component analysis was used to find the direction of the largest possible variance for each vertex of the mid-myocardium surface. The motion was analyzed by projecting the 3D displacement along that vector with the positive direction defined as pointing outside of the mid-myocardium. With these displacement signals, we computed a displacement-based septal-to-lateral wall delay (DSLD) and displacement homogeneity index (DHI). Results were expressed with degree (°). With the same sets of data from acquisition to reconstruction, the software itself would result in reproducible outcomes.

Statistical Analysis

Statistical analysis was performed using GraphPad Prism (version 6.0; GraphPad software, San Diego, CA). The effects of dobutamine stress were investigated by repeated measures-

one way analysis of variance (ANOVA) for each phase parameter to consider any significant differences between dobutamine levels. Tukey's multiple comparison post-tests were just implemented if the *P* value of ANOVA was significant. Continuous variables are presented as the mean ± SD. A two-tailed *P*-value of < 0.05 was considered statistically significant.

Results

Baseline Assessments

Cardiac hemodynamic and thermodilution characteristics of animals including in this study were recorded for 5 dogs due to inaccessibility of Millar software, while volumes, LV ejection fraction (LVEF), and all phase analyses were measured from all six animals. The mean baseline heart rate and RR-interval during GMPS were 111.6 ± 19.0 bpm and 558 ± 87.9 ms, respectively. The mean baseline cardiac output (CO) and LVEF were 3.7 ± 1.0 L/min and 36.7 ± 8.7%, respectively; Table 1. The value of LVEF in baseline measurements was not a normal expected value at rest for the normal samples, which might be due to the deep sedation of animals.

Functional Effects in Response to Dobutamine Stress

Hemodynamic and functional effects of dobutamine stress stimulation are shown in Table 1. The mean value for RR-interval was significantly decreased with the increase of the dobutamine level in a linear trend, which reflects the shortening of the cardiac cycle during the stress stimulation ($P<0.01$). Dobutamine infusion resulted in a significant increase in LV

systolic performance. CO increased from 3.7 ± 1.0 L/min at rest to 8.4 ± 2.6 L/min at 20 μg/kg/min dobutamine level (P<0.0001). The dP/dt_{max} indicated a significant systolic contractile state between baseline and 5 and 10 μg/kg/min dobutamine levels; Table 1, Figure 1-5. A significant increase in contractility index (CI) was measured only between baseline and 5 μg/kg/min (P<0.05); Table 1, Figure 1-5. CI was defined as the dP/dt_{max} divided by the pressure at this point. It seems that there is a dose-response effect with a plateau at 10 ± 5 μg/kg/min in almost all the hemodynamic parameters.

Also, LVEF showed a significant difference with an increase of the dobutamine from baseline to 20 μg/kg/min (P<0.001). The same trend was measured for stroke volume (SV) (P<0.01). There was a significant reduction in LV end-systolic volume (LVESV) at low dose dobutamine infusion (2.5, 5 μg/kg/min) with respect to the baseline; however, LV end-diastolic volume (LVEDV) remained unchanged; Table 1.

Phase analysis in QGS via Dobutamine Infusion

Figure 1-6 illustrates the variation of phase parameters, acquired by QGS software, in response to the dobutamine infusion. As it is been shown, all the dyssynchrony parameters demonstrate a falling trend with an increase of the dobutamine level, suggesting more synchronous mechanical activation during stress. Baseline GMPS phase analysis made a mean histogram bandwidth of 93.0° ± 38.8° (range 36°-150°) and a mean phase SD of 25.7° ± 11.7° (range 9.5°-44.4°). There was a significant decrease in both histogram bandwidth and phase SD (45.0° ± 15.5° and 11.7° ± 4.6°, respectively; P<0.05) while increasing the dobutamine dose to 20 μg/kg/min. However, there was no apparent difference between baseline and other stress levels in both bandwidth and phase SD after post-tests. Analysis of mean phase revealed that,

except for dobutamine level of 2.5 μg/kg/min, there is a significant difference between the baseline and other stress levels (110.1° ± 29.6° at baseline vs 77.1° ± 22.4° at 2.5, 68.1° ± 21.5° at 5 and 54.5° ± 25.8° at 20 μg/kg/min; $P<0.001$). Furthermore, entropy has changed significantly through the infusion between the baseline and dobutamine levels of 5 and 10 μg/kg/min (55.2% ± 8% at baseline vs 43.5% ± 8.5% at 5 and 43.0% ± 3.7% at 10 μg/kg/min; $P<0.01$). Reduction of entropy in these dobutamine levels may reflect more LV contraction synchrony. The variations of all phase parameters in function of dobutamine stimulation mostly appear around the dose of 5 μg/kg/min dobutamine.

Phase Analysis in MHI_4MPI via Dobutamine Infusion

The dyssynchrony parameters acquired by MHI_4MPI, with the thickening vs displacement method, in the function of dobutamine level are shown in Figure 1-7. Mean phase angles measured by the thickening method indicated a significant difference between baseline and 10 and also 20 μg/kg/min dobutamine levels; Figure 1-7A (-78.0° ± 32.3° at baseline vs -108.0° ± 21.7° at 10 and -122.7° ± 30.5° at 20 μg/kg/min; $P<0.05$). In comparison, mean phase calculated by the displacement method did not reveal any significant difference between baseline and higher dobutamine levels (-89.7° ± 43.0° vs -129.5° ± 34.5° at 20 μg/kg/min; $P>0.05$). As it has been shown in Figure 1-7B, TSLD and DSLD also did not indicate any significant difference with variation of dobutamine levels (-5.5° ± 22.5° at baseline vs -1.0° ± 7.3° at 20 μg/kg/min, $P>0.05$; 25.3° ± 18.9° vs 45.17° ± 21.4°; $P>0.05$, respectively). THI had a slight increase through increase of dobutamine level; Figure 1-7C, (91.7% ± 5.5% at baseline vs 98.2% ± 0.75% at 20 μg/kg/min; $P=0.02$). In the case of DHI, no significant difference between the mean values of each level was seen (64.7% ± 20.3% at baseline versus

77.5% ± 14.9% at 20 μg/kg/min; *P*>0.05). Moreover, there was an excellent correlation between the mean phase calculated by MHI_4MPI and that of QGS software at each level of dobutamine; Pearson r > 0.9; Figure 1-8.

Discussion

This is the first under-stress analysis of LV mechanical dyssynchrony using phase analysis of gated SPECT MPI. This study demonstrates the influence of dobutamine stress on LV mechanical dyssynchrony and its functional characteristics. According to the entire results, the increase of dobutamine level is in accordance with improvement in LV functional capacity and reduction in dyssynchrony parameters. In fact, the considerable enhancement in cardiac functional capacity due to dobutamine infusion is because of improvement in ventricular synchrony. The evidence for this claim is a significant increase of LVEF, CO, dP/dt_{max} along with improvement in THI, and also drop-off entropy value (27.8%) with dobutamine infusion. It seems that most of the variations in parameters (Figures 1-5, 1-6) happened at low dose (5, 10 μg/kg/min) dobutamine levels and there are dose-response effects with a plateau at 10 ± 5 μg/kg/min in almost all parameters.

Cardiac dyssynchrony analysis based on wall thickening seems to be more robust and sensitive than the global wall displacement. In fact, average TSLD at baseline was close to zero (-5.5°, 1.8°, -0.1°, -1.3°, -1° for 0, 2.5, 5, 10 and 20 μg/kg/min of dobutamine respectively). In contrast, the average measurements for DSLD were completely positive (25.3°, 21.8°, 27.8°, 31°, and 45.1° for 0, 2.5, 5, 10, 20 μg/kg/min of dobutamine, respectively). Although, the positive values did not reveal a significant difference, indicated a

later contraction in the lateral wall than in the septal wall, which is more likely to happen in patients with left bundle branch block (LBBB)[17], not in our cohort. The same observation was seen for baseline DHI indicating a low magnitude for a normal cohort, which is not plausible. In contrast, baseline THI was around 90% and there was a slight improvement with response to the dobutamine stress level. Also, thickening-based mean phase in MHI_4MPI showed an excellent correlation with that of QGS software for LV dyssynchrony analysis in each dobutamine level.

The preference of the thickening method was also observed by other groups in perfusion and functional assessments of coronary artery bypass surgery patients using gated SPECT.[20,21] In the presence of normal septal thickening, wall motion analysis was shown as an underestimation of septal and overestimation of lateral motions which appear typically in post-cardiac surgery patients. The authors recommended the thickening as it is more accurate for evaluation of pseudo-paradoxical motion in these patients. Van Kriekinge et al. investigated the global and regional phase analysis of GMPS in normal and LBBB patients with QGS software.[17] They found an average timing difference around zero for both global and regional septal and lateral wall contractions in normal patients (-1.1° and -1.7° for wall- and segmental-based calculations, respectively). Their results are comparable with ours for TSLD which is close to zero.

The effects of different kinds of stress-induced factors on ventricular dyssynchrony have had contradictory results. Some studies have mentioned that mechanical dyssynchrony did not change during cardiac stimulation using stressors like exercise or pharmacological agonists.[22-24] Lafitte et al. assessed the effects of exercise on ventricular dyssynchrony in patients with normal and depressed LV function.[22] They mentioned that dyssynchrony

parameters did not significantly differ between rest and exercise in normal subjects. However, exercise could modify the extent of dyssynchrony parameters (20%-26%) as reflected by its shortening or reverse. However, Chattopadhyay et al. studied the effects of dobutamine on intraventricular dyssynchrony in patients with LV systolic dysfunction vs control subjects.[25] They found that dobutamine shortened the intraventricular delay in all the segments of LV in healthy subjects on stress echocardiography. A comparison with our results remains difficult due to major differences in methodology used. Kasama et al. demonstrated that dobutamine in ^{99m}Tc gated SPECT could predict improvement of cardiac function in patients with dilated cardiomyopathy.[26] The authors mentioned that the exact mechanism responsible for the improvement in systolic function during dobutamine infusion is unclear. However, as mentioned before, in our point of view, a desirable cardiac performance during the administration of dobutamine stress is due to the improvement in ventricular synchrony.

As a matter of fact, the value of LVEF at baseline measurements in our study was not a normal expected value at rest for the normal samples. Several reasons could result in acquiring underestimated LVEF in the present study. The precision of LVEF measurements for animals is unknown in QGS software. Also, the software cannot rely on the accuracy of count-based LVEF in myocardial perfusion imaging. However, it might be the result of the deep sedation of the animals through the entire experiments. Even so, improvement in EF after dobutamine stress injection was definitely apparent.

The results of phase analyses have been expressed using degree (°) instead of millisecond in this study as we believe that using the absolute value of a parameter for describing a cyclic mechanical behavior is not accurate specifically to compare normal ranges between species or for comparing results from the same subject with significantly different

HRs (rest vs stress). Also, the use of degrees should give heart rate independent accuracy; since the acquisition is adjusted automatically to have exactly 16 time measurements every 360°. Moreover, the sign of the delay gives the ability to define which wall (septum or lateral) contracts first.

Above all, we found that inter-animal variation of phase parameters decreased with the increase of dobutamine concentration. Although this kind of variability seems to be normal at baseline due to the individual mechanical and electrical characteristics,[27,28] dobutamine is able to eliminate it by synchronizing the septum and lateral wall at the time of contraction. In general, the results of this study confirm that the levels of cardiac activity could change the cardiac contraction synchrony and take these changes into account would be essential in the CRT optimization process, in particular, in the stress condition.

Limitations

There are several limitations in our study. One of the major limitations is that the number of animals was limited in this study as it is always a restriction in animal experiments. Therefore, MHI_4MPI requires more validation due to this problem. In addition, Laplacian edge detection does not permit the exact measurement of wall thickness in the cardiac structure. However, it could help us correctly position a coherent mid-myocardial wall. Also, GMPS is not ideal for acquiring the accurate volume and LVEF. Phase analysis measurement in high dobutamine levels was difficult since ventricles had completely collapsed. Moreover, the gating process in HF patients with irregular heart rhythm (e.g., atrial fibrillation) would be complicated and it is hard to get good image quality of the average heart beat in these patients. Besides the normal cohorts, further analysis within the HF animal model is needed to compare

the dyssynchrony results, which is already on hand. Finally, analysis of dyssynchrony parameters before and after resynchronization therapy would be interesting to see the efficiency of predictors on CRT response.

New knowledge gained

The increase of dobutamine level is in accordance with the improvement of LV functional capacity and reduction of dyssynchrony parameters. Cardiac dyssynchrony analysis based on wall thickening seems to be more robust and sensitive than the global wall displacement.

Conclusion

As phase analyses of GMPS indicated, dobutamine significantly increases the LV synchrony of contraction in normal cohorts. The proposed MHI_4MPI software with useful indexes using the thickening- and displacement-based methodologies could indicate the mechanical synchrony alterations. Evaluation of thickening- and displacement-based results demonstrates the reliability and sensitivity of thickening-based over the displacement-based method for identifying the mechanical dyssynchrony.

Disclosures

This work was supported by a grant from the: *Fonds de Recherche en Santé du Québec*.

References

(1) Henneman MM, Chen J, Dibbets-Schneider P, Stokkel MP, Bleeker GB, Ypenburg C et al. Can LV dyssynchrony as assessed with phase analysis on gated myocardial perfusion SPECT predict response to CRT? J Nucl Med 2007;48:1104-11.

(2) Boogers MM, Van Kriekinge SD, Henneman MM, Ypenburg C, Van Bommel RJ, Boersma E et al. Quantitative gated SPECT-derived phase analysis on gated myocardial perfusion SPECT detects left ventricular dyssynchrony and predicts response to cardiac resynchronization therapy. J Nucl Med 2009;50:718-25.

(3) van Bommel RJ, Bax JJ, Abraham WT, Chung ES, Pires LA, Tavazzi L et al. Characteristics of heart failure patients associated with good and poor response to cardiac resynchronization therapy: a PROSPECT (Predictors of Response to CRT) sub-analysis. Eur Heart J 2009;30:2470-7.

(4) White JA, Yee R, Yuan X, Krahn A, Skanes A, Parker M et al. Delayed enhancement magnetic resonance imaging predicts response to cardiac resynchronization therapy in patients with intraventricular dyssynchrony. J Am Coll Cardiol 2006;48:1953-60.

(5) Dauphin R, Nonin E, Bontemps L, Vincent M, Pinel A, Bonijoly S et al. Quantification of ventricular resynchronization reserve by radionuclide phase analysis in heart failure patients: a prospective long-term study. Circ Cardiovasc imaging 2011;4:114-21.

(6) Yu CM, Bax JJ, Gorcsan J, 3rd. Critical appraisal of methods to assess mechanical dyssynchrony. Curr Opin Cardiol 2009;24:18-28.

(7) Abraham T, Kass D, Tonti G, Tomassoni GF, Abraham WT, Bax JJ et al. Imaging cardiac resynchronization therapy. JACC Cardiovasc Imaging 2009;2:486-97.

(8) Oyenuga OA, Onishi T, Gorcsan J, 3rd. A practical approach to imaging dyssynchrony for cardiac resynchronization therapy. Heart Fail Rev 2011;16:397-410.

(9) Chung ES, Leon AR, Tavazzi L, Sun J-P, Nihoyannopoulos P, Merlino J et al. Results of the Predictors of Response to CRT (PROSPECT) trial. Circulation 2008;117:2608-16.

(10) Chen J, Garcia EV, Folks RD, Cooke CD, Faber TL, Tauxe EL et al. Onset of left ventricular mechanical contraction as determined by phase analysis of ECG-gated myocardial perfusion SPECT imaging: development of a diagnostic tool for assessment of cardiac mechanical dyssynchrony. J Nucl Cardiol 2005;12:687-95.

(11) Boogers MM, Chen J, Bax JJ. Myocardial perfusion single photon emission computed tomography for the assessment of mechanical dyssynchrony. Curr Opin Cardiol 2008;23:431-9.

(12) Trimble MA, Borges-Neto S, Velazquez EJ, Chen J, Shaw LK, Pagnanelli R et al. Emerging role of myocardial perfusion imaging to evaluate patients for cardiac resynchronization therapy. Am J Cardiol 2008;102:211-7.

(13) Chen J, Henneman MM, Trimble MA, Bax JJ, Borges-Neto S, Iskandrian AE et al. Assessment of left ventricular mechanical dyssynchrony by phase analysis of ECG-gated SPECT myocardial perfusion imaging. J Nucl Cardiol 2008;15:127-36.

(14) Trimble MA, Velazquez EJ, Adams GL, Honeycutt EF, Pagnanelli RA, Barnhart HX et al. Repeatability and reproducibility of phase analysis of gated single-photon emission computed tomography myocardial perfusion imaging used to quantify cardiac dyssynchrony. Nucl Med Commun 2008;29:374.

(15) Harel F, Finnerty V, Gregoire J, Thibault B, Marcotte F, Ugolini P et al. Gated blood-pool SPECT versus cardiac magnetic resonance imaging for the assessment of left ventricular volumes and ejection fraction. J Nucl Cardiol 2010;17:427-34.

(16) Harel F, Finnerty V, Grégoire J, Thibault B, Khairy P. Comparison of left ventricular contraction homogeneity index using SPECT gated blood pool imaging and planar phase analysis. J Nucl Cardiol 2008;15:80-5.

(17) Van Kriekinge SD, Nishina H, Ohba M, Berman DS, Germano G. Automatic global and regional phase analysis from gated myocardial perfusion SPECT imaging: application to the characterization of ventricular contraction in patients with left bundle branch block. J Nucl Med 2008;49:1790-7.

(18) Buck S, Maass AH, Nieuwland W, Anthonio RL, Van Veldhuisen DJ, Van Gelder IC. Impact of interventricular lead distance and the decrease in septal-to-lateral delay on response to cardiac resynchronization therapy. Europace 2008;10:1313-9.

(19) Andersson L, Wu K, Wieslander B, Loring Z, Frank T, Maynard C et al. Left ventricular mechanical dyssynchrony by cardiac magnetic resonance is greater in patients with strict vs. conventional ECG criteria for left bundle branch block. J Cardiovasc Magn Reson 2013;15:P152.

(20) Giubbini R, Rossini P, Bertagna F, Bosio G, Paghera B, Pizzocaro C et al. Value of gated SPECT in the analysis of regional wall motion of the interventricular septum after coronary artery bypass grafting. Eur J Nucl Med Mol Imaging 2004;31:1371-7.

(21) Nakajima K, Tamaki N, Kuwabara Y, Kawano M, Matsunari I, Taki J et al. Prediction of functional recovery after revascularization using quantitative gated myocardial

perfusion SPECT: a multi-center cohort study in Japan. Eur J Nucl Med Mol Imaging 2008;35:2038-48.

(22) Lafitte S, Bordachar P, Lafitte M, Garrigue S, Reuter S, Reant P et al. Dynamic Ventricular DyssynchronyAn Exercise-Echocardiography Study. J Am Coll Cardiol 2006;47:2253-9.

(23) Kurita T, Onishi K, Dohi K, Tanabe M, Fujimoto N, Tanigawa T et al. Impact of heart rate on mechanical dyssynchrony and left ventricular contractility in patients with heart failure and normal QRS duration. Eur J Heart Fail 2007;9:637-43.

(24) Da Costa A, Thévenin J, Roche F, Faure E, Roméyer-Bouchard C, Messier M et al. Prospective validation of stress echocardiography as an identifier of cardiac resynchronization therapy responders. Heart Rhythm 2006;3:406-13.

(25) Chattopadhyay S, Alamgir MF, Nikitin NP, Fraser AG, Clark AL, Cleland JG. The effect of pharmacological stress on intraventricular dyssynchrony in left ventricular systolic dysfunction. Eur J Heart Fail 2008;10:412-20.

(26) Kasama S, Toyama T, Kumakura H, Takayama Y, Ichikawa S, Tange S et al. Dobutamine stress 99mTc-tetrofosmin quantitative gated SPECT predicts improvement of cardiac function after carvedilol treatment in patients with dilated cardiomyopathy. J Nucl Med 2004;45:1878-84.

(27) Harel F, Finnerty V, Gregoire J, Salimian S, Thibault B. Effects of dobutamine stress on cardiac contraction synchronism in a canine model. Physiol Meas 2013;34:1387-97.

(28) Golovchiner G, Dorian P, Mangat I, Korley V, Ahmad K, Sharef K et al. Electrogram-based optimal atrioventricular and interventricular delays of cardiac resynchronization change individually during exercise. Can J Cardiol 2011;27:351-7.

Figures

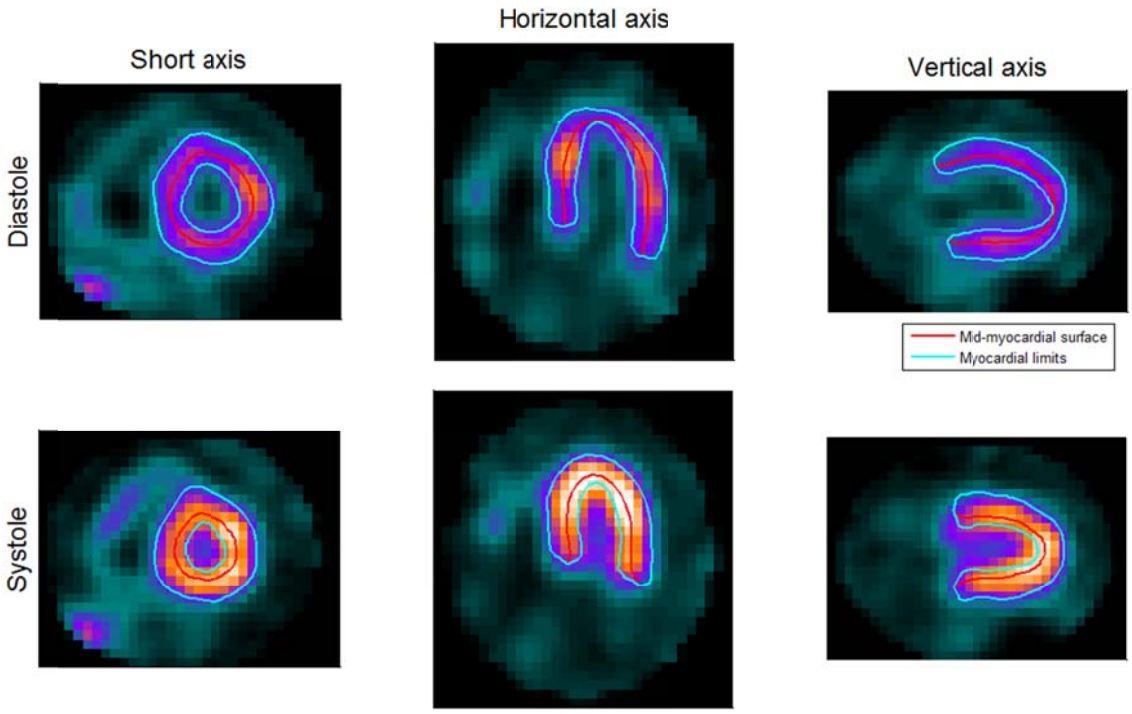

Figure 1-1: An example of the segmentation process by MHI4MPI algorithm during systole and diastole at different axes

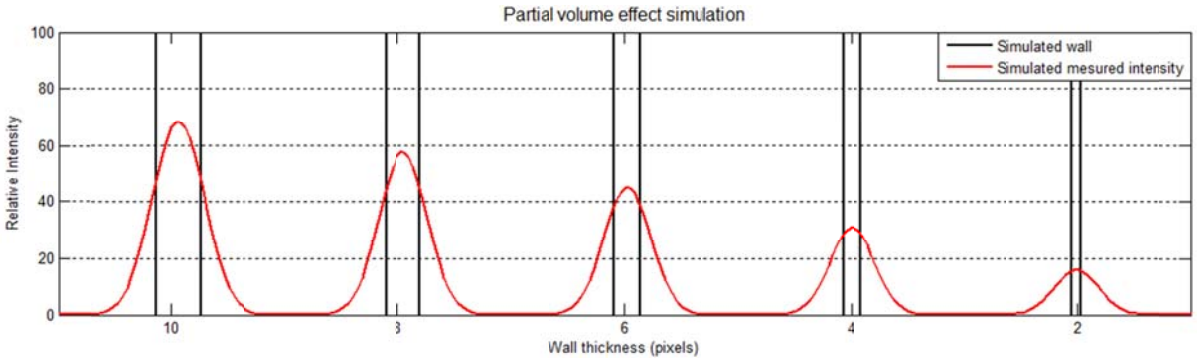

Figure 1-2: The simulation of partial volume effect that leads to a greater decrease in maximum counts (relative intensity) when the myocardium is thinner.

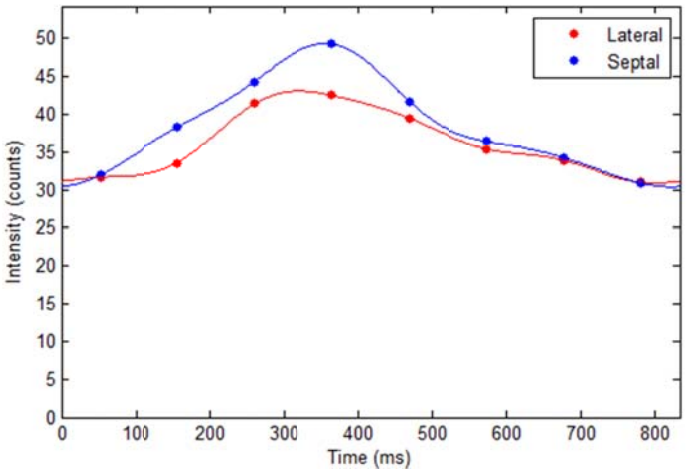

Figure 1-3: Intensification of mid-myocardial septal and lateral wall through time

.

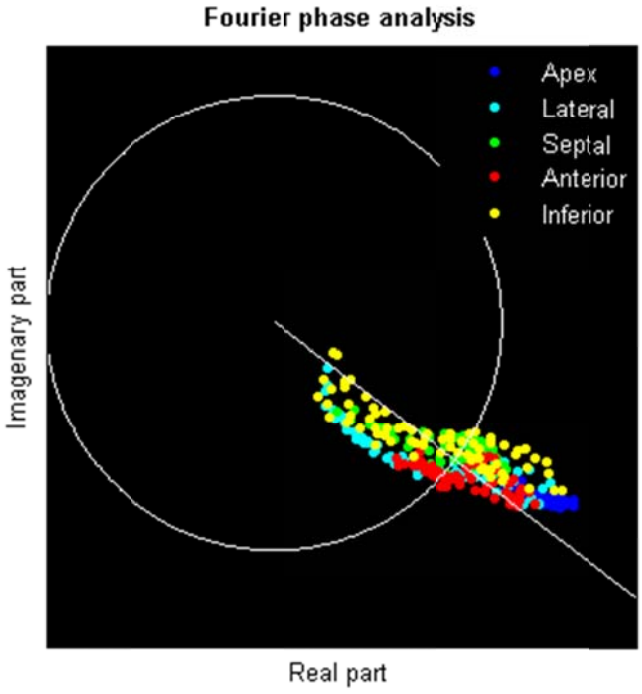

Figure 1-4: Fourier phase analyses of thickening signals. Each point is an actual vertex on the surface. The average amplitude is presented by the circle and the average phase direction is represented by the line. The average efficiency is the projection along the direction of the mean phase and is negative if the vertex phase differs from the mean phase for more than a

quarter of the cardiac cycle. THI is measured by the average efficiency divided by average amplitude.

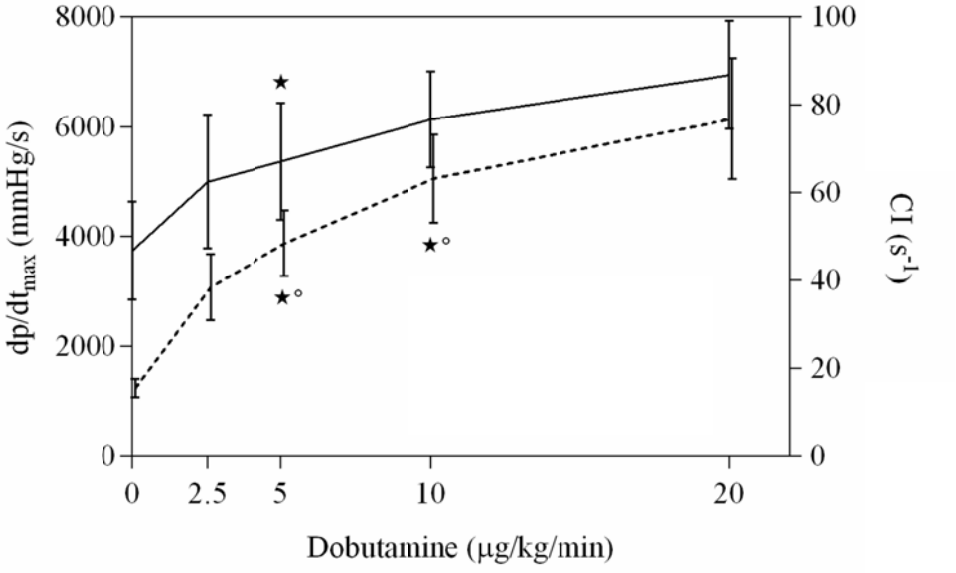

Figure 1-5: Hemodynamic effects of dobutamine stress variations of dP/dt_{max} in (mmHg/s) and contractility index (CI) in (s^{-1}) in response to the dobutamine stress stimulation. Dash line is related to dP/dt_{max} variations and solid line shows the CI variations; asterisks = $P \leq 0.05$ vs baseline, open circles = $P \leq 0.05$ vs 2.5 μg/kg/min.

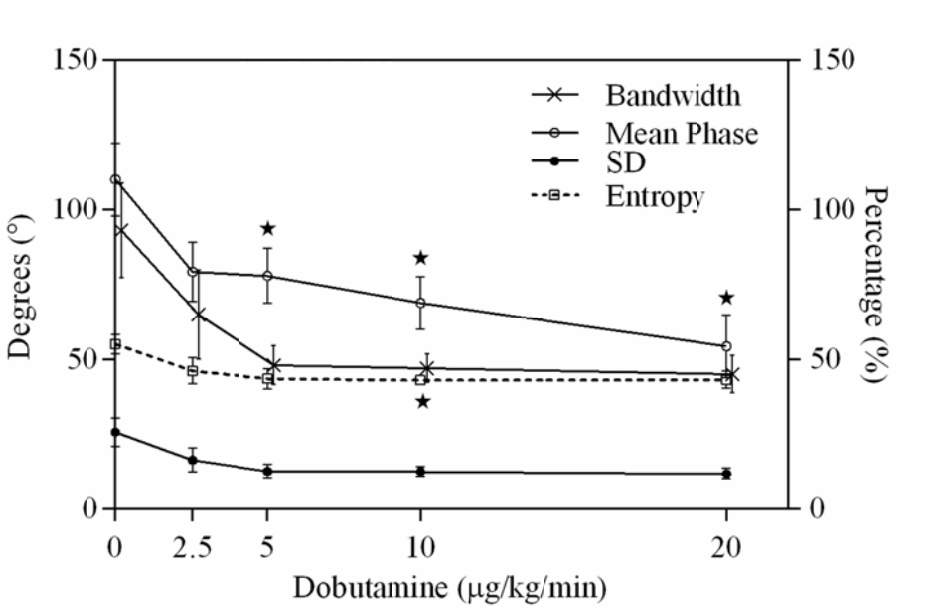

Figure 1-6: Variation of dyssynchrony parameters related to increasing the dobutamine stress level measured by QGS, (bandwidth, mean phase, and SD in degree and entropy in %). Asterisks = $P \leq 0.05$ vs baseline.

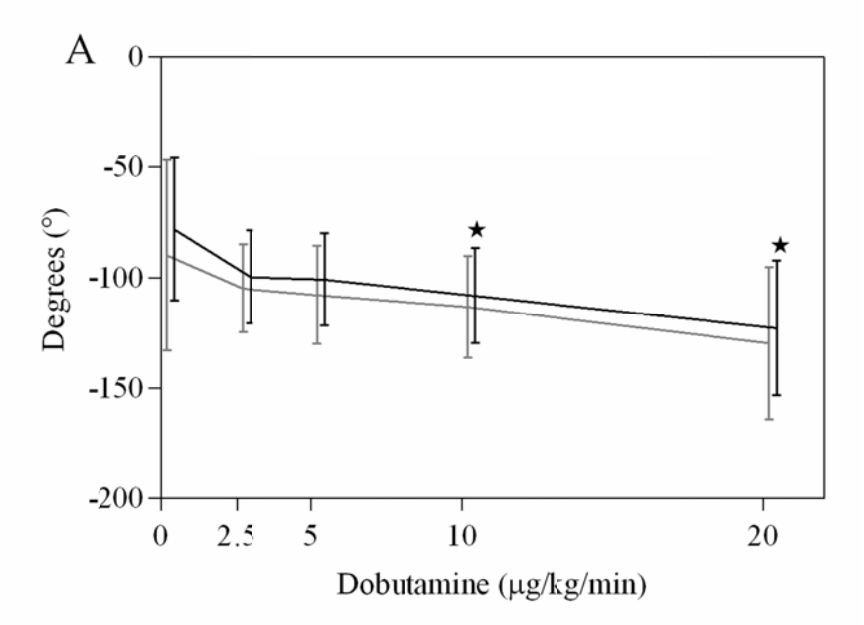

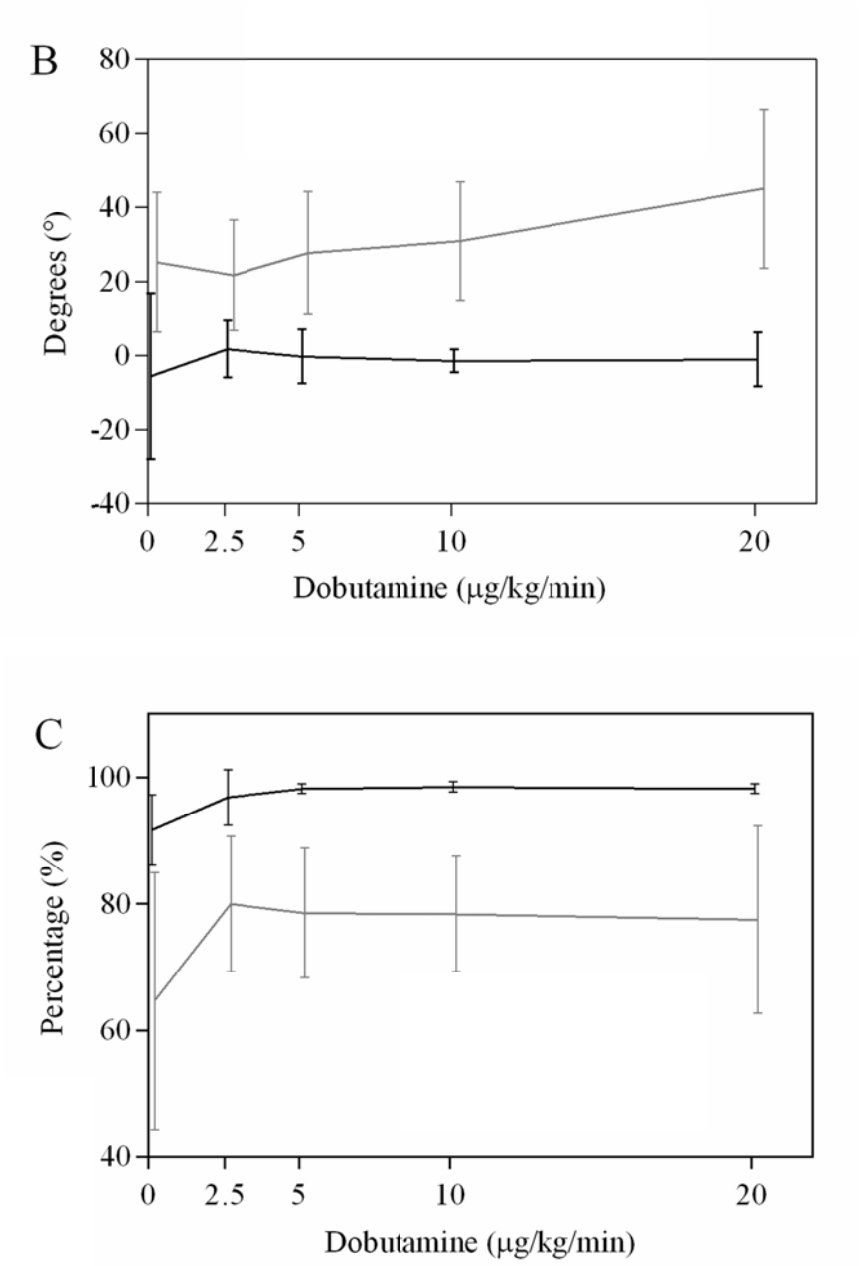

Figure 1-7: Comparison between the thickening- and displacement-based methods for dyssynchrony parameters acquired with MHI4MPI in response to dobutamine stress level increasing. (A) Mean phase (in degree), (B) septal-to-lateral delay (in degree), (C) homogeneity index (in %). Grey lines are measurements for a displacement-based method and black lines are that of the thickening-based method; Asterisks = $P \leq 0.05$ vs baseline.

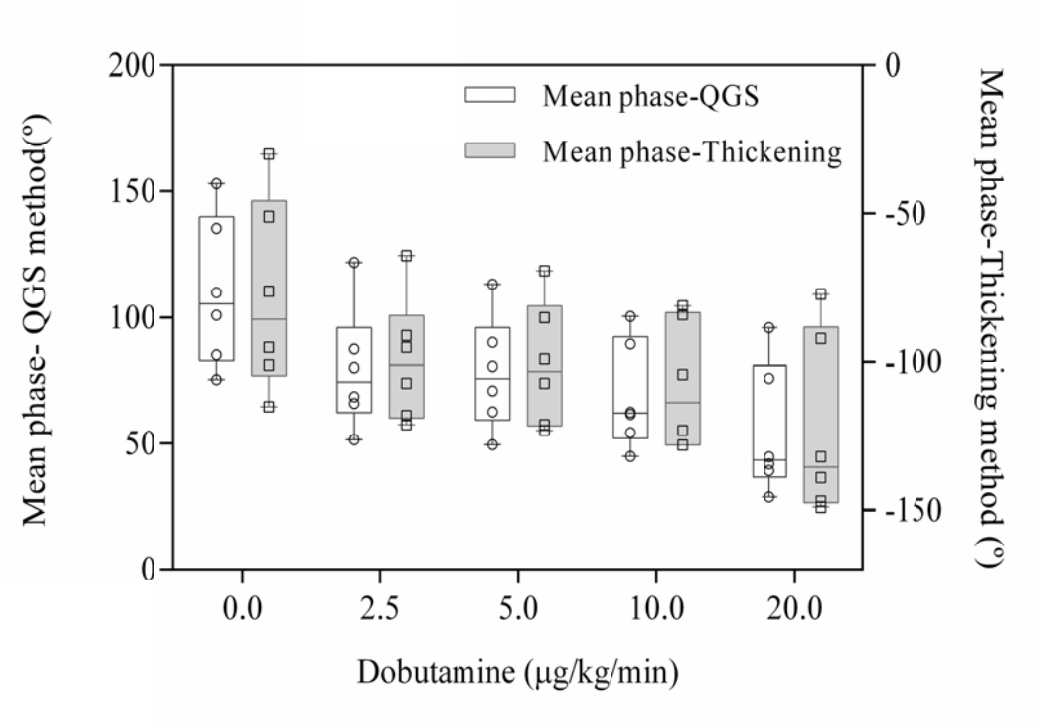

Figure 1-8: Graphical illustration of the distribution of the mean phase measured by each of the QGS and thickening method. For each dobutamine level, the median and spread of the phase value are indicated by a box plot. The line in the box marks the median and the whiskers indicate the range of observations with 5th-95th percentile. Pearson's correlations in each dobutamine level: $r > 0.9$

Tables

Table 1-1: LV functional parameters during rest and levels of dobutamine stress

Index	Dobutamine (µg/kg/min)				
	0	2.5	5	10	20
LVEDV (mL)	54.7±11.5	47.8±9.8	48.7±9.4	49.7±9.6	53.0±8.3
LVESV (mL)	34.8±9.7	24.3±6.7*	24.0±5.3*	25.2±5.6	24.2±5.8
LVEF (%)	36.7±8.7	49.0±10.5*	50.8±9.3*	49.0±10.9*	53.7±12.3*
SV (mL)	19.8±5.3	23.5±7.7	24.7±7.5	24.5±8.7	28.8±9.1*
HR (bpm)	111.6±19.1	152.4±51.9	232.6±88.6	248.4±149.6	254.0±153.6
QRS width (ms)	43.8±3.7	46.4±4.7	47.8±3.7	47.2±6.3	47.0±6.0
R-R (ms)	558.0±87.2	452.2±78.4	380.6±90.3*	347.0±127.9*	335.6±136.8 *
Pmax (mmHg)	74.4±8.8	104.3±16.1*	113.8±12.3*	131.7±18.7*	161.2±45.2*
dP/dt_{max} (mmHg/s)	1247±382	3075±1340	3875±1342*#	5062±1800*#	6155±2465
CI (s^{-1})	46.9±25.0	62.5±34.2	67.2±29.8*	76.8±24.5	86.9±27.4
CO (L/min)	3.7±1.0	5.4±1.9	6.6±2.2*	7.5±2.0*#ǂ	8.4±2.6*#ǂ

n=5 for all except LVEDV, LVESV, SV and LVEF (n=6). Data are presented as mean ± SD. *=$P \leq 0.05$ vs baseline; #=$P \leq 0.05$ vs 2.5; ǂ=$P \leq 0.05$ vs 5 µg/kg/min (RM ANOVA, Tukey's). LVEDV, left ventricular end-diastolic volume; LVESV, left ventricular end-systolic volume; LVEF, left ventricular ejection fraction; SV, stroke volume; HR, heart rate, R-R, time between R-R interval; P_{max}, maximum pressure of left ventricle; dP/dt_{max}, maximum rate of left ventricular pressure change; CI, contractility index; CO, cardiac output.

Chapter 2

Phase analysis of gated blood pool SPECT for multiple stress testing assessments of ventricular mechanical dyssynchrony in a tachycardia-induced dilated cardiomyopathy canine model

Samaneh Salimian, MSc,[a] Bernard Thibault, MD,[b] Vincent Finnerty,[a] MSc, Jean Grégoire, MD,[a] and François Harel, MD, PhD[a]

[a]Department of Nuclear Medicine, Montreal Heart Institute, and Université de Montréal, Montreal, QC, Canada

[b]Department of Medicine, Montreal Heart Institute, and Université de Montréal, Montreal, QC, Canada

Received Jun 12, 2015; accepted Nov 6, 2015; published online: 18 Dec 2015

doi:10.1007/s12350-015-0338-6

J Nucl Cardiol. *in press*

Abstract

Background: Stress-induced dyssynchrony has been shown to be independently correlated with clinical outcomes in patients with dilated cardiomyopathy (DCM) and narrow QRS complexes. However, the extent to which stress levels affect inter- and intraventricular dyssynchrony parameters remains unknown.

Methods: Ten large dogs were submitted to tachycardia-induced DCM by pacing the right ventricular apex for 3-4 weeks to reach a target ejection fraction (EF) of 35% or less. Stress was then induced in DCM dogs by administering intravenous dobutamine up to a maximum of 20 μg/kg/min. Hemodynamic and ventricular dyssynchrony data were analyzed by left ventricular (LV) pressure measurements and gated-blood pool SPECT (GBPS) imaging. In order to assess mechanical dyssynchrony in DCM subjects and compare it with that of 8 normal counterparts, we extracted the following data: count-based indices of LV contraction homogeneity index (CHI), entropy and phase standard deviation (SD), and interventricular dyssynchrony index.

Results: A significant LV intraventricular dyssynchrony (CHI: 96.4% ± 1.3% in control *vs* 78.6% ± 10.9% in DCM subjects) resulted in an intense LV dysfunction in DCM subjects (EF: 49.5% ± 8.4% in control *vs* 22.6% ± 6.0% in DCM), compared to control subjects. However, interventricular dyssynchrony did not vary significantly between the two groups. Under stress, DCM subjects showed a significant improvement in ventricular functional parameters at each level (EF: 22.6% ± 6.0% at rest *vs* 48.1% ± 5.8% at maximum stress). All intraventricular dyssynchrony indices showed a significant increase in the magnitude of synchrony from baseline to stress levels of greater than or equal to 5 μg/kg/min dobutamine. There were individual

differences in the magnitude and pattern of change in interventricular dyssynchrony during the various levels of stress.

Conclusions: Based on GBPS analyses, different levels of functional stress, even in close intervals, can have a significant impact on hemodynamic and intraventricular dyssynchrony parameters in a DCM model with narrow QRS complex. (J Nucl Cardiol 2015)

Keywords: Ventricular dyssynchrony **.** gated blood pool SPECT **.** dobutamine stress **.** dilated cardiomyopathy with narrow QRS.

Introduction

Ventricular mechanical dyssynchrony, defined as a timing disparity in ventricular regional contraction, seems to be present in almost all chronic heart failure (HF) patients.[1] Wall motion discoordination is not exclusively caused by electrical conduction delays; regional heterogeneity in myocardial contractility properties can also modify the synchronicity of contraction.[1, 2] The presence of mechanical dyssynchrony with preserved electrical conduction is apparent in a substantial proportion of patients with dilated cardiomyopathy (DCM) and narrow QRS complexes.[3]

Exercise-induced intraventricular dyssynchrony has been independently correlated with clinical outcomes (combined endpoint of death, heart transplant, or assist device implantation) in patients with idiopathic DCM and narrow QRS complexes.[4] However, few studies[4-7] have investigated the effect of stress on mechanical dyssynchrony in such patients and none have examined the range of difference in inter- and intraventricular dyssynchrony parameters when the patients are submitted to various levels of stress. Moreover, the quantification of stress dyssynchrony in those studies has been performed by different echocardiography-based methods. However, an intrinsic property of these methods lies in their limited reproducibility, since they are largely subject-dependent, both in the case of image acquisition and analysis.[8] Also, there is no standardized methodology with accurate and robust parameters for detecting mechanical dyssynchrony using echocardiographic imaging tools.[9]

In comparison with echocardiographic methods, phase analysis of nuclear cardiology modalities such as gated single-photon emission computed tomography (SPECT) myocardial perfusion imaging (GMPS)[10] and gated blood-pool SPECT (GBPS)[11] have shown a high reproducibility to effectively assess cardiac mechanical dyssynchrony. While both methods have

shown a clear applicability in this field, GBPS has been preferred in some cases since it is based on volume rather than myocardial wall thickness. In addition, it can provide both inter- and intraventricular dyssynchrony data.

Consequently, we used GBPS in our study to investigate the effects of various levels of dobutamine-induced stress on inter- and intraventricular dyssynchrony parameters in an animal model of tachycardia-induced DCM, a well-characterized model of non-ischemic cardiomyopathy in terms of left ventricular (LV) dilation and systolic dysfunction.[12] This study follows our previous work performed on a control cohort.[13]

Methods

Study Protocol

Ten large dogs of either gender (mixed races with mean weight of 40.2±4.5kg) were submitted to tachycardia-induced HF by pacing the right ventricular apex at 240 bpm for 3-4 weeks until the LV ejection fraction (EF) fell below 35%; we selected a moderate to severely reduced EF to assess variations toward upper or lower EF categories. Experiments were initiated within 48hr of achieving the target LVEF. The protocol was approved by the institutional Research Ethics Board and all procedures followed the Canadian Council on Animal Care.

The animals underwent general anesthesia with isoflurane 1.5% after induction with doses of 5 mg/kg ketamine and 0.25 mg/kg diazepam. SaO_2 was monitored using a standard biomedical cardiac monitor (Eagle 4000, Marquette Medical System, Milwaukee, WI, USA). The dogs' bladders were catheterized in order to prevent radioactive urine spills. Venous and arterial accesses were obtained in carotid and femoral arteries as well as jugular and femoral

veins. Those vascular accesses were used to install the following devices. First, a Swan-Ganz catheter (931HF75, Edward Life Sciences, Mississauga, ON, Canada) was introduced in a segmental pulmonary artery to measure the cardiac output using a thermodilution method.[14] This was followed by bolus injections of 10 mL of sterile saline cooled at 4°C to increase the signal stability. We used the cardiac monitor to measure cardiac outputs. Second, a pressure catheter was introduced into the right femoral artery in order to acquire systemic arterial pressure signals. Signals were conditioned by a dedicated control unit and acquired by a signal acquisition system. Dobutamine was infused using the venous access in the left leg. Another pressure catheter (Ventricath 507S, 5F, straight tip, Millar, Houston, TX, USA) was installed in the LV via the left carotid artery access. Signals were conditioned (MPVS Ultra 753-2083, Millar), digitized (ITF156, Emka Technologies, Falls Church, VA, USA), and subsequently analyzed with a dedicated software (Iox2, ver. 2.5.1.6, Emka). It has to be mentioned that hemodynamic results were recorded for eight dogs out of ten because the Millar system was unavailable. Surface ECGs were recorded using a standard 3-lead configuration (Cardiac Trigger Monitor 3000, Ivy Biomedical Systems Inc., Branford, CT, USA).

The GBPS and surface ECGs were acquired at baseline and for each dobutamine-induced stress level of 2.5, 5, 10 and 20 μg/kg/min. The acquisition of GBPS was performed after red blood cell labeling using the UltraTag®-^{99m}Tc kit. A single dose of radiopharmaceutical of 1223 MBq in average was injected to animals and baseline images were acquired. Cardiac stress was induced by a dobutamine infusion prepared in 500 μg/mL of normal saline solution and continuously infused over average times of 43.5, 28.4, 36.4 and 34.8 min while increasing the outflow to reach the predetermined dosage (Figure 2-1). Because of dobutamine's short half-life of approximately 2.3 min, we used the continuous infusion to create a stable dobutamine stress effect for acquiring the SPECT images. On average, the total infusion duration was 143.0 min,

during which a total volume of 415 mL was infused. Immediately after reaching a target dobutamine concentration level, image acquisition was initiated. There were no rest periods during the entire experiment. Cardiac and peripheral hemodynamic data, as well as cardiac contraction synchrony data (using GBPS) were recorded at each stress level. The duration of GBPS acquisition was adjusted throughout the day to reach equal count statistics in spite of ^{99m}Tc decay time; average times of 10.8, 13.4, 14.3 and 14.8 min, respectively, were used for each dobutamine-induced stress level. Overall, the dobutamine-induced stress effect lasted approximately 208.1 min, with the heart rate continuously increasing at each level. Because of humane considerations, we euthanized the dogs at the end of the experiment with the administration of isoflurane 5% and an intravenous overdose of potassium chloride.

GBPS Acquisition and Reconstruction

Data were acquired on a dual head gamma camera with low-energy high-resolution collimators and 64 projections dispatched on a 360˚ configuration using 64×64 matrix. Data acquisition involved 16 frames per cardiac cycle. Transaxial reconstructions were performed with the ramp filtered back projection and subsequently filtered by 8mm Gaussian filter.

GBPS Data Processing and Dyssynchrony Analysis

Images were manually reoriented into LV short axis sections (Figure 2-2). Segmentation was performed using an algorithm based on the invariance of the Laplacian previously developed by our group to deliver a dynamic surface of approximately 400 vertices.[15] In summary, simple geometric assumptions were made to separate LV from RV and atria. Two smoothed isosurfaces (LV and RV) were then determined inside both ventricular regions (LV left of the RV, both

below the atria). The GBPS images were filtered with a variable cutoff frequency, and Laplacian was computed for each data set. Profiles were extracted from each Laplacian image by sampling along 400 vectors perpendicular to each of the ventricular isosurfaces (LV and RV). These profiles were used to find a pivotal point, where values were the least variable between filtered data sets. Since this position was resolution-independent, it represented a true edge estimation. This surface was then replaced by 3D self-organizing maps (LV and RV) using standard surfaces to get regular sampling over the ventricles. Again 400 profiles normal to these surfaces were analyzed to determine the invariance of the Laplacian for each bin of all 16 temporal bins (Figure 2-3). Lastly, post-processing was executed on the surfaces to ensure spatial and temporal continuity. After the segmentation, dynamic regions of interest (ROIs) were estimated over both ventricles. The LV ROI was defined as the pixels totally or partially inside the LV plus all pixels under the valvular plane and within 8mm (2 pixels) of the LV, but all pixels closer to the RV than the LV were excluded (Figure 2-4). The same approach was applied to define the RV ROI. Time-activity curves (TACs) for the LV and RV were generated using these ROIs (Figure 2-4). Count-based LVEF and RVEF were measured directly using the TACs. However, in order to measure the stroke volume (SV) in mL, we had to estimate count-based volumes by adjusting the TACs (dividing by the average TAC and multiplying by the average geometric volume, a method previously shown to be well correlated with magnetic resonance imaging volumetric results[16]).

A three-harmonic inter-correlation of the RV and LV TACs was used to compute the phase differences between RV and LV (count-based RVLV delay). These results were expressed in degrees and converted to milliseconds to accommodate readers from different specialties (echocardiography, electrocardiography, etc.). It has to be noted that any comparison between RVLV delays measured by GBPS and with other modalities will not be accurate since the methods for acquiring RVLV delays using various modalities are totally different.

In addition, we extracted TACs for different regions of the LV from the LV ROI. First, the basal slices (where the surface's normal angle to basal direction was less than 45°) were discarded. Then, apical slices were extracted to evaluate the apical TAC separately. The pixels from remaining median slices were split into four regions (anterior, lateral, inferior and septal) using their angular position in the short axis slice around the LV center (Figure 2-5). We first estimated Fourier harmonics of each regional TAC to obtain the phase and amplitude of each LV region. In order to compute the LV intraventricular dyssynchrony parameters, a static ROI was used containing the voxels where the LV dynamic ROI was present at least in half of the temporal frames. Three-harmonics Fourier analysis of all voxel TACs and subsequent count-based amplitudes (A) and phases (θ) were acquired within this ROI. In addition to the phase and amplitude, efficiency (E) of contraction of each voxel was also determined, namely, the portion of amplitude in phase with the remainder of the ventricle.[17] In other words, E represents the portion of amplitude in the direction of the mean phase. Thus, E could be calculated as complex harmonic of each voxel TAC ($Ae^{i\theta}$) divided by the mean phase ($\bar{\theta}$), which is the mean angle of all complex harmonics, as following:

$$E = \frac{A_1 e^{i\theta_1}}{e^{i\bar{\theta}}} \qquad \bar{\theta} = \angle\overline{Ae^{i\theta}} \tag{2-1}$$

Based on the above equation, E is actually the projection along the direction of the mean phase in the Fourier space. It would be negative if the voxel phase differed from the mean phase for more than a quarter of the cardiac cycle. In fact, the E index was used to calculate a global contraction homogeneity index (CHI)[17] which was defined as the mean E divided by the mean A. In our point of view, CHI could be interpreted as the proportion of wall movement (endocardial-blood interface movement) that contributes to the stroke volume.

In addition to CHI, phase standard deviation (phase SD) and entropy of the phase histogram were extracted within the LV static ROI. These dyssynchrony parameters have been previously evaluated in planar and radionuclide ventriculography phase analysis.[11, 18, 19] Entropy is a degree of randomness of the phase distribution within the ROI. In the case of reduced contraction homogeneity, entropy is able to identify the degree of random and uncoordinated contraction by computing the probability of occurrence of phase angle i (P_i) in a given number of bins (M) of a phase histogram as following:

$$\text{Entropy} = -\frac{\sum_{i=1}^{M} P_i \log_2(P_i)}{\log_2(M)} \qquad (2\text{-}2)$$

We used the same equation and method proposed by O'Connell *et al*. to measure the entropy values.[18] It ranges from 0 with complete order and 1 with complete disorder.

Statistical Analysis

Statistical analysis was performed using GraphPad Prism version 6.00 for Windows (GraphPad Software, La Jolla, California, USA). The D'Agostino-Pearson test was used to confirm that the distribution of the hemodynamic. as well as dyssynchrony variables were not significantly different from a normal distribution at different dobutamine levels.

Comparisons between rest and dobutamine-induced stress levels for functional and dyssynchrony parameters were made using ANOVA test for repeated measures with Tukey post-test. Also, comparisons between control and DCM groups were made using the unpaired Student *t* test. In addition, a correlation test was used to assess the relation between various cardiac output measurements. Statistical significance was defined as a two-tailed *P*-value <0.05. Data are shown as mean values ± SD for the continuous variables.

Results

Effects of Stress on Functional Parameters

Functional parameters at rest and during levels of dobutamine-induced stress in DCM dogs are shown in Table 1. D'Agostino-Pearson test confirmed that the distribution of the hemodynamic variables was not significantly different from a normal distribution ($P > 0.1$). The progressive dobutamine infusion resulted in a marked increase in heart rate, from 107.1 ± 10.5 bpm at rest to 134.7 ± 12.2 bpm for the maximum level of pharmacological stress. Immediately after the initial pharmacological stimulation with a small amount of dobutamine, a significant increase in LVEF (22.6% ± 6.0% in baseline *vs* 29.5% ± 7.5% in 2.5 μg/kg/min; $P < 0.02$) was observed. Further significant differences were shown at higher levels ($P < 0.0001$). Interestingly, the same results were seen in RVEF ($P < 0.0001$). Also, a significant increasing trend was observed in the cardiac output by both radionuclide and thermodilution methods with the increase of dobutamine doses ($P < 0.0001$), and methods indicated a good correlation in cardiac output measurements (Pearson's correlations at each dobutamine level > 0.7). Modulations of LV end-systolic and diastolic volumes (ESV, EDV) with increasing doses of dobutamine enhanced the stroke volume. Although the LV end-diastolic pressure (EDP) was still preserved in response to doses of dobutamine, volume alterations produced a constant progression in the maximum rate of rise of LV pressure (dP/dt_{max}; 949.5 ± 238.5 mmHg/s at baseline *vs* 3,020.8 ± 568.9 mmHg/s at 20 μg/kg/min; $P < 0.0001$). QRS duration was almost constant and did not change significantly with the varying stress levels.

Effects of Stress on Intraventricular Dyssynchrony

Dyssynchrony parameters at rest and during dobutamine-induced stress levels in DCM *vs* control dogs are shown in Table 2. The D'Agostino-Pearson test confirmed that the distribution of the dyssynchrony variables did not significantly differ from a normal distribution ($P > 0.2$). All subjects revealed a significant amount of LV dyssynchrony at rest. However, dobutamine significantly increased the synchrony of contraction in all subjects. Figure 2-6 (A-C) shows the count-based LV contraction phase of a control *vs* DCM dog at baseline and at maximum stress level. As has been shown, LV regions in a DCM subject contract according to different phases and amplitudes. Although these uncoordinated contractions are substantially normalized at maximum stress level, they still show some differences when compared to the normal pattern. In the control group, a plateau was observed at the dobutamine level of 5 μg/kg/min for CHI and entropy values, meaning that 5 μg/kg/min dobutamine was an appropriate amount to generate maximum contraction efficiency in those subjects. In comparison, CHI showed a significant improvement from baseline to stress levels of 5 μg/kg/min dobutamine or greater ($P < 0.05$) in DCM subjects. Similar results were found for entropy and phase SD. Septal displacement was significantly out of phase with the LV (later than the lateral wall at rest). However, it was normalized at peak dobutamine stress; this contrasts with the apex, which showed a significant difference relative to the LV phase and remained out of phase even at maximum stress ($P < 0.002$, Figure 2-7). An example of one DCM dog with reduced apex and septum contraction efficiency is shown in Figure 2-8.

Effects of Stress on Interventricular Dyssynchrony

Interventricular dyssynchrony was negative in all except one DCM subject at rest. A delay is defined as negative when the LV contracts earlier than the RV (Figure 2-9). Although a visual trend toward improvement of RVLV synchrony (approaching to zero) was observed with 2.5 μg/kg/min dobutamine, overall no significant change was seen between rest and the maximum stress level in this parameter, even when considering absolute values (-20.9 º ± 21.1º (-33 ± 33.4 ms) at baseline *vs* -22.2 º ± 11.5º (-27.6 ± 14.6 ms) at 20μg/kg/min, $P < 0.25$; 25.0º ± 15.4º at baseline *vs* 22.2º ± 11.5º at 20μg/kg/min, in absolute values, $P < 0.08$; Table 2). In fact, as has been shown in Figure 2-9, there were individual differences in the magnitude and pattern of change in interventricular dyssynchrony during the various levels of dobutamine stress and it was hard to draw a certain direction of change in RVLV delay measurements.

Control versus DCM Group

Comparison of LV dyssynchrony and functional parameters between the DCM and control dogs at rest and at maximum stress level is shown in Table 3. In general, DCM dogs showed a depressed ventricular function (EF, dP/dt_{max}). Also, all intraventricular dyssynchrony indices in this cohort showed significant differences in comparison to the control subjects both at rest and under maximum stress levels (all lower than normal values). In the DCM cohort, septal contraction always occurred later than LV lateral wall contraction. The introduction of cardiac stress did not change the pattern of mechanical contraction in the DCM cohort, which was always a lateral-to-septal (Figure 2-7), compared to LV contraction in the control group, where dobutamine-induced stress resulted in a septal-to-lateral pattern. There was no significant difference between the DCM and control subjects in interventricular mechanical dyssynchrony at

rest ($P < 0.08$) and notably at maximum dobutamine stress ($P < 0.91$). In average, LV contraction preceded RV contraction in both groups at rest. Due to the increase in ventricular conduction speed, a progressive early LV contraction was apparent in subjects with normal cardiac contraction under dobutamine-induced stress. However, the interventricular synchrony was not hampered during the stress condition in these subjects. In comparison, individual differences in the magnitude and pattern of change in interventricular dyssynchrony precluded the existence of a statistically significant trend of change in this parameter during the various stages of dobutamine stress in the DCM cohort.

Discussion

The range of difference in ventricular dyssynchrony parameters between rest and levels of stress has rarely been studied in cardiac failure subjects. The current study performed by GBPS showed that, even in close intervals, different levels of dobutamine stress could have a significant impact on ventricular function and intraventricular dyssynchrony parameters in DCM subjects with narrow QRS complexes.

GBPS for Assessing Stress Dyssynchrony

In echocardiography, a few points in space and a few heartbeats are used to estimate either maximum temporal delay or standard deviation of delays over the entire LV segments. In contrast, GBPS uses several hundred data points in space and multiple data points in time that are taken from the analysis of a complete cardiac cycle which has been averaged over hundreds of cardiac cycles at the time of acquisition. Cross-correlation of the mean phase of all points, either

regionally or globally, thus results in the direct measurement of mechanical dyssynchrony. GBPS is fully automated (in our case more than 90%) and provides highly reproducible dyssynchrony indices.[10] In comparison, several different and complicated segmental analyses in echocardiography result in substantial errors and high inter- and intraobserver variability.[8] Currently, GMPS plays a central role in the visual and quantitative characterization of LV dyssynchrony. However, it cannot replace GBPS, since GBPS can provide both inter- and intraventricular dyssynchrony data, especially in the presence of perfusion defects. Recently, GBPS has also been used to gain a better understanding of mechanical dyssynchrony and its efficacy in predicting the response to cardiac resynchronization therapy in HF patients.[20, 21]

Ventricular Dyssynchrony and Narrow QRS

The evidence found in literature highlight the fact that QRS duration does not correlate with intraventricular dyssynchrony and has only a limited relationship with interventricular dyssynchrony.[22] In a model with narrow QRS complex, we observed significant LV dyssynchrony and non-significant RVLV delay, which is in accordance with previous reports. In fact, QRS duration incorporates both right and left ventricular activation, and one's delayed activation can be balanced by the other's rapid activation. In so doing, a normal QRS complex is preserved, in spite of a significant LV mechanical dyssynchrony. In the current study, while disparity in the timing of ventricular mechanical contraction was obviously affected by levels of dobutamine stress, no specific alteration was observed in the duration of the QRS complex.

Dobutamine Stress and Ventricular Dyssynchrony

A limited number of echocardiographic studies have specifically addressed the effect of stress on mechanical dyssynchrony in DCM patients with narrow QRS complexes.[4-7] In these studies, three distinct groups of patients could be identified based on a specific dyssynchrony parameter: the first group showed no difference between rest and stress, the second showed an induced dyssynchrony when going from rest to stress, and the last showed a normalized dyssynchrony when going from rest to stress. The reason the patients manifested such variable responses to exercise or dobutamine stress is not clear. What we observed in our study was the same response from all DCM subjects, with exactly the same induced pathology, in terms of LV intraventricular dyssynchrony parameters at stress. Based on our regional analysis, improvement of LV mechanical dyssynchrony at stress was attributable to the early contraction of previously delayed-contracting regions that were mostly seen in the LV apex and septum. Our observations concur with the evidence collected by Somsen *et al*., according to whom the septal wall is the typical site of dyskinesia and reduced contractility in patients with DCM,[23] as well as with a recent canine study performed by strain echocardiography which showed a larger decrease on strains of apical segments in DCM dogs.[12] Under induced stress, only the late septal contraction was normalized. The absence of any protection from the mitral annulus and papillary muscles in the apex could be the cause of severe tachycardia-induced effects in this region rather than on other walls at the time of evolution of LVDCM.[12]

Intermediate levels of dobutamine stress caused significant changes in homogeneity of contraction and ventricular function in the DCM cohort. Applied LV dyssynchrony indices allowed for a clear distinction between those changes during the various stages of stress. Even in control subjects, CHI and entropy sensitivity were promising in specifying the dyssynchrony

variations during the stress condition. This observation concurred with what was previously seen in wall thickening-derived CHI and entropy when these were used to evaluate stress dyssynchrony in a control group.[24] However, because phase values were well peaked in control subjects, phase SD could not show the small variances during the induction of dobutamine stress. Overall, our LV dyssynchrony parameters did not contradict, but rather complemented, each other in the stress analysis, in contrast to the previously seen discordance between the parameters of dyssynchrony measured by stress echocardiography in HF patients.[5]

In the current study, interventricular mechanical dyssynchrony was found to be insignificant in DCM subjects compared to their normal counterparts. A similar observation was made by another group who showed that interventricular mechanical dyssynchrony is less frequently noted in HF patients with narrow QRS complexes.[25] The main point here is the variability of the baseline direction of contraction (1 out of 10 subjects with positive RVLV delay), also seen in the control group (2 out of 8 dogs showed positive RVLV delays).[13] Moreover, there was an individual difference in the magnitude and pattern of change in RVLV delays during the dobutamine stress that was also seen in the control group. We could not explain the reason for such variability in RVLV delays between individuals, which might be related to individual cardiac mechanical characteristics.

Limitations

The current study was performed in dogs; consequently, even though the applied methodology may seem transferable, our findings are not directly transferable to humans. The number of animals was limited in this study. The inadequate number of subjects, as well as inter-animal variability in RVLV delays, precluded any definitive conclusion about the effects of maximum

stress in interventricular dyssynchrony. Due to the limited spatial resolution of the SPECT system, we relied on a count-based analysis to quantify dyssynchrony indices, an alternative superior to volume-based measurements, since it is more reproducible and accurate. The apparent ventricular movement was actually the movement of the blood-endocardial interface. Consequently, a global cardiac motion was also present during ventricular systole along with myocardial contraction, which made it impossible to distinguish the real endocardial movements. Although the global cardiac motion was likely to be small in LV, it could severely affect the RV due to its geometrical shape. For this reason, we did not measure the RV intraventricular dyssynchrony indices. The best scenario for RV was probably to be in synchrony with the LV which is thicker and more concentric (RVLV delay). Finally, differences in synchrony between rest and stress episodes could be interpreted as being due to a better image resolution and count statistics caused by higher heart rates rather than by the intrinsic physiologic effects of stress. This hypothesis was previously evaluated by positron emission tomography and results revealed that count statistics are not responsible for the difference in dyssynchrony indices at stress.[26] However, this might not be as clear-cut in the case of SPECT images when image quality and count statistics are different.

New knowledge gained

Stress ventricular dyssynchrony analysis can be assessed in a straightforward and fully automated manner by phase analysis of GBPS imaging. Different levels of dobutamine stress, even in close intervals, can have a significant impact on intraventricular dyssynchrony parameters in DCM subjects with narrow QRS complexes. The changing trends are mostly seen as going toward the

perfection of synchrony. The dyssynchrony indices of CHI, entropy, and phase SD have the same sensitivity to distinguish between various stress levels in DCM subjects.

Conclusion

In this study with a non-ischemic DCM model and narrow QRS complex, GBPS could identify the extent and pattern of ventricular contraction dyssynchrony at rest and during dobutamine stress levels. Different levels of functional stress, even in close intervals, made significant positive changes in hemodynamic and intraventricular dyssynchrony parameters. Since evidence of stress-induced mechanical dyssynchrony may be helpful in predicting the response to cardiac resynchronization therapy, further research is warranted to assess whether lower ventricular mechanical dyssynchrony indices induced by stress and measured by GBPS have the ability to predict the response to resynchronization therapy.

Acknowledgments

This study was conducted with the collaboration of the Electrophysiology Service of the Montreal Heart Institute. We wish to thank Marc-Antoine Gillis, Evelyn Landry, Marie-Pierre Mathieu and Sophie Marcil for their expert technical assistance.

References

1. Kass DA. An epidemic of dyssynchrony: but what does it mean? J Am Coll Cardiol 2008;51:12-7.
2. Matsumoto K, Tanaka H, Tatsumi K, Kaneko A, Tsuji T, Ryo K et al. Regional heterogeneity of systolic dysfunction is associated with ventricular dyssynchrony in patients with idiopathic dilated cardiomyopathy and narrow QRS complex. Echocardiography 2012;29:1201-10.
3. Ghio S, Constantin C, Klersy C, Serio A, Fontana A, Campana C et al. Interventricular and intraventricular dyssynchrony are common in heart failure patients, regardless of QRS duration. Eur Heart J 2004;25:571-8.
4. D'andrea A, Mele D, Nistri S, Riegler L, Galderisi M, Losi MA et al. The prognostic impact of dynamic ventricular dyssynchrony in patients with idiopathic dilated cardiomyopathy and narrow QRS. Eur Heart J Cardiovasc Imaging 2013;14:183-9.
5. Lafitte S, Bordachar P, Lafitte M, Garrigue S, Reuter S, Reant P et al. Dynamic ventricular dyssynchrony: an exercise-echocardiography study. J Am Coll Cardiol 2006;47:2253-9.
6. Chattopadhyay S, Alamgir MF, Nikitin NP, Fraser AG, Clark AL, Cleland JG. The effect of pharmacological stress on intraventricular dyssynchrony in left ventricular systolic dysfunction. Eur J Heart Fail 2008;10:412-20.
7. Yagishita-Tagawa Y, Abe Y, Arai K, Yagishita D, Takagi A, Ashihara K et al. Low-dose dobutamine induces left ventricular mechanical dyssynchrony in patients with dilated cardiomyopathy and a narrow QRS: a study using real-time three-dimensional echocardiography. J Cardiol 2013;61:275-80.

8. Chung ES, Leon AR, Tavazzi L, Sun JP, Nihoyannopoulos P, Merlino J et al. Results of the Predictors of Response to CRT (PROSPECT) trial. Circulation 2008;117:2608-16.

9. Lancellotti P, Moonen M. Left ventricular dyssynchrony: a dynamic condition. Heart Fail Rev 2012;17:747-53.

10. Trimble MA, Velazquez EJ, Adams GL, Honeycutt EF, Pagnanelli RA, Barnhart HX et al. Repeatability and reproducibility of phase analysis of gated single-photon emission computed tomography myocardial perfusion imaging used to quantify cardiac dyssynchrony. Nucl Med Commun 2008;29:374.

11. Lalonde M, Birnie D, Ruddy TD, Wassenaar RW. SPECT blood pool phase analysis can accurately and reproducibly quantify mechanical dyssynchrony. J Nucl Cardiol 2010;17:803-10.

12. Kusunose K, Zhang Y, Mazgalev TN, Thomas JD, Popovic ZB. Left ventricular strain distribution in healthy dogs and in dogs with tachycardia-induced dilated cardiomyopathy. Cardiovasc Ultrasound 2013;11:43.

13. Harel F, Finnerty V, Gregoire J, Salimian S, Thibault B. Effects of dobutamine stress on cardiac contraction synchronism in a canine model. Physiol Meas 2013;34:1387-97.

14. Ganz W, Donoso R, Marcus HS, Forrester JS, Swan HJ. A new technique for measurement of cardiac output by thermodilution in man. Am J Cardiol 1971;27:392-6.

15. Harel F, Finnerty V, Ngo Q, Gregoire J, Khairy P, Thibault B. SPECT versus planar gated blood pool imaging for left ventricular evaluation. J Nucl Cardiol 2007;14:544-9.

16. Harel F, Finnerty V, Grégoire J, Thibault B, Marcotte F, Ugolini P et al. Gated blood-pool SPECT versus cardiac magnetic resonance imaging for the assessment of left ventricular volumes and ejection fraction. J Nucl Cardiol 2010;17:427-34.

17. Harel F, Finnerty V, Grégoire J, Thibault B, Khairy P. Comparison of left ventricular contraction homogeneity index using SPECT gated blood pool imaging and planar phase analysis. J Nucl Cardiol 2008;15:80-5.

18. O'Connell JW, Schreck C, Moles M, Badwar N, DeMarco T, Olgin J et al. A unique method by which to quantitate synchrony with equilibrium radionuclide angiography. J Nucl Cardiol 2005;12:441-50.

19. Wassenaar R, O'Connor D, Dej B, Ruddy TD, Birnie D. Optimization and validation of radionuclide angiography phase analysis parameters for quantification of mechanical dyssynchrony. J Nucl Cardiol 2009;16:895-903.

20. Lalonde M, Birnie D, Ruddy TD, Beanlands RS, Wassenaar R, Wells RG. SPECT gated blood pool phase analysis of lateral wall motion for prediction of CRT response. Int J Cardiovasc Imaging 2014;30:559-69.

21. Lalonde M, Wells RG, Birnie D, Ruddy TD, Wassenaar R. Development and optimization of SPECT gated blood pool cluster analysis for the prediction of CRT outcome. Med Phys 2014;41:072506.

22. Hawkins NM, Petrie MC, MacDonald MR, Hogg KJ, McMurray JJ. Selecting patients for cardiac resynchronization therapy: electrical or mechanical dyssynchrony? Eur Heart J 2006;27:1270-81.

23. Somsen GA, Verberne HJ, Burri H, Ratib O, Righetti A. Ventricular mechanical dyssynchrony and resynchronization therapy in heart failure: a new indication for Fourier analysis of gated blood-pool radionuclide ventriculography. Nucl Med Commun 2006;27:105-12.

24. Salimian S, Thibault B, Finnerty V, Grégoire J, Harel F. The effects of dobutamine stress on cardiac mechanical synchrony determined by phase analysis of gated SPECT myocardial perfusion imaging in a canine model. J Nucl Cardiol 2014;21:375-83.

25. van Bommel RJ, Tanaka H, Delgado V, Bertini M, Borleffs CJW, Marsan NA et al. Association of intraventricular mechanical dyssynchrony with response to cardiac resynchronization therapy in heart failure patients with a narrow QRS complex. Eur Heart J 2010;31:3054-62.

26. AlJaroudi W, Alraies MC, DiFilippo F, Brunken RC, Cerqueira MD, Jaber WA. Effect of stress testing on left ventricular mechanical synchrony by phase analysis of gated positron emission tomography in patients with normal myocardial perfusion. Eur J Nucl Med Mol Imaging 2012;39:665-72.

Figures

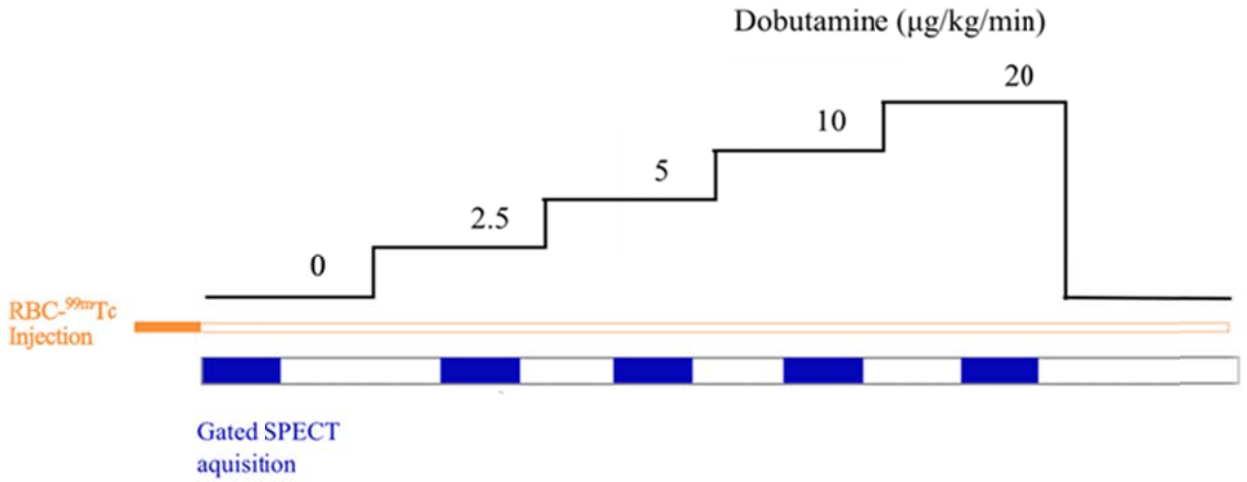

Figure 2-1: Illustration of dobutamine stress infusion and GBPS acquisition protocol. After injection of a single dose of red blood cells labeled ^{99m}Tc, baseline GBPS images were acquired. Cardiac stress was then induced by a continuous infusion of dobutamine at different levels of 2.5, 5, 10 and 20 µg/kg/min. After reaching a stable stress effect at each dobutamine level, GBPS acquisition was performed.

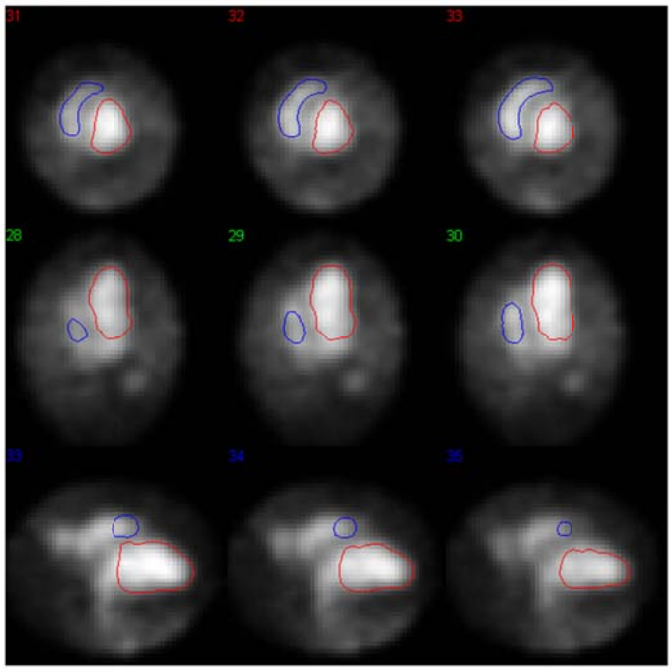

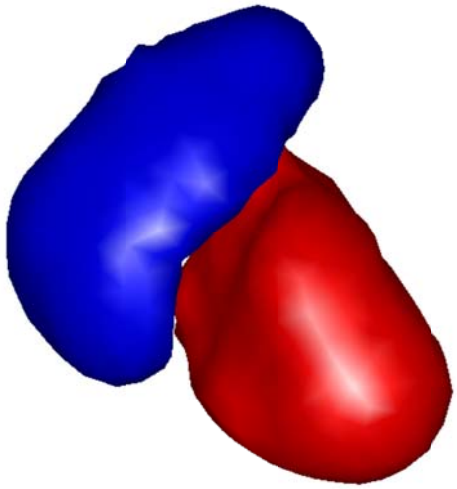

Figure 2-2: Illustration of GBPS images in short, horizontal and vertical long axis views, respectively. Regions of interest are drawn over both ventricles. Final 3D segmented right (blue) and left (red) ventricles derived from those ROIs are shown in the right side of the figure.

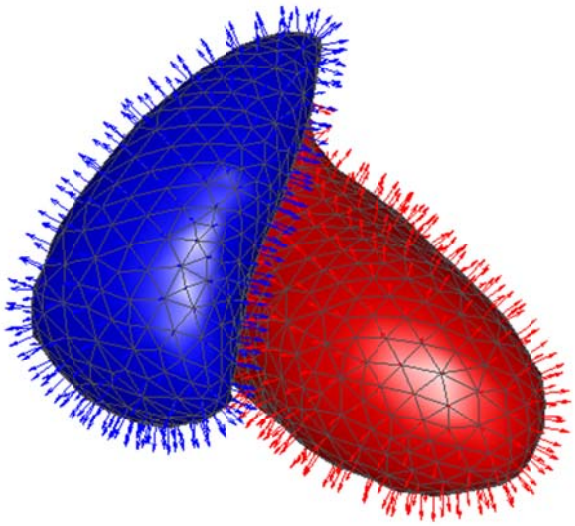

Figure 2-3: Dynamic surface of approximately 400 vertices over the LV and RV. Vertices are linked together making triangular shapes and surface tetrahedrons then are used to estimate the final geometric volumes. Also, 400 profiles normal to the initial surface are shown for both ventricles that are used to estimate the dynamic motion of the surfaces.

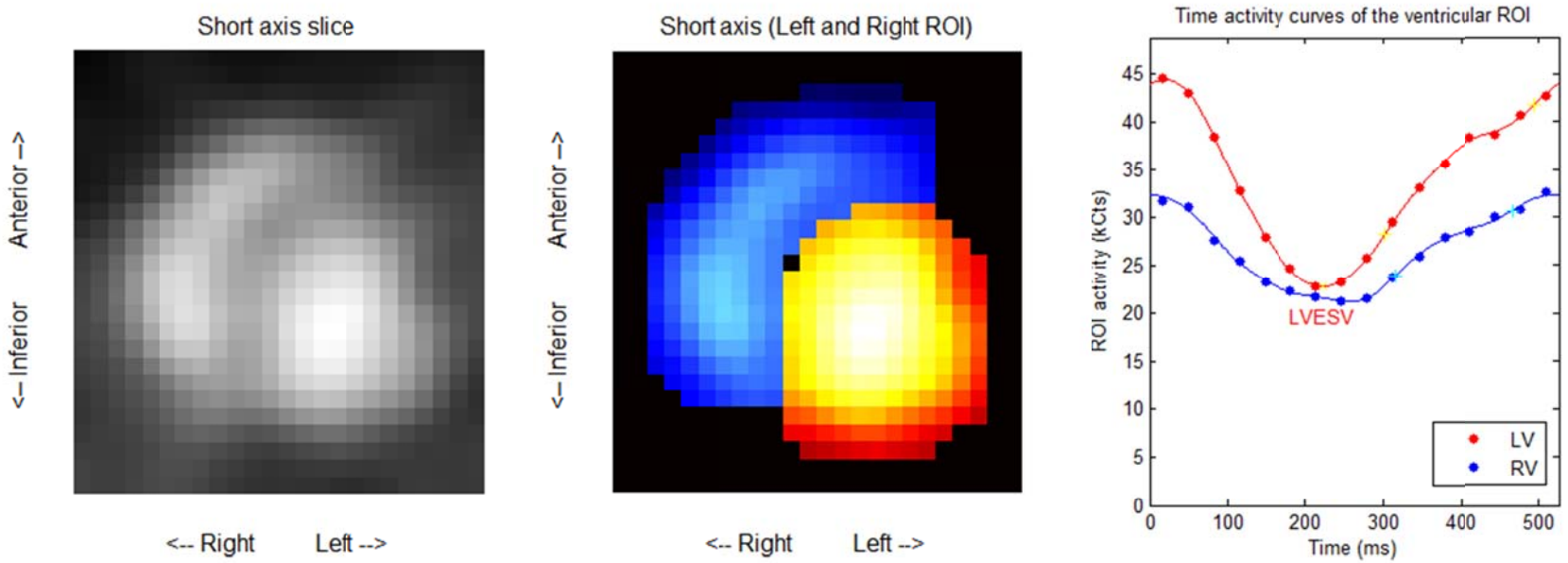

Figure 2-4: Left and right regions of interest in short axis view and related time activity curves in 16 bins.

.

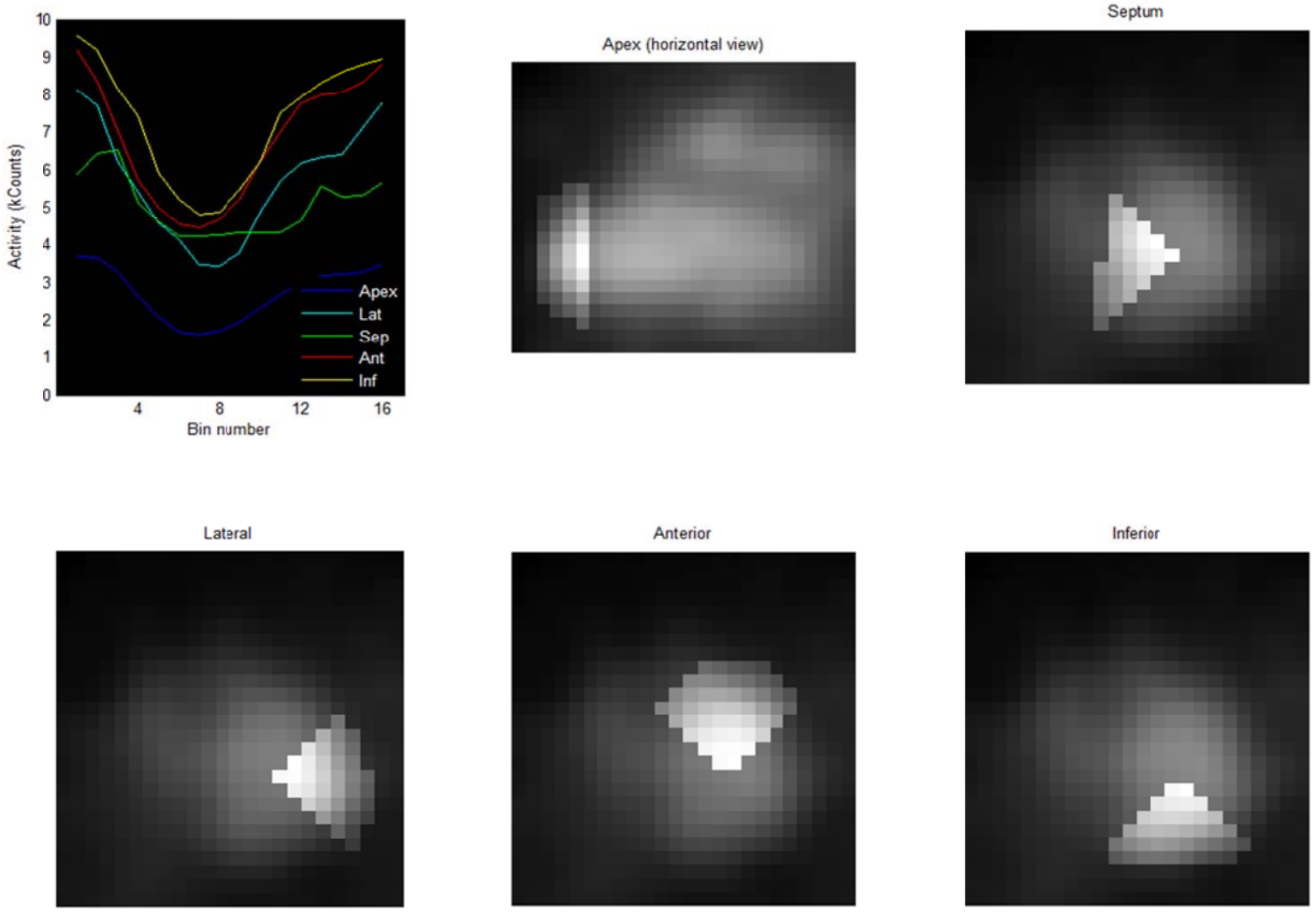

Figure 2-5: Illustration of time-activity curves for different regions of the LV as well as regional LV ROIs: anterior, lateral, inferior and septal regions in short axis and apex in horizontal long axis view.

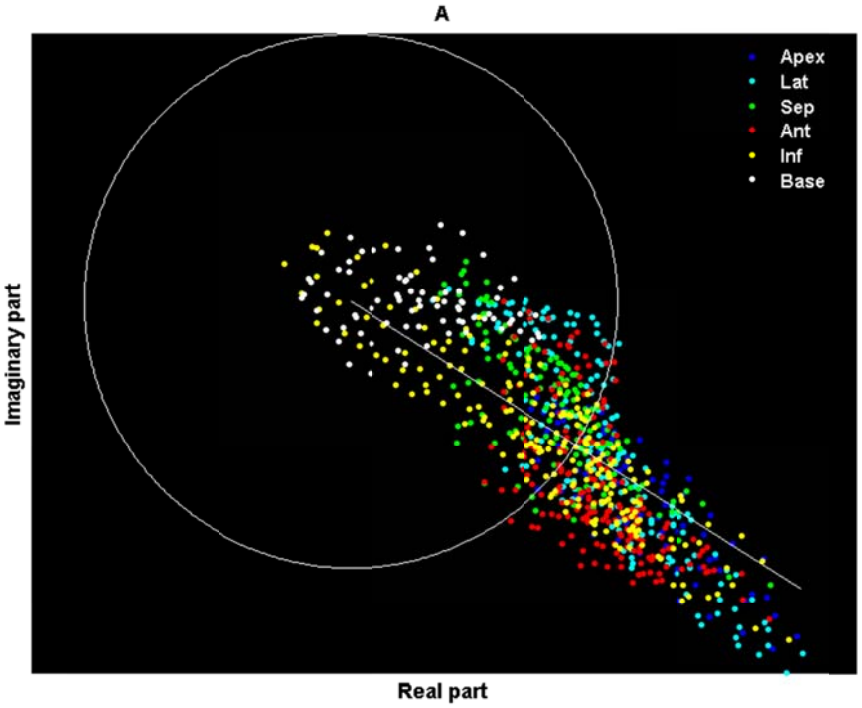
A
Apex
Lat
Sep
Ant
Inf
Base
Imaginary part
Real part

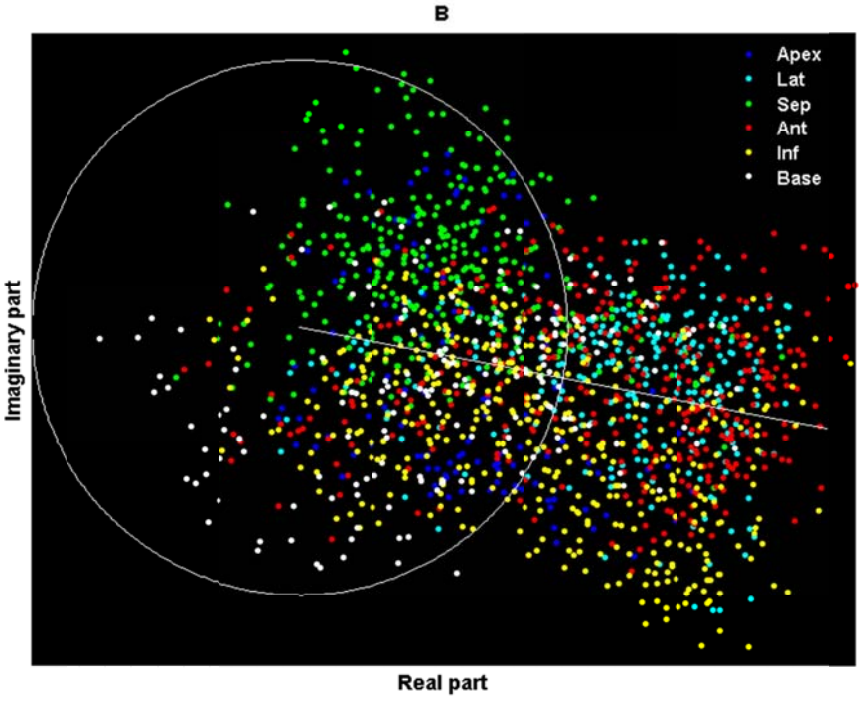
B
Apex
Lat
Sep
Ant
Inf
Base
Imaginary part
Real part

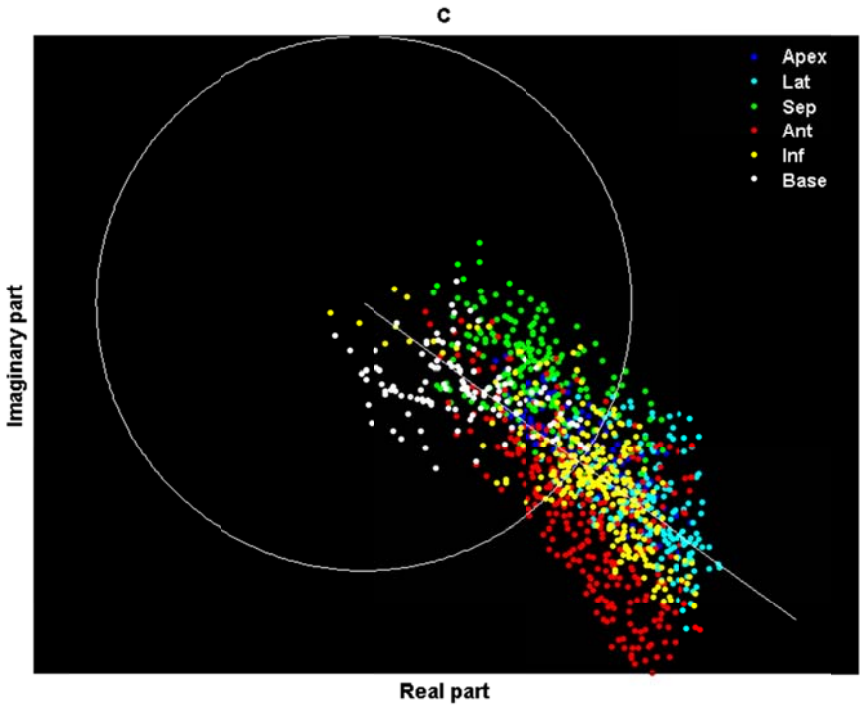

Figure 2-6: Illustration of count-based LV contraction phase in a control dog at baseline (A) and in a DCM dog at baseline (B) and at 20 μg/kg/min dobutamine level (C). Each of the 400 dots contains both amplitude and phase of an actual voxel within the LV ROI. They are expressed as a complex harmonic which contains both amplitude and phase ($Ae^{i\theta}$), represented in a polar coordinate system with a radius and angle that correspond to amplitude and phase, respectively. The white circle represents the average amplitude and the line is the direction of the average phase. In the normal subject, regional dots (complex harmonics) are homogenously distributed around the mean phase and amplitude. However, in the DCM subject, the distribution of dots is almost uncoordinated around the circle. During the stress episodes, their distribution become more homogenous, potentially getting closer to the mean phase and amplitude, but still shows differences compared to the normal pattern.

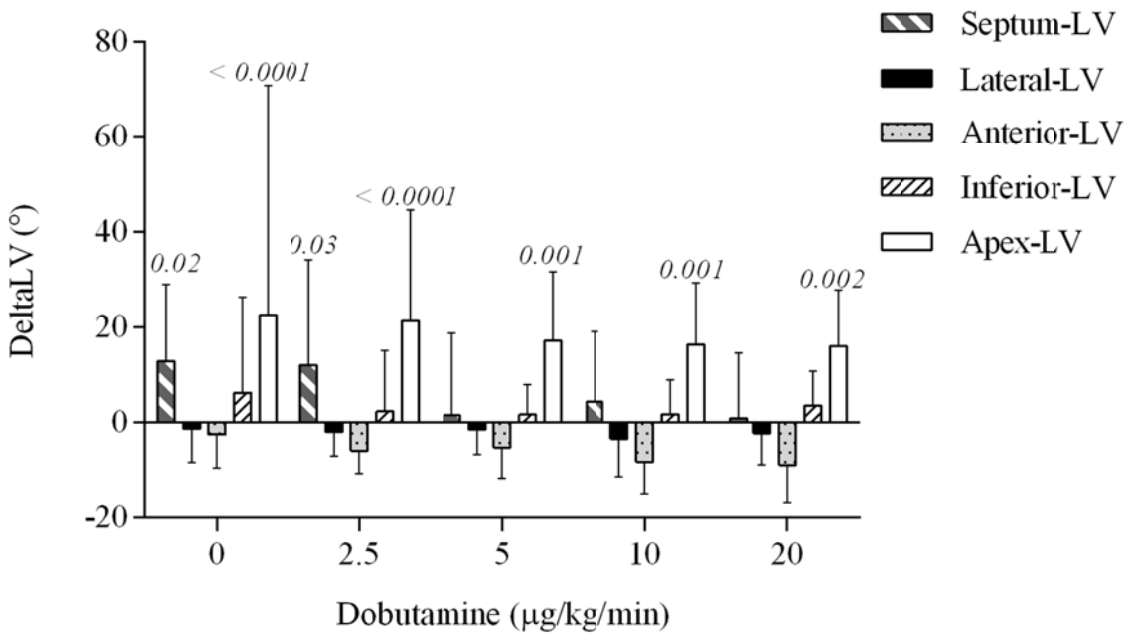

Figure 2-7: Left ventricular regional wall phase differences at baseline and at each dobutamine level. LV phase is the origin (zero) and each regional wall phase delay has been individually shown during the induction of dobutamine stress. Negative phases are earlier and positive values are more delayed sites of contraction. *P* values show the significant phase differences from zero.

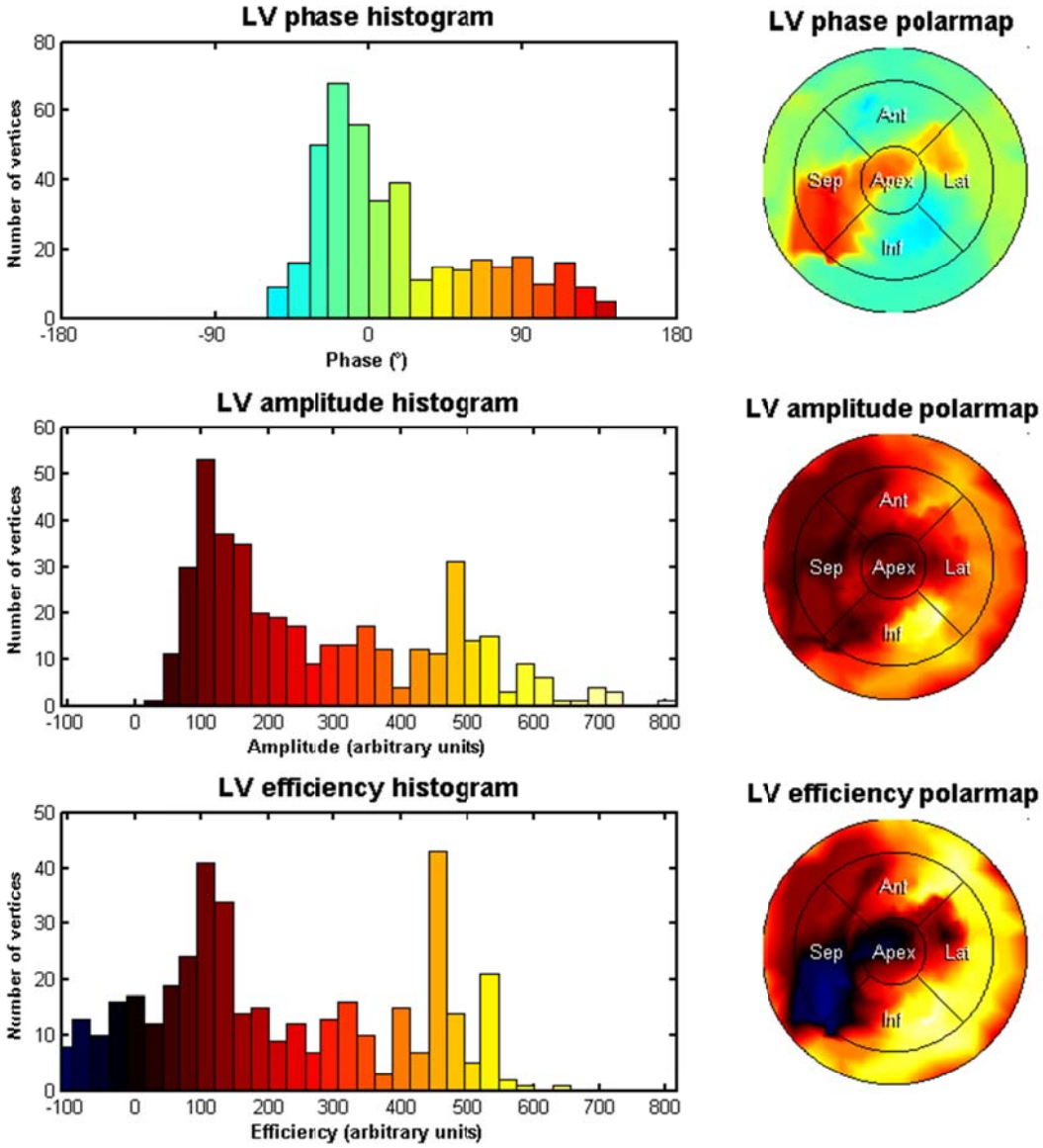

Figure 2-8: Illustration of phase, amplitude and efficiency of all vertices in the LV of a DCM dog as an example in histogram and polarmap displays. For this subject, the most important phase delays are located in the apex and septum. The apex shows approximately 90º phase delay (orange) compared to the average phase and lower amplitude (dark red) compared to the anterolateral or inferior regions as well as zero efficiency (black). For the septum, the overall amplitude is lower than the rest of the ventricle, which is normal, since it is in the center of the ventricle and we measured the movements of the regions of the ventricle rather than the wall

thickening. However, in this case, the septal delay is remarkable relative to other regions in the LV (red) which gives a negative efficiency or blue region in the efficiency polarmap. For this example, the CHI has been reduced to 82% and the entropy increased to 73%.

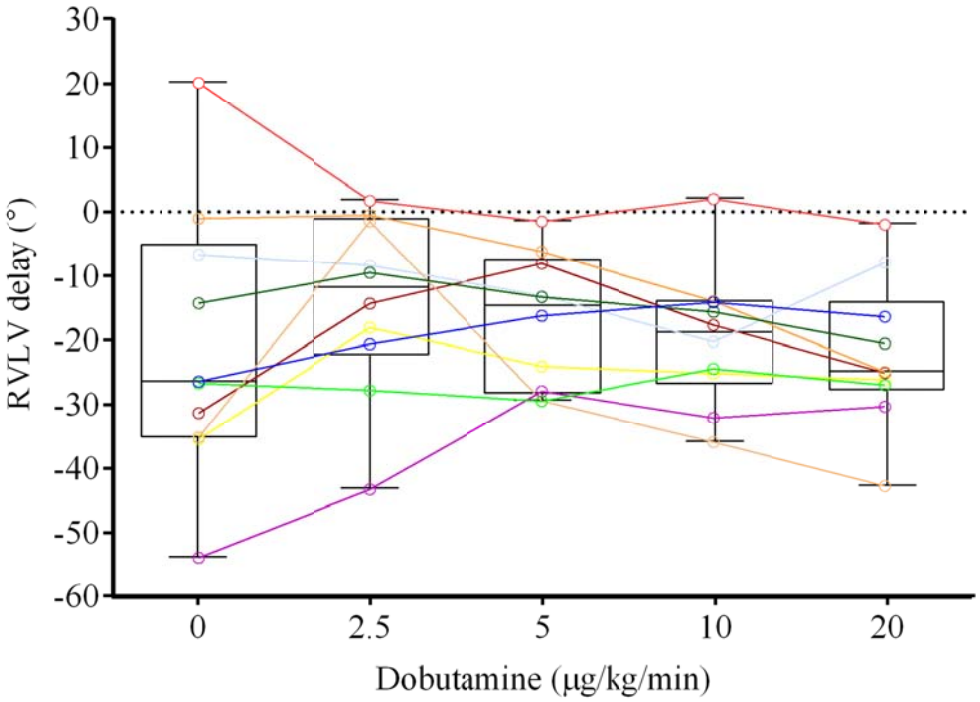

Figure 2-9: Interventricular mechanical dyssynchrony (RVLV delay) at rest and during different levels of dobutamine stress. For each dobutamine level, median and spread of phase delays are indicated in a box-and-whiskers plot. The line in the box marks the median and the hinges (limits of the box) indicate the range of observation with 5^{th}-95^{th} percentile. Whiskers show the minimum and maximum values in a column. Also, the trend of variations of RVLV delays during the dobutamine stress is shown for each dog in color lines

.

Tables

Table 2-1: Functional parameters at rest and during levels of dobutamine-induced stress in DCM dogs

Index	Dobutamine (µg/kg/min)				
	0	2.5	5	10	20
HR (bpm)	107.1±10.5	112.7±12.2	117.8±12.4*#	125.7±11.7*#♮	134.7±12.2*#♮¶
QRS interval	79.1±10.2	80.4±9.7	79.5±9.5	78.1±8.7	78.2±7.7
LVEDP	16.9± 5.5	16.8± 8.5	16.5± 8.5	13.7± 9.1	16.1± 10.7
dP/dt_{max}	949.5±238.5	1343.2±277.3*	1660.5±296.9*#	2309.7±396.9*#♮	3020.8±568.9*#♮¶
LVEDV (ml)	129.5±34.1	124.2±35.8	118.4±34.5	115.4±34.7	110.3±39.1
LVESV (ml)	97.4±29.3	84.3±26.4*	74.8±25.0*#	66.5±24.2*#♮	56.7±22.0*#♮¶
LVSV (ml)	29.2±11.0	36.6±14.6	41.5±13.3*	46.3±12.6*#♮	52.2±17.2*#
LVEF (%)	22.6±6.0	29.5±7.5*	35.2±5.5*#	41.0±5.9*#♮	48.1±5.8*#♮¶
RVEDV (ml)	94.2±28.8	87.1±29.5	82.0±25.8*	80.6±24.2*	82.7±25.8
RVESV (ml)	80.0±26.8	67.8±26.8	59.2±20.2*	55.5±19.2*#♮	53.5±21.7*#
RVEF (%)	15.8±4.5	23.1±7.5*	28.3±4.5*#	32.1±7.6*#	36.9±9.8*#♮
CO_Cb	3.1±1.1	4.2±1.8	4.9±1.7*	5.8±1.8*#♮	7.1±2.6*#♮
CO_Th	3.8±2.0	6.0±3.1*	7.4±3.2*	9.4±4.0*#	11.7±5.2*#

N=10 for all parameters except CO_Th and dP/dt_{max} (N=8) for DCM dogs. Data are presented as mean ± SD. *= $P \leq 0.05$ *vs* baseline; # = $P \leq 0.05$ *vs* 2.5; ♮ = $P \leq 0.05$ *vs* 5; ¶ = $P \leq 0.05$ *vs* 10 µg/kg/min (RM ANOVA, Tukey). HR, heart rate; QRS interval, QRS complex duration; LVEDP, left ventricular end-diastolic pressure; dP/dt_{max}, maximum rate of LV pressure change; LVEDV and RVEDV, left and right end-diastolic volume; LVESV and RVESV, left and right end-systolic volume; LVSV, left ventricular stroke volume; LVEF and RVEF, left and right ventricular ejection fraction; CO_Cb, cardiac output by count-based method; CO_Th, cardiac output by thermodilution method.

Table 2-2: Dyssynchrony parameters at rest and during dobutamine-induced stress levels in DCM vs control dogs

	Index	Dobutamine (µg/kg/min)				
		0	2.5	5	10	20
DCM						
	LVCHI (%)	78.6±10.9	84.5±9.4	89.8±5.2*	90.6±5.4*#	92.4±3.9*#
	LV Entropy	0.78±0.09	0.71±0.11	0.65±0.09*#	0.63±0.09*#	0.59±0.08*#♮
	LV Phase SD (°)	49.4±14.8	41.0±14.9	33.3±10.6*#	31.9±12.2*#	27.1±10.7*#
	RVLV delay (°)	-20.9±21.1	-14.1±13.9	-16.8±10.2	-19.6±10.7	-22.2±11.5
	RVLV delay (ms)	-33.3±33.4	-20.3±19.4	-23.4±13.9	-25.8±14.5	-27.6±14.6
Control						
	LVCHI (%)	96.4±1.3	97.9±0.6	98.7±0.9*	98.6±1.0	98.4±1.2
	LV Entropy	0.52±0.04	0.43±0.03*	0.36±0.09*	0.37±0.10	0.38±0.01
	LV Phase SD (°)	25.4±5.1	17.8 6.4	12.8±7.7	13.6±8.0	15.0±10.3
	RVLV delay (°)	-6.3 ±2.6	-10.7±3.4	-19.3 ±1.4*	-21.3±3.6*	-21.6 ±3.1*
	RVLV delay (ms)	-13.9 ±11.8	-17.2 ±13.7	-17.8 ±7.6	-23.8 ±9.5	-23.5 ±11.5

N=10 for DCM dogs. N=8 for Normal dogs. Data are presented as mean ± SD. *= $P \leq 0.05$ *vs* baseline; # = $P \leq 0.05$ *vs* 2.5; ♮ = $P \leq 0.05$ *vs* 5; ¶ = $P \leq 0.05$ *vs* 10 µg/kg/min (RM ANOVA, Tukey). LVCHI, LV contraction homogeneity index; RVLV delay, interventricular delay.

Table 2-3: Comparison of LV dyssynchrony and functional parameters between DCM and control dogs.

	Rest			Maximum stress		
	Normal	DCM	P value	Normal	DCM	*P* value
HR (bpm)	112.1±19.1	107.1±10.5	0.49	182.9±15.6	134.7±12.2	<0.0001
QRS interval (ms)	76.5±5.7	79.1±10.2	0.52	71.1±9.0	78.2±7.7	0.09
LVEDV (ml)	52.2±15.7	130.1±34.3	< 0.0001	37.4±14.5	110.3±39.1	0.0001
LVESV (ml)	30.9±7.0	97.8±29.4	< 0.0001	16.7±2.8	56.7±22.0	0.0001
SV (ml)	25.8±9.4	29.2±11.0	0.49	31.3±12.3	52.2±17.2	0.01
LVEF (%)	49.5±8.4	22.6±6.0	< 0.0001	69.9±12.4	48.1±5.8	0.0001
dP/dt_{max} (mmHg/s)	1588±374	949.5±238.5	0.001	8004±710	3020.8±568.9	< 0.0001
CO_Cb (L/min)	2.8±1.0	3.1±1.1	0.55	5.7±2.2	7.1±2.6	0.24
CO_Th (L/min)	3.2±1.3	3.8±2.0	0.47	7.9±4.2	11.7±5.2	0.13
LVCHI (%)	96.4±1.3	78.6±10.9	0.0003	98.4±1.2	92.4±3.9	0.0008
LV Entropy	0.52±0.04	0.78±0.09	0.0001	0.38±0.10	0.59±0.08	0.0002
LV Phase SD (°)	25.4±5.1	49.4±14.8	0.0005	15.0±10.3	27.1±10.7	0.03
RVLV delay (°)	-6.3±2.6	-20.9±21.1	0.08	-21.6±3.1	-22.2±11.5	0.91
RVLV delay (ms)	-13.9±11.8	-33.3±33.4	0.14	-23.5±11.5	-27.6±14.6	0.53

N=10 for all parameters except CO_Th and dP/dt_{max} (N=8) in DCM dogs. N=8 for all except dP/dt_{max} at 20 μg/kg/min dobutamine (N=6) in control dogs. Data are presented as mean ± SD. Abbreviations are the same as previous Tables.

Chapter 3

Effect of various modes of ventricular pacing on left ventricular mechanical synchrony under stress as assessed by phase analysis of gated myocardial perfusion SPECT in a canine model of atrioventricular block and normal function.

Samaneh Salimian, MSc,[a] Bernard Thibault, MD,[b] Vincent Finnerty,[a] MSc, Jean Grégoire, MD,[a] and François Harel, MD, PhD[a*]

[a]Department of Nuclear Medicine, Montreal Heart Institute, and Université de Montréal, Montreal, QC, Canada

[b]Department of Medicine, Montreal Heart Institute, and Université de Montréal, Montreal, QC, Canada

Abstract

Background: It is still not known whether biventricular (BiV) pacing is the best pacing mode in every patient with atrioventricular block (AVB) and normal function and whether the optimal pacing mode at rest can be the best one during the exercise.

Methods: Five large dogs were submitted to AV node ablation and pacing leads were placed in the right atrium for sensing, in the right ventricular (RV) apex, and in posterolateral LV vein for pacing in five modes of left ventricular (LV), BiV with 20 ms of LV pre-activation (LVRV20), BiV, BiV with 20 ms of RV pre-activation (RVLV20) and RV pacing. Stress was induced by administering intravenous dobutamine up to a maximum of 20 μg/kg/min. Hemodynamic and dyssynchrony data were analyzed by LV pressure measurements and gated SPECT myocardial perfusion (GMPS) phase analysis by either the QGS or MHI_4MPI software.

Results: A significant LV dyssynchrony was seen at LV pacing versus other interventions which was normalized at maximum stress level (bandwidth: 177.6º ± 41.7º at rest *vs* 68.4º ± 21.0º at maximum stress). Although RV pacing produced lower contraction homogeneity (THI) mostly cause of lowered amplitude (THI: 90.3% ± 10.3%) at rest, it was improved at 5 μg/kg/min level (97.2% ± 2.3%) and remained stable at higher stress level. At maximum stress, LV dyssynchrony was further normalized at LV-based pacing modes and worsened at BiV or RV-based pacing modes. LVRV20 pacing showed the lowest degree of LV dyssynchrony versus single-site pacing modes at maximum stress (entropy: 37.8% ± 3.0% in LVRV20 *vs* 52.6% ± 5.3% in LV pacing and 51.0% ± 8.2% in RV pacing).

Conclusions: Stress changed the extent of resting LV dyssynchrony at all the pacing modes and resulted in more accurate dyssynchrony assessment with lesser variability in our subjects than the resting condition. BiV pacing with pre-activation of the LV closely resembled the intrinsic ventricular activation in developing normal mechanical contraction at higher levels of stress.

Keywords: Left ventricular dyssynchrony **.** gated myocardial perfusion SPECT **.** dobutamine stress **.** atrioventricular block and normal function.

Introduction

Ventricular pacing is an inevitable treatment in patients with congenital or acquired atrioventricular block (AVB) for eliminating the bradycardia as a trigger for initiation of ventricular arrhythmia and further dysfunctions.[1] Right ventricular apex (RVA) pacing has been the ideal site of stimulation for decades in patients with AVB and typically normal ventricular activation pattern and normal systolic function.[2] However, recognition of deleterious effects of RVA pacing on left ventricular (LV) function,[3,4] mechanical synchrony,[5,6] and structure[7] has shifted the interest toward the alternative pacing modes.

Among pacing alternatives which are routinely used for different heart failure patients with intraventricular conduction disorders, simultaneous biventricular pacing (BiV) has been mostly considered by both preclinical and clinical studies in patients with AVB and normal ventricular function.[8-11] Comparative acute and chronic studies of the effects of RVA and BiV pacing confirmed the superiority of BiV pacing in preserving the LV performance and function due to inducing a more physiologic and synchronous ventricular activation sequence in such patients.[8-11] While, it is still not known whether BiV pacing is the best mode in every patient with AVB and normal function, other types of stimulation have rarely been studied in such patients. Also, it is unknown whether the optimal pacing mode at rest can be the best one during the exercise and increased heart rates in these patients.

The potential mechanism in the superiority of BiV pacing is thought to be related to the mechanical dyssynchrony as studied by echocardiography.[9,11] Considering the fact

that echocardiographic techniques are not reliable in LV dyssynchrony measurements due to high inter and intra-observer variability,[12] it is of special interest to verify the dyssynchrony produced by different ventricular activation sequence, especially at stress, with a more reliable, reproducible though possibly an automated imaging modality. In comparison with echocardiography, phase analysis of gated single-photon emission computed tomography (SPECT) myocardial perfusion imaging (GMPS), has been shown to be highly repeatable and reproducible for LV dyssynchrony measurements.[13]

Accordingly, we used phase analysis of GMPS to quantify the acute changes in LV function and mechanical synchrony during RV pacing compared to various pacing modes of LV, simultaneous and sequential biventricular pacing under the rest and dobutamine stress levels in a canine model of AVB and normal function.

Methods

Study Protocol

The protocol was approved by the institutional Research Ethics Board and all procedures followed the Canadian Council on Animal Care. Five adult dogs (mixed races; mean weight 38.3 ± 1.9 kg) underwent general anesthesia with isoflurane 1.5% after induction with doses of 5 mg/kg ketamine and 0.25 mg/kg diazepam. SaO_2 was monitored using a standard biomedical cardiac monitor (Eagle 4000, Marquette Medical System, Milwaukee, WI, USA). The dogs' bladders were catheterized in order to prevent radioactive urine spills. A pressure catheter (Ventri-cath 507S, 5F, straight tip, Millar

Instruments, Houston, TX, USA) was inserted into the LV via the left carotid artery to monitor chamber pressure. Signals were conditioned (MPVS Ultra 753-2083, Millar), digitized (ITF156, Emka Technologies, Falls Church, VA, USA) and subsequently analyzed with a dedicated software (Iox2, ver. 2.5.1.6, Emka). It has to be mentioned that hemodynamic data were recorded for four dogs out of five because the Millar system was unavailable. An access was positioned in the femoral venous of the left leg for dobutamine infusion. Surface ECGs were recorded using a standard 3-lead configuration (Cardiac Trigger Monitor 3000, Ivy Biomedical Systems Inc., Branford, CT, USA). At the end of the experiment, dogs were euthanized with the administration of isoflurane 5% and an intravenous overdose of potassium chloride.

Pacing Protocol

The atrioventricular (AV) node was ablated with a 4-mm electrode-tip radiofrequency ablation catheter (Cordis-Webster, Johnson, and Johnson). Pacing leads were placed in the right atrium for sensing, in the RV apex (via the jugular vein guided by fluoroscopy), and in a branch of the coronary sinus (posterolateral LV vein) for pacing. Devices were programmed in an atrial synchronous tracking mode without atrial pacing (VDD mode) for five pacing modes performed in a regular order as following: LV pacing, biventricular pacing with 20 ms of LV pre-activation (LVRV20), biventricular pacing (BiV), biventricular pacing with 20 ms of RV pre-activation (RVLV20) and right ventricular pacing (RV). The optimal AV delay used for the protocol was individually adjusted during BiV pacing mode and was the smallest which provided no changes in hemodynamic properties. The AV delay was fixed for each set of tested configuration.

Dobutamine Stress GMPS Acquisition

The GMPS and surface ECGs were simultaneously acquired at baseline and dobutamine-induced stress levels of 5 and 20μg/kg/min for each pacing configuration. First, baseline images were acquired with ^{99m}Tc-tetrofosmin (Myoview, GE Healthcare) at each pacing mode started from LV and continued by predetermined modes to the RV. Radiotracer dose was adjusted to dogs' weight. Data were collected after 10 min of pacing at each configuration to achieve the equilibrium before data acquisition. Then, cardiac stress was induced by a dobutamine infusion prepared in 500 μg/mL of normal saline solution and continuously infused over average times of 37.4 and 30.6 min while increasing the outflow to reach the predetermined dosage. Because of dobutamine's short half-life (≈ 2.3 min), a continuous infusion was used to create a stable dobutamine stress effect allowing the acquisition of the SPECT images. Immediately after reaching a target dobutamine concentration level, image acquisition was initiated for each of five pacing modes. There was no rest period during the entire experiment.

In average, the stress dobutamine effect for each level of 5 and 20 μg/kg/min lasted around 106.2 and 84.6 min which a total volume of 42.2 and 132.1 mL of solution was infused. The duration of GMPS acquisition was adjusted throughout the day to reach equal count statistics in spite of ^{99m}Tc decay time; average time of image acquisition was 8 min for each of pacing modes. Cardiac hemodynamic, as well as cardiac contraction synchrony data (using GMPS) were recorded for each pacing mode at rest and during the stress levels. Data were acquired on a dual-head gamma camera (e.cam; Siemens PA, USA), low-energy high-resolution collimators and 64 projections dispatched on a 360°

arc. The gated data were acquired as 16 frames per cardiac cycle and stored in a 64 × 64 matrix.

GMPS Data Processing and Phase Analysis

All the gated data were reconstructed using a 2D-OSEM algorithm with 10 iterations and 8 subsets and then filtered by a Gaussian filter of 8.4 mm with a reconstructed pixel size of 4.8 mm. All reconstructed data were reoriented manually using a camera software package (Siemens Autocardiac 8.5.10.1) to produce gated short axis images which were then submitted to phase analysis of LV dyssynchrony assessment. Short axis images were submitted into automatic segmentation QGS® 2009 software including the phase analysis plug-in (Cedars-Sinai Medical Center, Los Angeles, CA, USA). LV dyssynchrony parameters throughout a cardiac cycle in QGS were phase histogram bandwidth (the width of the band with 95% of the samples over the entire LV), SD (standard deviation of the phase histogram) and entropy (the probability of occurrence of phase angle *i* in a phase histogram).[14] As a note, entropy would be equal to zero when the synchrony of contraction is at the maximum level.[14] In fact, in the case of reduced contraction consistency, entropy is able to identify the degree of random and uncoordinated contraction. In addition, LV functional volumes, ejection fractions, and septal-to-lateral delay were obtained from this software.

Short axis images were also submitted into the automatic segmentation software MHI_4MPI with thickening-based mechanical synchrony analysis measurement. Details of segmentation and calculation of synchrony parameters have been previously described elsewhere.[15] Briefly, after constructing the myocardial wall edges, a three harmonics

Fourier analysis was used to estimate the phase (timing) and amplitude of contraction in different walls of anterior, septal, inferior, lateral and apex. In fact, the phase, measured as an angle, was the base of all synchrony parameters. The cross-correlation of the septum and lateral mean thickening phases was used to obtain the thickening-based septal-to-lateral wall delay (TSLD) as an index of intraventricular mechanical synchrony. Also, the thickening homogeneity index (THI) which represents the proportion of wall thickening that is in synchrony with the average LV thickening was calculated as the mean efficiency, the portion of amplitude that is in the direction of mean phase, divided by the mean amplitude.

Statistical Analysis

Statistical analyses were performed using dedicated software (SPSS Statistics 21.0, Chicago, IL). Also for graphical illustrations, we used the GraphPad Prism version 6.00 for Windows (GraphPad Software, La Jolla, California, USA). Data are reported as mean ± SD. QGS and MHI_4MPI phase measurements, as well as functional parameters in different pacing modes under rest and stress levels were compared by a linear mixed model with levels of stress, type of stimulation and their interactions as fixed effects and with repeated measures on animals as random subjects using compound symmetry variance structure. A dog with missing data in RVLV20 pacing at rest for the gating problem and a dog with missing data in LVRV20 pacing at 20 μg/kg/min dobutamine which was never made a mistake at the day of the experiment were included in the model. Also, a dog with missing data in RV pacing at 20 μg/kg/min dobutamine due to the segmentation difficulty through the MHI_4MPI software was included in the model. P

< 0.05 was considered statistically significant. Multiple comparisons were performed with Bonferroni's post-hoc test whenever the F-ratio for the factors was significant.

Results

Hemodynamic Data

LV hemodynamic parameters in the effect of various pacing modes have been shown at rest and during dobutamine-induced stress levels in Table 1 and 2 respectively. At baseline, established LVEF and dP/dt_{max} indicated a normal systolic function, within the normal range,[15] in the effect of different pacing interventions. However, a single favorable functional response cannot be seen among different pacing modes. Both parameters were significantly improved during the levels of dobutamine stress during each of the stimulation patterns. RV pacing did not indicate an increase in SV and cardiac output (CO) during the stress levels and had the lowest value among other stimulation modes during the maximum stress. The reason why the CO and SV at RV pacing failed to reach a statistical significance with those of LVRV20 pacing, while the related values in LVRV20 pacing were fairly high relative to the RV pacing, could be the effect of a missing data in LVRV20 pacing mode and the expectation and replacement of that missing value in the statistical model. In fact, the calculation of SV and CO requires two variables of EDV and ESV for the SV, and SV and heart rate for the CO, which because of missing data at each parameter, the expected error might be doubled during the LVRV20 pacing mode.

The contractility index (CI) defined as the maximal rate of pressure rise normalized to instantaneous pressure (a contractility index with less load sensitivity) was profoundly improved during each pacing mode at maximum stress level but reached the statistical significance at BiV , RVLV20 and RV pacing interventions. The reason of this significance was the augmented variance between the subjects at 20 μg/kg/min dobutamine in the mentioned pacing modes, while the mean values were nearly the same (Figure 3-1). Heart rate was constantly increasing by the stress levels, no matter which pacing mode was used and BiV pacing showed a significantly higher heart rate in comparison with the LV pacing at maximum stress level. QRS duration was significantly higher in LV pacing compared to RV and RVLV20 both at baseline and stress levels.

Regional Mechanical Contraction

Regional LV phase delays were not significantly different from the LV mean phase at rest and 5 μg/kg/min dobutamine as shown in Figure 3-2 A, B. During the LV and RV pacing, the standard deviation of the phase delays in some LV regions were remarkable at rest; however, it was largely reduced during the stress levels. There was only a significant difference between inferior wall and mean LV contraction phase at maximum stress level during the LV and RVLV20 pacing modes ($P = 0.04$ and $P = 0.03$ at LV and RVLV20 pacing modes, respectively; Figure 3-2 C), showing an incomplete synchrony perfection at LV inferior wall during the LV pacing (despite more synchronous contraction in other walls) and a little synchrony decline at inferior wall during the RVLV20 pacing at maximum stress level. Figure 3-3 A-J shows the thickening-based LV contraction phase of a dog at baseline and maximum stress level during various

pacing modes as an example. As it has been shown, the pattern of contraction in regions of the LV is different during each pacing mode at rest. For instance, lateral and anterior walls of the LV at RV pacing contract according to different phases and amplitudes and later than mean LV phase. Although the spatial distribution of the regions (phase and amplitude of LV regional contractions) has been improved at maximum stress level, they still show differences with the mean phase and amplitude. Comparing the pacing modes with respect to the uniformity of contraction, LVRV20 shows the most homogeneous and coordinated regional contraction at maximum stress among other modes in this case (Figure 3-3 H).

Dyssynchrony Parameters

LV dyssynchrony parameters in the effect of various pacing modes have been indicated at rest and during dobutamine-induced stress levels in Table 3 and 4, respectively. Also as an example, Figure 3-4 A-J shows phase analysis of GMPS as assessed by QGS software in a dog, same dog as shown in Figure 3-3, at rest and maximum stress while various pacing modes were applied. LV pacing significantly increased the dyssynchrony in comparison with other interventions at rest based on bandwidth and phase SD. It has to be mentioned that these parameters were significantly higher than the range reported previously for normal dogs (93.0° ± 38.8° with the range of 36°-150° for bandwidth and 25.7° ± 11.7° with the range of 9.5°-44.4° for phase SD in normal dogs[15]). Also, LVRV20 pacing had a significantly higher bandwidth compared to BiV and RVLV20 pacing modes; however it is within the normal range. SLD in LV pacing was considerable and negative in comparison with other pacing modes. Also, LV pacing

showed a significant higher entropy versus BiV and RVLV20 pacing modes (LV: 60.0% ± 3.0% *vs* BiV: 45.6% ± 8.2% and RVLV20: 47.7% ± 13.7%; $P < 0.05$).

Based on THI, the more synchronous contraction was seen during sequential pacing either LV first or RV and less synchronous one was seen for RV pacing stimulation. However, both single-pacing sites indicated close values and were lower than BiV pacing in terms of homogeneity of contraction. TSLD showed an early lateral wall contraction phase in LV pacing compared to other interventions meaning that the contraction of septum first happened in all other stimulations. Thus, the phase delay between the lateral wall and septum did not differ between interventions and only the first contracted wall was different in LV pacing compared to other pacing modes at rest and at maximum stress.

During the stress, dyssynchrony (bandwidth and phase SD) was significantly diminished in LV based pacing modes. However, phase SD and entropy were still significantly higher in LV pacing in respect to the BiV-based pacing modes at 5 μg/kg/min dobutamine level. BiV and RV-based pacing modes did not show significant differences with each other at baseline; unless RV pacing had lower THI versus RVLV20 pacing. A considerable decrease in LV dyssynchrony (based on entropy) happened at 5 μg/kg/min dobutamine-induced stress at these pacing modes while further stress level returned the dyssynchrony to the baseline value. LVRV20 pacing showed further decrease in entropy at maximum stress relative to the single pacing sites. Moreover, at maximum stress level, sequential pacing modes evoked the least entropy compared to both single site pacing modes. High SLD during LV pacing was normalized and significantly decreased during both levels of stress. THI was significantly improved in

single-site ventricular pacing modes with the intermediate level of dobutamine and remained constant through further stress level. However, the THI in other BiV pacing modes were already high at baseline and did not significantly change. Additionally, the amplitude of contraction was considerably augmented in all the pacing modes at 5 μg/kg/min dobutamine and only under the RV pacing further improvement was seen in the magnitude of contraction with maximum stress level (Figure 3-5).

Discussion

The actual incidence of pacing-induced cardiomyopathy is not clear in patients with normal LVEF due to non-subgroup analysis in most studies; however, it seems to be lower than patients with a depressed LVEF.[16] Although priority of BiV over RV pacing has been shown by PACE trial which was particularly designed for patients with bradycardia and preserved LVEF,[10,11] based on a recent long-term study, the use of preventive BiV pacing has no clinical benefits in terms of heart failure (HF) hospitalizations or mortality in patients with AVB.[17] Consequently, indications for BiV pacing in patients with preserved LV function who require long-term pacing is still not well-defined in current guidelines and it is still not known whether it is the best mode in every patient with AVB and normal function. However, the identification of LV dyssynchrony may help to select a subgroup that could benefit from an alternative pacing as it was successfully used to predict the response of HF patients to cardiac resynchronization therapy (CRT).[18]

In this study with a model of AVB and normal function, we could not find a significantly better acute response with BiV rather than RV pacing regarding the synchrony of mechanical contraction at rest or stress levels. It is in contrast to the findings of a previous echocardiographic study showing that BiV pacing could induce lower LVSLD in comparison with the RV pacing in an immature animal model of AVB and normal function.[9] Interestingly, rather than BiV pacing, sequential pacing modes were the most prominent in reducing the contraction dyssynchrony compared to the RV pacing at rest and at maximum dobutamine stress in our study. This finding may bring new idea about using individual optimization of the interventricular delay (sequential pacing), which has been a recognized strategy in patients receiving CRT, to improve the long-term response of the patient. However, this hypothesis must be verified by the clinical comparative trials.

Alteration of the pacing modes did not induce a significant difference in acute hemodynamic response in our model either at rest or at stress levels. All hemodynamic parameters were considerably improved with the administration of dobutamine stress during each of the pacing modes. Only the RV pacing did not make a change in SV and CO with the maximum stress level and showed significant difference with other interventions at this stress level. The reason could be observed by the non-significant difference in synchrony with the RV pacing during the maximum activity as assessed by the phase parameters. Although the amplitude of contraction was significantly increased with the dobutamine stress levels during the RV pacing, it still did not make considerable effects on the hemodynamic results.

It is worth mentioning that the LV dyssynchrony results measured by QGS or MHI_4MPI software did not contradict, but rather complemented, each other in the stress analysis in contrast to the disagreement formerly seen between the parameters of dyssynchrony measured by stress echocardiography.[19] Hence, various components of mechanical contraction (phase and amplitude) by variables of both methods were used in this study. At baseline, decreased amplitude during the RV stimulation offset the increased uncoordinated contraction phase during the LV pacing to achieve a comparable amount of ventricular homogeneity about 90% using single-site pacing modes. Thus, the randomness of the phase of contraction at baseline was more prominent during the LV pacing versus BiV and RV-based pacing modes at rest which did not reflect any sensible effect on ventricular contractility. Also , by LV pacing longer time was needed to activate the entire ventricles relative to using RV-based pacing modes and this electrical dyssynchrony remained constant at maximum stress level, despite mechanical synchrony was significantly improved. Although the electrical dyssynchrony matched the mechanical dyssynchrony at resting condition, the link was faded away at maximum stress level. Based on a comprehensive study in normal subjects, QRS duration is not sensitive to the variation of heart rates and activity levels.[20] Although in our model, the electrical stimulations were propagated through various sites and different myocardial pathways rather than the Purkinje system, their behavior with the increased heart rates was the same as normal electrical propagations and did not change with activity levels. Moreover, QRS duration incorporates the electrical activation timing of both ventricles, not the mechanical activation of LV. Also, it has been previously proved that it does not correlate with intraventricular dyssynchrony.[21]

Although the LV-induced dyssynchrony was normalized significantly through the 5 μg/kg/min dobutamine, synchrony improvement was seen in all the pacing modes resulted in an identical pattern of difference between the LV and other pacing modes at baseline. Further stress level made the considerable decline in synchrony of mechanical contraction (entropy) at BiV and RV-based pacing modes, enforced them to return the baseline values. Thus, improvement in LV synchrony remained stable over a range of heart rates and activity levels only in LV-based pacing modes. Moreover, LVRV20 pacing was the most effective stimulation which produced maximum LV synchrony with 98% THI at stress condition. The reason why the electrical stimulation induced from BiV pacing with pre-activation of the LV develops a progressing synchrony with increasing the levels of stress may be found in the timing of electrical propagation through the normal ventricular myocardium. Since more time is needed for the LV epicardial wavefronts to move transmurally toward the endocardium relative to the RV endocardial wavefronts from RV apical site,[22] earlier proceeding of electrical signals from the LV site and, with a time interval, from the RV endocardium can make a coincidence in myocardial activation from both sites which may provide a proper timing synchrony in ventricular contractions. As it has been shown in the current study, higher heart rates do not hamper this activation coincidence but rather strengthen, making the synchrony of mechanical contractions more efficient.

Dobutamine stress may induce regional differences in myocardial contractility, thus may change the presence and extent of LV dyssynchrony either in normal subjects or heart failure patients.[15,19] Our results, in accordance with the previous findings, show that clear synchrony differences exist between the rest and stress episodes in subjects with

AVB and normal function submitted to various pacing modes. The aforesaid difference could be mostly due to the intrinsic physiologic effects of stress rather than better image resolution and count statistics at higher heart rates, as previously been examined.[23] Dobutamine-induced variation in dyssynchrony parameters was positive at the level of 5 μg/kg/min dobutamine for all the pacing interventions. However, further stress level up to 20 μg/kg/min dobutamine did not make a considerable change at LV-based pacing modes and even worsened the synchrony of contraction at BiV or RV-based pacing modes. The variation was attributed to the extent of approaching to or moving away from the mean LV contraction phase, amplitude or both together.

It is worth mentioning that the inter-subject variability in mechanical response to the pacing stimulations was substantially decreased with the administration of dobutamine stress according to the phase parameters. Since high variability reduces the ability to detect statistical significance, assessing the LV dyssynchrony under stress allows a better statistical power mostly in the case of using small sample sizes.

Limitations

The number of subjects was limited in this study. Moreover, the number of imaging sessions and data collected from each animal was very high that made it impossible to record all the information without any missing data. We used the GMPS for acquiring the volumes and LVEFs which might not be an ideal method for the accurate measurements. Also, focusing only on the dP/dt_{max} and contractility index was insufficient and might neglect many other aspects of systolic function and ventricular performance affected by pacing interventions.

Conclusion

In this study with a model of AVB and normal function, GMPS could clearly identify the pattern of LV regional contraction and the extent of LV dyssynchrony at rest and at dobutamine stress levels while various pacing modes were applied. The mechanical response of the LV myocardium to a specific type of pacing intervention may be overestimated or underestimated at rest. However, intrinsic physiologic effects of stress result in a more accurate dyssynchrony assessment with lesser variability in subjects underwent pacing. BiV with LV pre-activation seems to be the preferred site of stimulation in this model rather than single-site pacing mode. Due to the importance of ventricular pacing in patients with AVB and concerns about the generated ventricular dyssynchrony with pacing, further research is warranted in a larger group to assess if the stress dyssynchrony measured by GMPS could be efficient as a method for optimizing the pacing in these patients.

Acknowledgments

This study was conducted with the collaboration of the Electrophysiology Service of the Montreal Heart Institute. We wish to thank Marc-Antoine Gillis, Evelyn Landry, Marie-Pierre Mathieu and Sophie Marcil for their expert technical assistance.

References

1. Sweeney MO, Prinzen FW. A new paradigm for physiologic ventricular pacing. J Am Coll Cardiol 2006;47:282-8.
2. Arenas IA, Jacobson J, Lamas GA. Routine Use of Biventricular Pacing Is Not Warranted for Patients With Heart Block. Circ Arrhythm Electrophysiol 2015;8:730-738.
3. Tops LF, Schalij MJ, Bax JJ. The effects of right ventricular apical pacing on ventricular function and dyssynchrony implications for therapy. J Am Coll Cardiol 2009;54:764-76.
4. Nahlawi M, Waligora M, Spies SM, Bonow RO, Kadish AH, Goldberger JJ. Left ventricular function during and after right ventricular pacing. J Am Coll Cardiol 2004;44:1883-1888.
5. Tops LF, Suffoletto MS, Bleeker GB et al. Speckle-tracking radial strain reveals left ventricular dyssynchrony in patients with permanent right ventricular pacing. J Am Coll Cardiol 2007;50:1180-1188.
6. Zhang H, Hou X, Wang Y et al. The acute and chronic effects of different right ventricular site pacing on left ventricular mechanical synchrony as assessed by phase analysis of SPECT myocardial perfusion imaging. J Nucl Cardiol 2014;21:958-966.
7. Karpawich PP, Rabah R, Haas JE. Altered cardiac histology following apical right ventricular pacing in patients with congenital atrioventricular block. Pacing Clin Electrophysiol 1999;22:1372-1377.

8. Frias PA, Corvera JS, Schmarkey L, Strieper M, Campbell RM, Vinten-Johansen J. Evaluation of Myocardial Performance with Conventional Single-Site Ventricular Pacing and Biventricular Pacing in a Canine Model of Atrioventricular Block. J Cardiovasc Electrophysiol 2003;14:996-1000.

9. Cojoc A, Reeves JG, Schmarkey L et al. Effects of Single-Site Versus Biventricular Epicardial Pacing on Myocardial Performance in an Immature Animal Model of Atrioventricular Block. J Cardiovasc Electrophysiol 2006;17:884-889.

10. Yu C-M, Chan JY-S, Zhang Q et al. Biventricular pacing in patients with bradycardia and normal ejection fraction. N Eng J Med 2009;361:2123-2134.

11. Chan JY-S, Fang F, Zhang Q et al. Biventricular pacing is superior to right ventricular pacing in bradycardia patients with preserved systolic function: 2-year results of the PACE trial. Eur Heart J 2011:ehr336.

12. Chung ES, Leon AR, Tavazzi L et al. Results of the Predictors of Response to CRT (PROSPECT) trial. Circulation 2008;117:2608-16.

13. Trimble MA, Velazquez EJ, Adams GL et al. Repeatability and reproducibility of phase analysis of gated single-photon emission computed tomography myocardial perfusion imaging used to quantify cardiac dyssynchrony. Nucl Med Commun 2008;29:374.

14. Van Kriekinge SD, Nishina H, Ohba M, Berman DS, Germano G. Automatic global and regional phase analysis from gated myocardial perfusion SPECT imaging: application to the characterization of ventricular contraction in patients with left bundle branch block. J Nucl Med 2008;49:1790-7.

15. Salimian S, Thibault B, Finnerty V, Grégoire J, Harel F. The effects of dobutamine stress on cardiac mechanical synchrony determined by phase analysis of gated SPECT myocardial perfusion imaging in a canine model. J Nucl Cardiol 2014;21:375-383.

16. Herweg B, Singh R, Barold SS. Cardiac Resynchronization Therapy Is Appropriate for All Patients Requiring Chronic Right Ventricular Pacing: The Pro Perspective. Card Electrophysiol Clin 2015;7:433-444.

17. Blanc J. Biventricular pacing for atril-ventricular block to prevent cardiac desynchronization (BIOPACE Trial). European Scientific Meeting, 2014.

18. Friehling M, Chen J, Saba S et al. A prospective pilot study to evaluate the relationship between acute change in left ventricular synchrony after cardiac resynchronization therapy and patient outcome using a single-injection gated SPECT protocol. Circ Cardiovasc Imaging 2011;4:532-539.

19. Lafitte S, Bordachar P, Lafitte M et al. Dynamic ventricular dyssynchrony: an exercise-echocardiography study. J Am Coll Cardiol 2006;47:2253-9.

20. Simoons M, Hugenholtz P. Gradual changes of ECG waveform during and after exercise in normal subjects. Circulation 1975;52:570-577.

21. Hawkins NM, Petrie MC, MacDonald MR, Hogg KJ, McMurray JJ. Selecting patients for cardiac resynchronization therapy: electrical or mechanical dyssynchrony? Eur Heart J 2006;27:1270-1281.

22. van Deursen C, van Geldorp IE, Rademakers LM et al. Left ventricular endocardial pacing improves resynchronization therapy in canine left bundle-branch hearts. Circ Arrhythm Electrophysiol 2009;2:580-587.

23. AlJaroudi W, Alraies MC, DiFilippo F, Brunken RC, Cerqueira MD, Jaber WA. Effect of stress testing on left ventricular mechanical synchrony by phase analysis of gated positron emission tomography in patients with normal myocardial perfusion. Eur J Nucl Med Mol Imaging 2012;39:665-72.

Figures

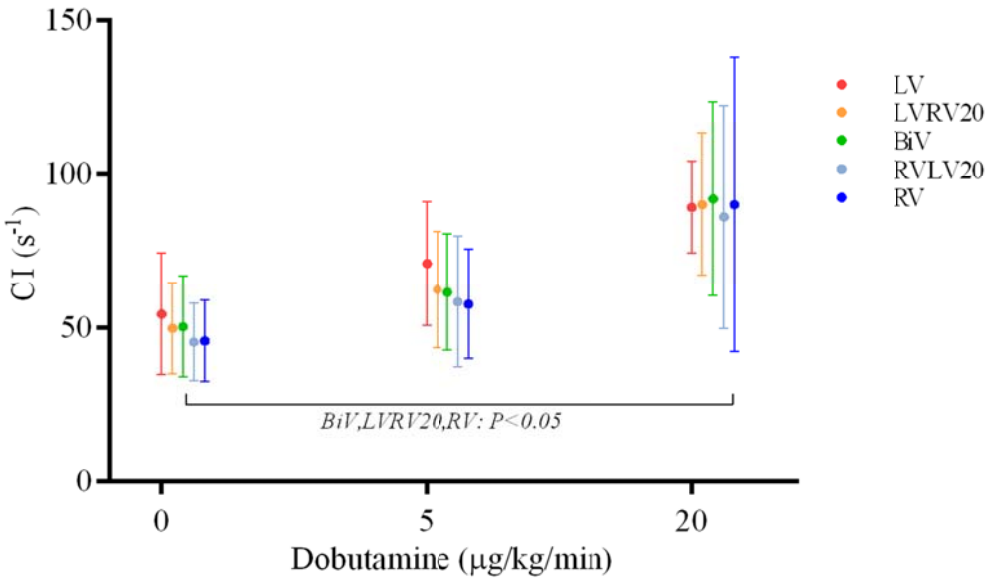

Figure 3-1: Variation of contractility index (CI) in effect of various pacing modes at baseline and different dobutamine stress levels.

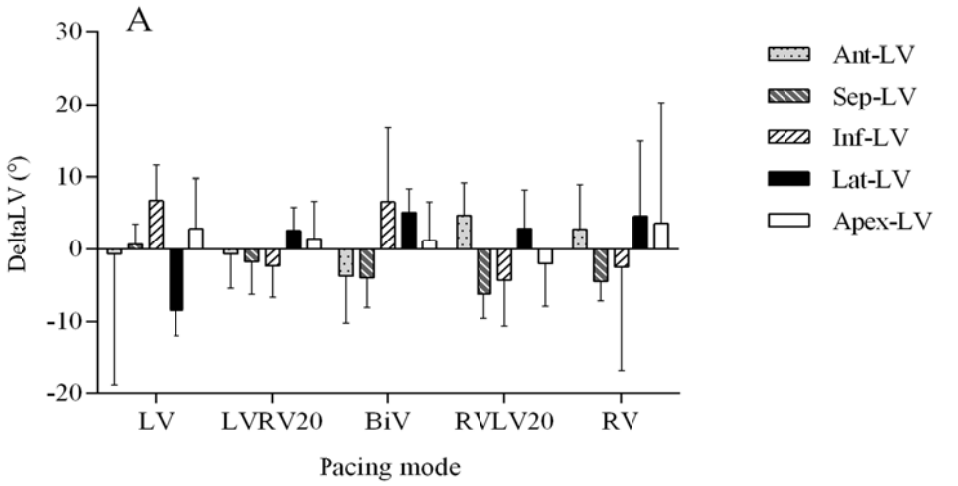
A
30
20
10
0
-10
-20
DeltaLV (°)
LV
LVRV20
BiV
RVLV20
RV
Pacing mode
Ant-LV
Sep-LV
Inf-LV
Lat-LV
Apex-LV

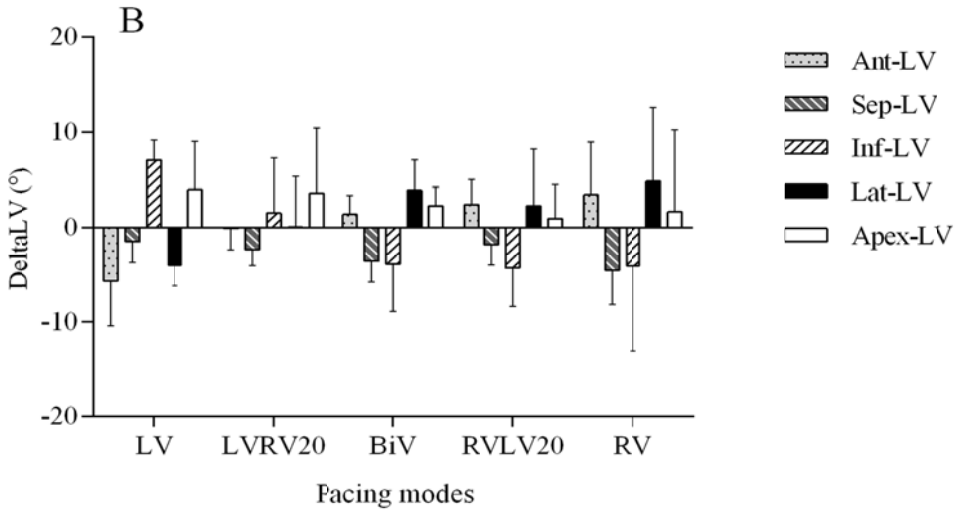
B
20
10
0
-10
-20
DeltaLV (°)
LV
LVRV20
BiV
RVLV20
RV
Pacing modes
Ant-LV
Sep-LV
Inf-LV
Lat-LV
Apex-LV

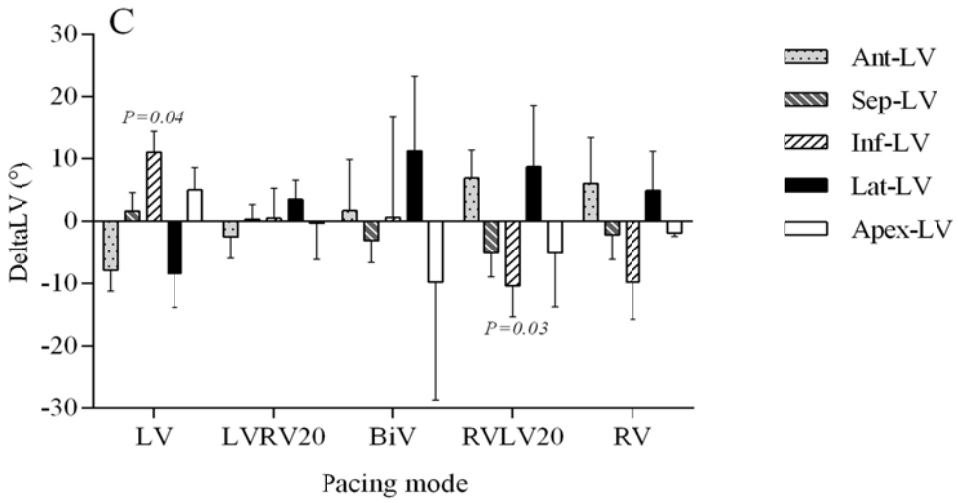
C
30
20
10
0
-10
-20
-30
DeltaLV (°)
P=0.04
P=0.03
LV
LVRV20
BiV
RVLV20
RV
Pacing mode
Ant-LV
Sep-LV
Inf-LV
Lat-LV
Apex-LV

Figure 3-2: Regional LV phase delays from the mean LV phase at baseline (A), levels of 5 (B) and 20 µg/kg/min (C) dobutamine stress in various pacing modes

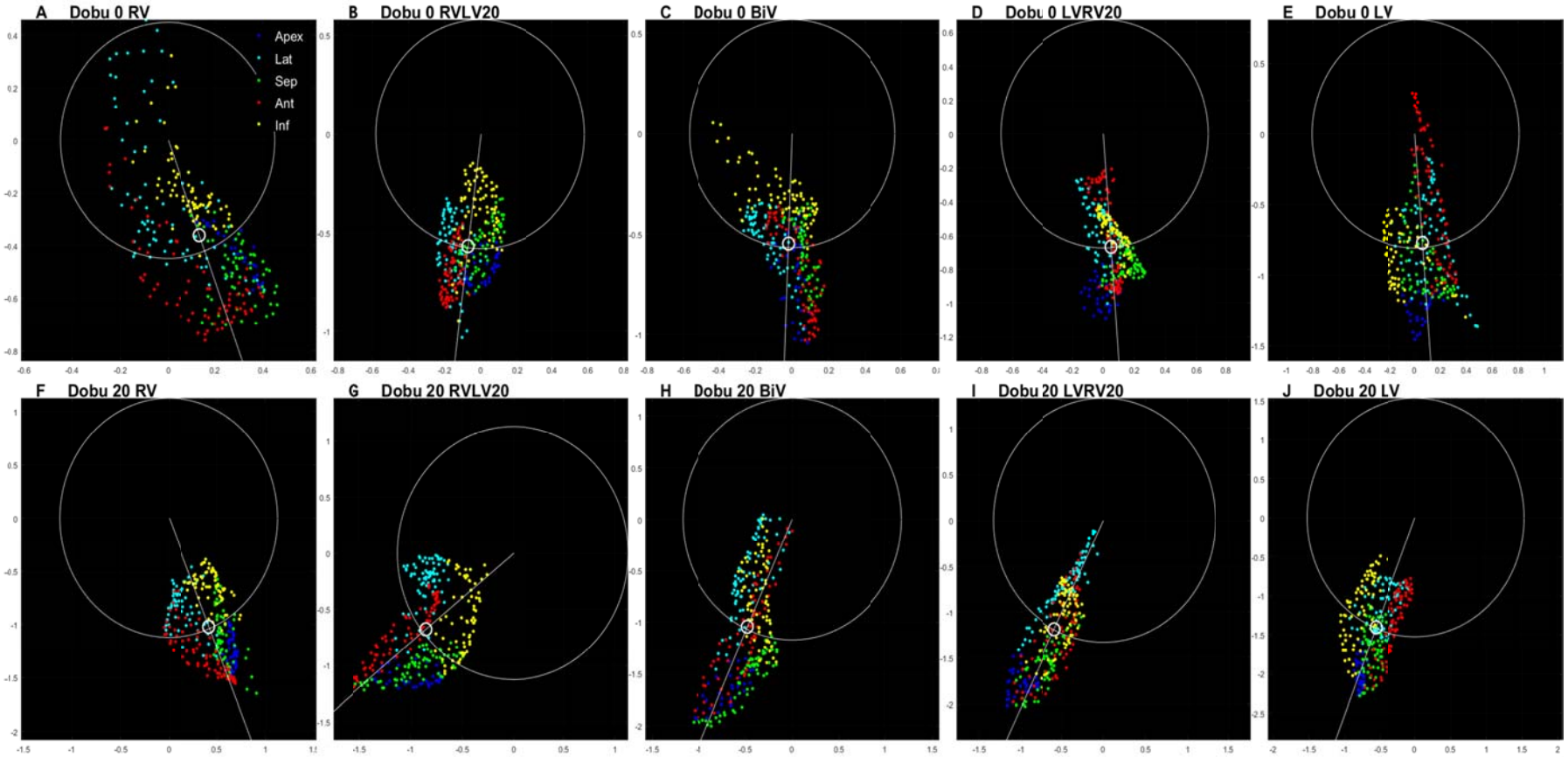

Figure 3-3: Thickening-based LV contraction phase of a dog during various pacing interventions at baseline (A-E) and at 20 μg/kg/min dobutamine (F-J) as an example. Each of the 400 dots contains both amplitude and phase of an actual vertex on the LV surface. They are expressed as a complex harmonic which contains both amplitude and phase, represented in a polar coordinate system with a radius and angle that correspond to amplitude and phase, respectively. The average amplitude (normalized to the percentage of average thickening) is presented by the circle and the average phase direction is represented by the line. The average efficiency presented by small circle is the projection along the direction of the mean phase and is negative if the vertex phase differs from the mean phase for more than a quarter of the cardiac cycle. While there is some sort of uncoordinated contraction at rest, in particular during RV and LV pacing, stress forced the LV walls to contract more homogeneously using increased amount of amplitude in nearly all pacing stimulations, especially during LVRV20 pacing.

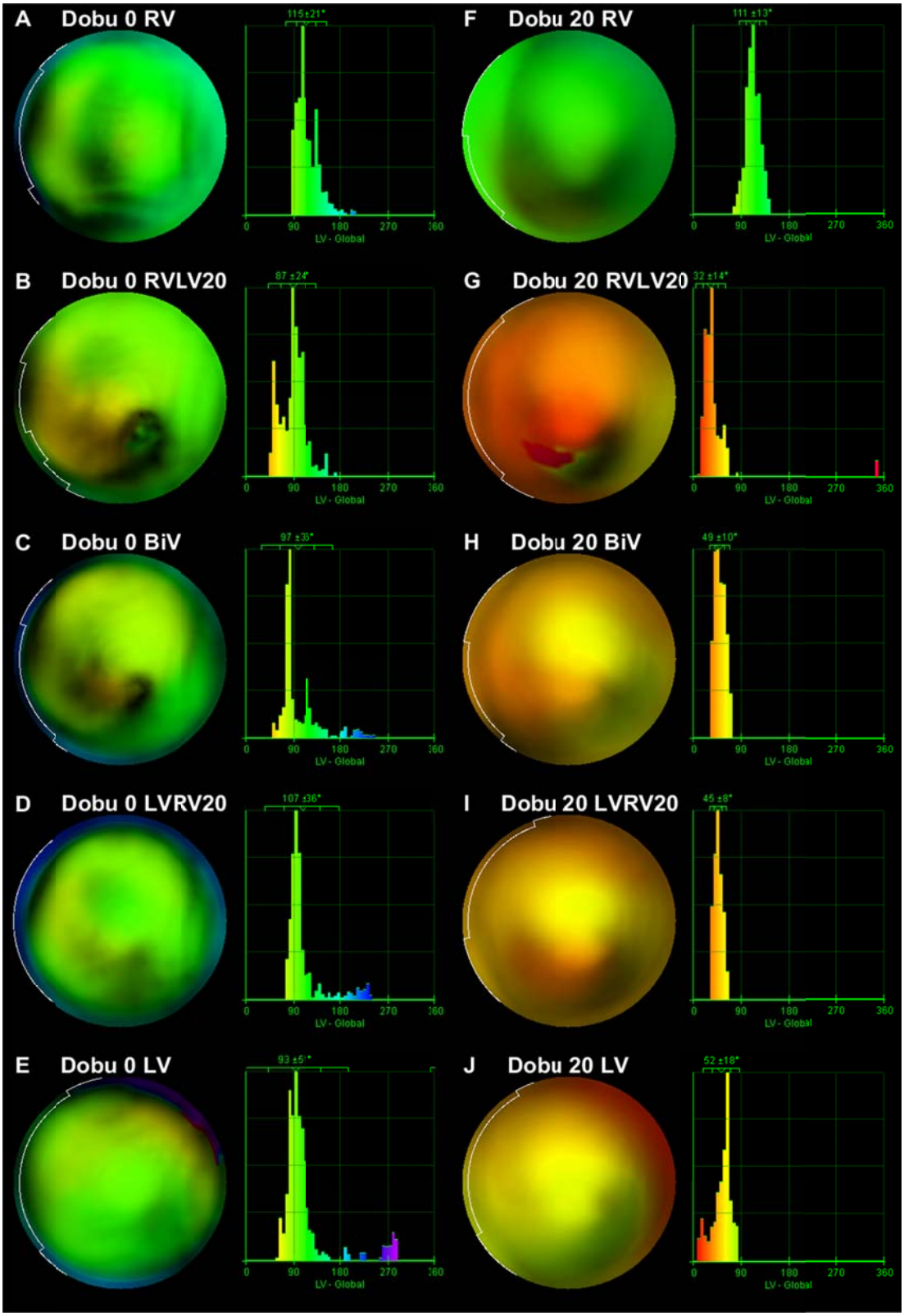
A Dobu 0 RV
116±21°
F Dobu 20 RV
111 ±13°
B Dobu 0 RVLV20
87 ±24°
G Dobu 20 RVLV20
32 ±14°
C Dobu 0 BiV
97 ±35°
H Dobu 20 BiV
49 ±10°
D Dobu 0 LVRV20
107 ±36°
I Dobu 20 LVRV20
45 ±8°
E Dobu 0 LV
93 ±5°
J Dobu 20 LV
52 ±18°
0 90 180 270 360
LV - Global

Figure 3-4: Phase analysis of GMPS as assessed by QGS software in a dog, same dog as shown in Figure 3-3, at baseline (A-E) and at 20 μg/kg/min dobutamine stress (F-J) during the stimulation through various pacing modes represented by polarmap and phase histograms.

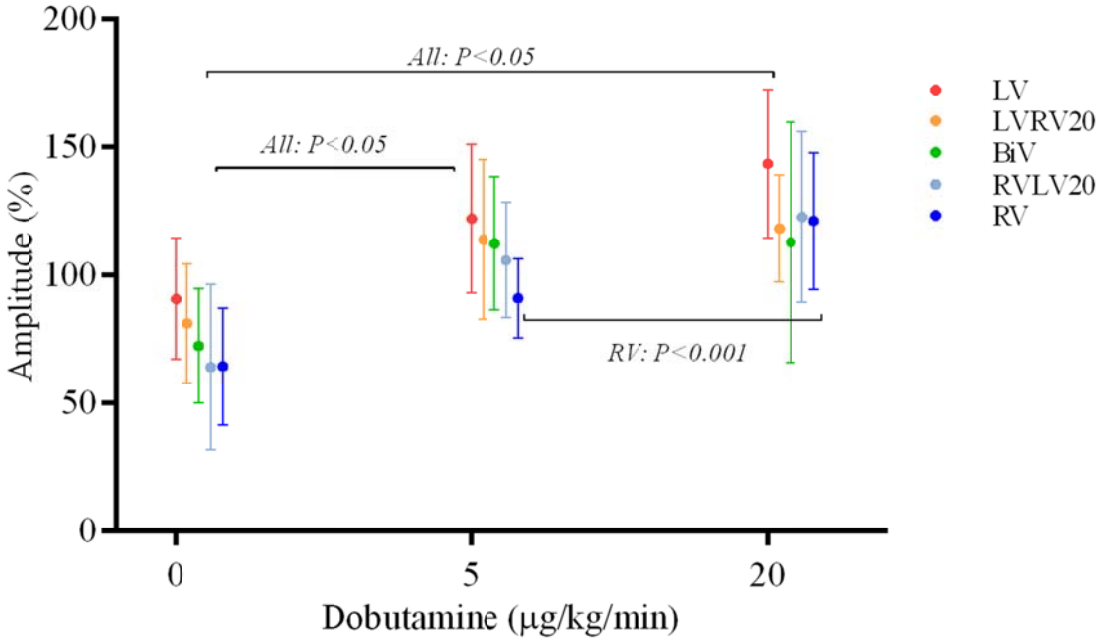

Figure 3-5: Variation of the amplitude of LV contraction with administration of levels of dobutamine stress when different pacing intervention is applied. The amplitude is normalized to the percentage of average thickening. Significant difference was found between rest and stress levels of 5 and 20 μg/kg/min dobutamine ($P < 0.05$) in all pacing modes; while only RV pacing showed significant improvement in contraction amplitude from 5 to 20 μg/kg/min stress level.

Tables

Table 3-1: LV hemodynamic parameters in effect of various pacing modes at rest.

Index	Dobutamine (μg/kg/min) =0				
	LV	LVRV20	BiV	RVLV20	RV
HR (bpm)	117.3±22.6§º	116.6±22.8§º	115.6±22.9§º	113.9±23.0§º	113.7±22.3 §º
QRS-interval (ms)	139.6±9.3	129.4±7.7	114.2±7.1	105.5±17.3*	100.3±26.4*
dP/dt_{max} ($mmHg.s^{-1}$)	1348±402§º	1449±514§º	1455±524§º	1339±511§º	1351±438§º
EDP(mmHg)	6.1±1.5	5.5±1.6	5.5±1.7	5.8±1.8	6.4±1.7
CI (s^{-1})	54.5±19.8	50.0±14.8	50.4±16.4§	45.4±12.6§	45.8±13.3§
EDV (mL)	43.8±15.3	43.2±16.8	42.8±15.7	43.5±14.5	42.8±17.6
ESV (mL)	25.4±11.1 º	25.4±12.0§º	26.0±13.4§º	27.3±11.9§º	25.8±14.1§º
LVEF (%)	42.6±11.3§º	42.6±10.0§º	41.4±11.5§º	40.5±9.4§º	42.2±9.8§º
SV (mL)	18.4±6.4§º	17.8±6.2§º	16.8±3.8§º	16.1±5.4§º	17.0±4.1
CO (L/min)	2.4±0.5§º	2.3±0.3§º	2.1±0.3§º	2.1±0.4§º	2.1±0.2

N=4. Data are presented as mean ± SD. $P < 0.05$ vs LV=*; RV=¥, LVRV20=¶; dobutamine levels of 5= º and 20 μg/kg/min =§. HR: heart rate; dP/dt_{max}, maximum rate of rise of LV pressure; EDP, end diastolic pressure; CI, contractility index; EDV, end-diastolic volume; ESV, end-systolic volume; LVEF, left ventricular ejection fraction; SV, stroke volume; CO, cardiac output.

Table 3-2: LV hemodynamic parameters in effect of various pacing modes during dobutamine-induced stress levels.

Index	Dobutamine (µg/kg/min) =5					Dobutamine (µg/kg/min) =20				
	LV	LVRV20	BiV	RVLV20	RV	LV	LVRV20	BiV	RVLV20	RV
HR (bpm)	136.6±15.2	136.8±15.1	136.5±15.7§	135.3±16.1	132.2±14.2	135.2±14.7	145.5±19.9	153.1±31.8*	141.8±19.0	138.6±16.8
QRS-interval (ms)	138.6±8.3	128.8±9.0	118.9±16.2	100.3±11.8*	104.3±19.3*	140.0±5.5	117.7±13.1	108.3±15.4*	91.7±16.3*	107.0±25.3*
dP/dt_{max} ($mmHg.s^{-1}$)	3194±1330	3565±1761	3625±1961	3411±1834	2875±976	4522±896	4586±939	4454±934	4340±939	4093±1035
EDP (mmHg)	5.7±1.5	4.8±1.1	5.3±1.2	5.0±1.2	5.1±1.4	7.7±1.2	5.8±1.7	9.6±5.6	10.2±8.4	9.5±5.9
CI (s^{-1})	70.9±20.1	62.5±18.9	61.7±18.9	58.6±21.2	57.8±17.8	89.3±14.8	90.1±23.1	92.1±31.5	86.2±36.2	90.1±47.9
EDV (mL)	42.8±12.6§	42.0±10.9	42.6±10.2	41.6±11.4	37.6±10.2	51.0±12.2¥	45.3±12.2	46.7±11.1¥	46.8±12.6¥	35.8±8.0
ESV (mL)	17.8±5.5	16.4±5.4	17.8±4.9	18.2±5.9	17.8±5.1	19.0±5.5	17.4±5.3	17.8±4.1	18.0±4.3	14.4±4.5
LVEF (%)	57.6±11.4	59.6±11.4	57.4±9.9	55.8±9.6	52.4±7.3	63.0±7.8	58.6±10.3	60.0±7.8	60.0±9.0	59.6±8.0
SV (mL)	25.0±9.8§	25.6±9.2	24.8±9.2	23.4±8.1	19.8±6.6	32.0±9.1¥	28.0±10.2	29.0±8.7¥	28.8±10.8¥	21.4±4.8
CO (L/min)	3.8±0.8	3.8±1.0	3.7±1.4	3.4±1.0	2.8±0.7	4.8±1.0¥	4.3±1.0	4.7±1.4¥	4.5±1.1¥	3.2±0.3

N=4. Data are presented as mean ± SD. $P < 0.05$ vs LV=*; RV=¥, LVRV20=¶; dobutamine levels of 5= º and 20 µg/kg/min =§.

HR, heart rate; dP/dt_{max}, maximum rate of rise of LV pressure; EDP, end diastolic pressure; CI, contractility index; EDV, end-diastolic volume; ESV, end-systolic volume; LVEF, left ventricular ejection fraction; SV, stroke volume; CO, cardiac output.

Table 3-3: LV dyssynchrony parameters in effect of various pacing modes at rest.

Index	Dobutamine (μg/kg/min) =0				
	LV	LVRV20	BiV	RVLV20	RV
QGS measurements					
Bandwidth (º)	177.6± 41.7§º	92.4± 44.6*§º	50.4± 23.8*¶	49.2±22.2*¶	73.2±30.4*º
Phase SD (º)	47.4±12.2 §º	26.3±11.3*§º	17.3±7.7*º	12.8±6.0*¶	18.8±8.6*º
Entropy (%)	60.0±3.0 º	51.8±8.0 §º	45.6±8.2*º	47.7±12.1*º	53.6±10.9º
SLD (º)	-27.3±25.5	-1.4±18.6*	8.3±15.9*	12.7±10.5*	5.7±13.7*
MHI_4MPI measurements					
THI (%)	91.9±4.3 º	97.6±1.3¥	95.0±4.3	97.6±1.3¥	90.3±10.3§º
TSLD (º)	-8.1±4.5	4.7±5.7*	7.8±8.6*	5.9±8.3*	7.8±16.3*

N=5. Data are presented as mean ± SD. P < 0.05 vs LV=*; RV=¥, LVRV20=¶; dobutamine levels of 5= º and 20 μg/kg/min =§. SLD, septal-to-lateral delay; THI, thickening homogeneity index; TSLD, thickening septal-to-lateral delay

.

Table 3-4: LV dyssynchrony parameters in effect of various pacing modes during dobutamine-induced stress levels.

Index	Dobutamine (µg/kg/min) =5					Dobutamine (µg/kg/min) =20				
	LV	LVRV20	BiV	RVLV20	RV	LV	LVRV20	BiV	RVLV20	RV
QGS measurements										
Bandwidth(º)	72.0±52.1	32.4±8.0*	33.6±6.8*	31.2±9.9*	40.8±10.7	68.4±21.0	40.3±18.1	44.7±11.4	44.4±19.7	52.8±15.5
Phase SD (º)	22.0±12.3	7.8±2.0*	7.3±2.0*	6.9±1.7*	10.0±3.0*	18.7±4.3	8.8±4.5*	11.4±2.2	12.1±4.3	13.5±3.3
Entropy (%)	51.0±7.0	38.8±6.3*	36.0±7.8*§	35.4±5.2*	41.8±6.8§	52.6±5.3	37.8±3.0*¥	48.4±6.5	42.2±10.8*	51.0±8.2
SLD (º)	-15.0±5.2	2.1±2.5	9.5±4.4*	2.7±3.7	10.8±5.0*	-17.2±7.3	0.2±3.2	10.0±6.0*	10.7±8.4*	11.6±9.4*
MHI_4MPI measurements										
THI (%)	97.9±0.9	97.9±0.8	98.7±0.4	98.0±1.9	97.2±2.3	96.3±2.0	98.5±0.5	95.0±2.8	95.7±2.4	97.1±0.6
TSLD (º)	-2.3±3.1	2.3±5.0	7.3±2.6	4.6±7.5	10.0±8.5*	-8.2±6.4	4.1±4.7*	11.8±9.4*	14.8±12.7*	7.4±8.8*

N=5. Data are presented as mean ± SD. P < 0.05 vs LV=*; RV=¥, LVRV20=¶; dobutamine levels of 5= º and 20 µg/kg/min =§.

SLD, septal-to-lateral delay; THI, thickening homogeneity index; TSLD, thickening septal-to-lateral delay.

Discussion and Conclusion

The current thesis was set out to explore the robust and accurate methods for quantifying mechanical dyssynchrony (MD) and also the role and impact of functional stress on inter- and intraventricular MD in three different experimental models of control, DCM, and AV block submitted to ventricular pacing.

The overall literature on ventricular "MD" subject and specifically in the context of "stress dyssynchrony" is inconclusive on several vital questions. The thesis sought to answer three of these questions:

1. Which nuclear methodology is more accurate and robust in the assessment of stress-MD?
2. What is the range of difference in inter- and intraventricular MD parameters when the patient is submitted to various levels of functional stress?
3. Is the optimal pacing solution at rest in terms of synchrony of contraction also the best one during the exercise and increased heart rates?

The response to these questions was searched and proposed as three manuscripts within the respective chapters. The main findings can be summarized here as following:

1. Which nuclear methodology is more accurate and robust in the assessment of stress-MD?

In the current thesis, two nuclear techniques of GMPS and GBPS were utilized for stress-MD assessments. While both methods could automatically identify the pattern and extent of under-stress ventricular contraction dyssynchrony, GMPS seemed to be more reliable; since the

global cardiac motion was always present in GBPS technique and it was non-separable from the endocardial motion and the associated MD. Moreover, the thickening-based approach was more accurate and robust than displacement-based measurements in GMPS as it yielded more realistic MD findings once the normal subjects were evaluated. Among different parameters of the phase analysis techniques, the sensitivity of entropy and CHI/THI was promising in specifying the MD variations during the stress conditions not only in the DCM but also in the case of normal ventricular anatomy and function.

2. What is the range of difference in inter- and intraventricular MD parameters when the patient is submitted to various levels of functional stress?

In chapter 1 with control subjects, synchrony of LV contraction in thickening increased from baseline to 5 μg/kg/min dobutamine and reached a plateau at 10 ± 5 μg/kg/min dobutamine. In chapter 2 with a DCM model, different levels of dobutamine stress, even in close intervals, had a significant impact on intraventricular MD parameters and the changing trends were mostly seen as going toward the perfection of synchrony. However, inter-subject variability and individual differences in the magnitude and pattern of change in interventricular delays precluded any definitive conclusion about the effects of dobutamine stress in interventricular MD. In contrast to the control group that intermediate levels (5 to 10 μg/kg/min) of dobutamine infusion were enough to generate maximum contraction efficiency (reaching a plateau), the outset point of MD improvement was 5 μg/kg/min dobutamine for the DCM group and it continued through further stress levels. Finally under ventricular pacing in chapter 3 with AV block model, dobutamine-induced variation in MD was positive at the level of 5 μg/kg/min dobutamine for all the pacing interventions both in the case of amplitude and uniformity of the timing of contraction. However, further stress level up to 20 μg/kg/min

dobutamine did not make a considerable change in the phase and amplitude of contraction at LV and LVRV20 and even worsened the synchrony of the phase of contraction at BiV, RVLV20, and RV pacing modes.

3. Is the optimal pacing solution at rest in terms of synchrony of contraction also the best one during the exercise and increased heart rates?

The results from Chapter 3 revealed that the mechanical response of the LV myocardium to a specific type of pacing intervention might be overestimated or underestimated at rest. However, intrinsic physiologic effects of stress resulted in more accurate MD assessments with lesser variability in subjects who underwent pacing. The synchrony of contraction both in the case of contraction onset within the cardiac cycle (phase) and regional stroke volume (amplitude) was significantly improved at a low-stress level in all the pacing modes. While further stress did not decrease the homogeneity of contraction in LV and LVRV20 pacing modes, it made a significant increase in the entropy of regional contraction in BiV, RV, and RVLV20 pacing modes. Hence, greater stress corresponded to a greater contraction dyssynchrony whether the stimulation via LV was not applied or was applied at the same time with the RV site or by 20 ms delay. In the case of BiV pacing, for instance, earlier contraction of the apex and later contraction of the lateral wall at maximum stress made total entropy of about 48% relative to the baseline value (46%) showing that higher stress can enforce higher discoordination in regional mechanical contraction. In fact, the sequence of induced electrical activation affects the myocardial response or the compatibility to the stress condition. BiV pacing with pre-activation of the LV closely resembles the intrinsic ventricular activation in developing normal mechanical contraction at higher levels of stress and higher heart rates do not hamper the activation coincidence between the two sides of the heart, but rather strengthen

it, making the synchrony of mechanical contractions more efficient. Overall, although, it was hard to find the optimal pacing solution at rest, some differences were lightened up by using the stress levels. Therefore, the optimization process of CRT devices is more robust to be done in the period of stress or exercise than resting condition that is routinely practiced. Since, dobutamine-induced stress may bring about differences in myocardial contractility, making stronger evidence to guide on the decision table for any prediction or optimization of response to the ventricular pacing.

The effect of adrenergic stress stimulation on regional LV function and myocardial deformation has been previously studied in normal canine and human subjects by tagged-MRI technique, mostly with the approach of using stress-MRI method in detecting myocardial ischemia.[109-111] A uniform increase in displacement, radial thickening, and circumferential shortening was seen in a dose-response pattern from baseline to 10 μg/kg/min dobutamine infusion in all those studies without additional increases at higher doses. Thus, similar to our finding based on the presence of a plateau in 10 μg/kg/min dobutamine, saturation of thickening homogeneity is consistent with the saturation of wall thickening and circumferential shortening at this stress level. The reason of such saturation in myocardial shortening has been under question. Scott et al.[110] assumed that the decrease of the preload (due to lower venous return) and thus a decrease in end-diastolic volume (EDV) in spite of an increased contractility could be the reason of lack of improvement in circumferential strains at high dobutamine doses. However, we observed no changes in LV EDV, same as the findings in the rat study, to support this hypothesis. Daire et al.[111] suggested two possible mechanisms for the observed saturation. The first one is based on the shortage of the tagging measurement

at higher heart rates in which the duration of the tagging pulse does not change with respect to the cardiac cycle and the myocardium tagging no longer occurs in end-diastole but rather in mid-systole. Hence a possible underestimation in circumferential shortening might occur at high dobutamine levels. They did not apply this hypothesis in their work to see whether introducing a trigger delay and tagging preparation at the end of the diastole would obviate the saturation. Scott et al. previously thank about the heart rate increase in their MRI study and compensated this problem but still found the same results. Thus, based on the findings of our first chapter, we advocate from Daire's second suggestion that successive doses of dobutamine may produce a desensitization of dobutamine receptors and consequently an underestimation of the dobutamine effect at higher doses (>10 μg/kg/min).[111]

The presence of MD in control subjects might seem very odd in the first chapter. How could it be possible to have some sort of heterogeneity in LV regional contractions in an intact heart? Also, how adrenergic stimulation can to some extent obviate this dyssynchrony? Baseline heterogeneity in LV regional and transmural contraction has also been shown in the studies performed by high spatial and temporal resolution tagged-MRI techniques.[110,111] A number of factors such as muscle fiber orientation, autonomic receptor density, and electrophysiologic properties could be involved in observed regional heterogeneity in myocardial contraction.[110] Since this thesis uses the pacing intervention in the third Chapter, it is pleasant to talk more about the heterogeneity of electrophysiologic properties in detail. The myocardial electrical activation sequence (the prerequisite for mechanical contraction) and the repolarization time across the LV walls have been extensively studied during the last two decades. One of the earliest studies in the human subject was performed by Franz et al.[9] that with monophasic action potential mapping in normal subjects suggested the presence of a

transmural gradient of repolarization in which epicardium repolarizes before the endocardium. With activation proceeding from endocardium to epicardium, they showed a negative correlation between the activation time (AT) and the action potential duration (APD). Sites with shortest AT had the longest APD in both the endocardium and epicardium. Though, progressively later activation was associated with progressively earlier repolarization. Although, their findings did not verify any regional ventricular gradient of endocardial AT and APD from apex to base or from septal to the lateral wall, they noted that APDs were markedly inhomogeneous even within a given region of the LV. The longest average APD was measured in the septal and inferior area and the shortest at anteroapical and posterolateral sites. Observations by Franz et al. about endocardial heterogeneity in electrophysiological properties even in closely adjacent areas were later seen by Cowan et al.[112] in the epicardium. However, after pooling data between patients, they found that activation and repolarization sequences were opposite in epicardium; meaning activation proceeded from septum to free wall and from apex to base, whereas repolarization proceeded from base to apex and from free wall to septum.

Therefore, a consensus about the presence of a transmural difference in action potential morphology and duration was yielded so that APDs were longest near the endocardium and shortest near the epicardium and since differences in APD supposed to be greater than AT, a transmural voltage gradient toward earlier recovery at epicardium was confirmed.[113] However, evidence from the recent studies[114] supported the heterogeneity of the AT-ADP relation in the whole human heart. In fact, while the relation of AT-ADP is negative in most parts of the LV, positive relations either with early AT and early repolarization time (RT) or late AT and late RT could be seen in LV regions.

Data above based on the heterogeneity in electrophysiological properties of ventricular myocardium due to the nonuniform expression of ion channels raise the question of how a myocardial cell recognize the time of repolarization besides all these heterogeneities within the ventricle? One assumption demonstrated by Franz et al.[9] from the earlier studies which then was emphasized in recent years[113] is the electrotonic interaction (i.e. ionic changes in the membrane of one myocyte can directly influence neighboring myocytes through gap junctions) that can relate APD to activation sequence. As mentioned by Franz et al., "During the cycle of ventricular depolarization and repolarization, electrotonic current from the area to be excited last may retard repolarization of areas excited earlier in the activation sequence, and current from the first area to repolarize may speed repolarization in areas not yet repolarized."[9] In diseased hearts, AT-APD relationships are attenuated, and more dispersion in RT could be seen in cardiomyopathies.[113]

Nevertheless, how dobutamine affects the electrical activation sequence and APDs in normal ventricular myocardium? In the human ventricle, John et al.[115] found a variable response of normal myocardium (posterolateral wall of LV and RV side of interventricular septum) to dobutamine with either lengthening or shortening of APD. This variable response was reported to be as the result of either the dobutamine alpha-beta adrenoreceptor influences, mechanoelectrical feedback whereby the force of contraction and degree of stretch alter repolarization, or the interactive effects of beta-stimulation on rate-adaptive mechanisms of APD. The study by John et al. once again confirmed the baseline electrical heterogeneity of regional ventricular myocardium while also showing the heterogeneity of subject response to dobutamine stress. The number of subjects was limited (n=7) in their study and action potential recording was not performed in several regions of LV myocardium to get to a

conclusive response to our question that what is the reason of increased LV contraction synchrony with the administration of dobutamine stress? As stated earlier in the introduction part, repolarization time is the sum of AT and APD. Though, the positive relationship between contraction synchrony and dobutamine might come from the effect of dobutamine stress on AT and depolarization gradient, overlooking the APD. Callaghan et al.[116] studied the effects of epinephrine, as a catecholamine, and the exercise stress on RV depolarization gradient. They concluded that catecholamines decrease the depolarization gradient in a dose-dependent response irrespective of underlying baseline pacing rate. Although it might be a notable outcome in our way through finding the reason for ventricular stress synchronization, it must be mentioned that we did not measure any significant alteration in QRS durations, as a depolarization gradient sensor, by dobutamine stress in our three sub-studies. Without a sensible decrease in ventricular activation times, nonetheless, increased contractility and enhanced contraction synchrony were clearly seen by the induction of dobutamine stress in our studies similar to the effect of other catecholamines.

It is worthwhile to come back once again to the APD and the study performed by Scott et al. in which dobutamine stress quickened the myocardial shortening and thereby obviated baseline variations in radial thickening of apical versus basal LV myocardium (apical thickening was less than basal thickening at rest).[110] Electrophysiological properties of apex resemble that of endocardium which activates early but has the longest functional refractory or repolarization period opposite to the epicardium or LV base.[117] Therefore, it might be possible that dobutamine stress stimulation leads to a reduced dispersion in APDs and an electrical homogeneity between the levels of LV myocardium (basal versus apical levels) and therefore improves the apical thickening and overall LV contraction synchrony. More

comprehensive studies about regional LV electrophysiological properties during rest and stress are needed for recognition of the causality of ventricular synchronization under stress.

Dispersion in repolarization does exist in normal myocardium and its amount is not at all sufficient to induce arrhythmias and significant MD as was shown in the first chapter. However, in diseased hearts, more dispersion in repolarization time happens and the AT-APD relationships are highly attenuated.[113] This phenomenon is accompanied by worsened MD even in the presence of normal electrical activation sequence or QRS width as seen in the second chapter. Although the underlying pathophysiological mechanisms leading to intraventricular MD in the presence of electrical synchrony is poorly understood in humans, it seems that regional variability of excitation-contraction coupling and myocardial contractile strength are the main problematic factors.[118] Several underlying electrophysiological and cellular changes can make those regional heterogeneities. It has been shown that APD change of one beat is inversely associated with the changes in contractility of the next beat.[119] Therefore, with respect to the hampered intrinsic property of the myocardium in the adaptation of APDs to their related ATs in cardiomyopathies, possible changes in APDs may play a role in the variability of myocardial contractile strength.[113,118] Also as further reviewed by Jackson et al.,[118] regional variability in multiple cell and molecular pathways including cytokines (cardiotrophin-1), calcium handling proteins, gap junction-alpha-1 protein (connexin 43), stress response kinases and tissue necrosis factor-alpha expression could be involved in excitation-contraction uncoupling and regional heterogeneity of myocardial thickening and mechanical contraction.[118] In addition, heterogeneous metabolism[120] and imbalance of myocardial blood flow can more fuel the regional heterogeneity in dilated cardiomyopathies. Thus, many mechanisms involve in developing dilated cardiomyopathies that can be

considered as the underlying mechanisms leading to the MD with the presence of electrical synergy.

As was shown in Chapter 2, dobutamine stress significantly reduced the variability of contraction timing in different regions of left ventricle. Since, the APD, contractility, and myocardial strain changes are interdependent factors, and considering the fact that dobutamine stress shortens the APDs in the area of weakened contractility properties,[115] it can be hypothesized that dobutamine stress improves the contraction homogeneity through reduction of the vast disparities in APDs among the LV regions.

Although all of MD underlying mechanisms and regional heterogeneities named before have been shown to normalize following CRT, it seems that a certain electrical substrate (LBBB)[32] is required by CRT to obviate all those problematic MD mechanisms. It means that all the mechanisms developed as the result of lacking or delayed electrical activation sequence that with induction of the appropriate electrical stimulation, the cellular mechanochemical inhomogeneities would disappear and then functional benefits would be conferred in CRT candidates. Therefore, although the MD with all of the mentioned underlying mechanisms could plausibly be present in patients with DCM and narrow QRS complex, the presence of normal excitation-activation sequences interfere with the induced ectopic wavefronts which might be harmful to the patients.

If we look back to the study performed by Rocchi et al.[48] who showed the superiority of exercise stress to rest-echo in predicting LV reverse remodelling and functional improvement after CRT, we realize that LV MD had a reduction from rest to the exercise stress at non-responders exactly opposite to what was seen for the responders (60±41 ms at rest vs 41±43 ms at stress in non-responders and 91±30 ms at rest vs 133±41 at stress in

responders). As they reported, 33% (21/64) of non-responders, in spite of possessing CRT selection criteria based on the current guidelines, were the patients who showed lesser dyssynchrony (or maybe better to say homogenous and improved excitation-activation-contraction coupling) at stress than rest condition. The role of stress on underlying MD mechanisms is not yet clear to explain the dual behavior of stress in the same cohort of patients. But what is apparent from the previous studies with narrow QRS patients is that, if the stress somewhat improves the MD, it means that the excitation-activation-contraction coupling could still be intrinsically established and using the ectopic stimulating fronts would not help anymore in this regard. Hence, we believe, as previous studies also suggested,[48,50] that one of the methods to dichotomize CRT responders and non-responders even in DCM and narrow QRS population could be to look at the LV MD response of the patients to the stress. As a note, although, RethinQ[121] and EchoCRT,[30] two multicenter randomized controlled trials, are evidence of negative clinical effects of CRT in patients with DCM and narrow QRS, there are lines of evidence on the positive effects of CRT in these patients. Thus, many definitive hypotheses about underlying MD mechanisms and whether they are potential targets for pacing are yet to be tested in this regard. As was seen in our study cohort in Chapter 2, lesser stress-MD among DCM subjects may show that establishing an appropriate activation-contraction coupling is still possible in ventricular myocardium and intrinsic physiologic effects of stress help to show this effect. Thus, even if CRT is supposed to help the DCM and narrow QRS patients, it will not have assisted in patients with lesser stress than rest-MD. As a conclusion, as stated by expert reviewers in 2015,[118] "CRT will have a role in narrow QRS patients, but this will be in a minor subgroup with a specific target for benefit with CRT." Also

as they believe, newer advanced techniques such as multisite and endocardial pacing can significantly reduce the amount of electropathy, improving the chance of benefit from CRT.

In the third chapter, the coordination of contraction between the right and left part of the LV myocardium was to some extent lost at higher heart rates, once the LV was paced by simultaneous BiV or RV pacing modes. In fact, the reason of the worsened contraction synchrony through the maximum level of stress under BiV, RV, and RVLV20 modes, contrary to the natural state in the control group, might be faster electrical conduction of the RV endocardial cells relative to the distant LV myocardium.[7] Therefore, for the later conduction of the signals from LV epicardial site and the fact that naturally the onset of LV activation is 10 ms before RV endocardial activation,[7,10] BiV pacing with pre-activation of LV closely resembles to the intrinsic ventricular activation in developing normal mechanical contraction at higher levels of stress. Hence, if the natural sequence of the electrical stimulation is not respected, it will be problematic (i.e. increase of MD) at higher heart rates. The mechanics of the LV contraction under single- and BiV pacing was previously studied by tagged-MRI. On a healthy canine model, it was shown that BiV pacing has a greater impact on correcting the spatial distribution of LV contraction than on improving the temporal synchronization of contraction.[122] This observation is in agreement with our results based on better temporal contraction synchrony with sequential (LVRV20) than the simultaneous pacing. Also, they showed that BiV pacing improved the spatiotemporal synchrony of contraction greater than RV apical pacing alone.[122] These two pacing modes did not show any significant difference in the case of MD and functional parameters in our study. Our results are also in contrast to similar dyssynchrony studies,[123-126] measured by echocardiographic methods, on the AV

block subjects with normal function, which demonstrated that BiV pacing was superior to the RV pacing in the case of SLD.

This thesis encountered a number of limitations, which need to be considered. The number of animals used for each sub-study was limited. While it is always a restriction in animal experiments, it can limit the statistical power of the tests used. For this reason, using the MHI_4MPI as a diagnostic tool for the assessment of MD in particular for the prediction or optimization of response to CRT requires more validation. Another constraint for the current thesis is the lack of an LBBB model among the models used; since it is amenable to CRT and the results of stress-MD assessments could be applicable on its potential target. Also, a non-ischemic cardiomyopathy model was chosen in the second chapter, since generating similar extent of ischemic pathology at all the subjects was difficult. Overall the pathologic model used in this study helped us to better understand the relationship between the stress-MD and HF. Transferring the methods and findings of this thesis directly to the clinical practice is a critical concern. One of the most important issues in this regard is the time of the experiment. The gradual increase in the dobutamine stress infusion up to 20 μg/kg/min has been previously performed on the clinical basis[110], and no unexpected, and inappropriate side effects were encountered in about 20 minutes infusion time. However, using of nuclear imaging techniques is totally different than the MRI or the echocardiography. For instance, after 2 minutes of dose change in MRI, about four sets of images could be obtained in only 3 minutes at each infusion rate. In comparison, at SPECT imaging at least 10 to 15 minutes is required for image acquisition at each dose change (at least about 1 hour for total analyses). Therefore, although the applied protocol and methodology may seem transferable, they must not be directly used in

the clinical study. Instead, if only one safe dobutamine stress dosage like 10 μg/kg/min (which develops a plateau at contractility and strain) is selected and the stress versus rest-MD is analyzed in the patient, then, the entire imaging techniques and phase analyses for MD assessments are completely transferable. Hence with an appropriate stress protocol, the stress-gated myocardial perfusion SPECT imaging can be performed for the stress-MD assessments in place of further CRT optimization or prediction purposes. Finally, low spatial resolution and count statistics of the SPECT images remains a limitation. However, there is an ongoing project in our group for quantification of MD with the purpose of CRT optimization by PET/computed tomography (CT) imaging that with higher tracer counts and better spatial resolution can solve the SPECT problem to a great extent.

One of the future directions for this thesis will be to search about whether the stress LV MD indices produced by the nuclear techniques specially GMPS can predict the response to CRT. In the meanwhile, it will be desirable to search for the perfect indicators of LV MD (among the MD parameters used in this thesis) at rest compared to stress condition in a large subset of CRT candidates. Also, it would be interesting to use the PET/CT system for MD assessments and to optimize the patient selection; since it provides a better spatial resolution besides valuable information about the tissue viability and leads placement. Thus, further prospective clinical studies in which automated assessment of stress-MD being considered, can more clarify the relationship between the MD and CRT non-responders.

As mentioned above, one of the future challenges in our group is to use the gated ^{18}F-fludeoxyglucose (FDG) PET/CT imaging for optimization of patient selection, lead placement,

and the response to CRT due to its advantages over GMPS imaging. Besides the importance of reliable MD assessment, to increase the CRT response rate, it is important that the LV lead(s) be placed in regions of viable tissue(s).[127] Although, both the GMPS[33,128] and gated PET[127,129] have been demonstrated to assess the LV MD and regional viability for the CRT patient selection and LV lead positions, studies on using the gated PET imaging in this field is quite limited. In the first part of ongoing research, our primary objective is to validate the FDG PET/CT imaging ability to measure the effects of three extremely different pacing modes (BiV versus single-site) on LV systolic function and LV intraventricular MD and to see the capability of using FDG PET in post-implant CRT programming optimization. Also, the assessment of lead placement in the patients receiving BiV pacing helps to identify if the LV leads are placed at or near the site of the viable segment with the latest activation.

Our preliminary results on three LBBB patients receiving a BiV pacing with LV multi-leads were satisfactory in showing the pacing-induced differences in function and MD parameters. However, the LV segmentation was not easy to perform in these patients; 2 of them had the myocardial area being infarcted and one of them indicated a non-homogenous FDG uptake within the LV (lack of uptake in the septum), made it difficult to find the LV contour properly. Using the CT images, we were able to mark the place of the LV leads and to fuse them into the 3-D FDG viability image. These first findings motivate us towards using PET-guided CRT LV lead placement in the cath lab. In fact, before the CRT implantation, an FDG PET/CT imaging not only can determine the amount of myocardial MD and scar tissue and therefore help in CRT patient selection but also if the patient being a candidate, this information would be applicable during the CRT implantation to find the optimal LV lead

position. Thus fusion of the fluoroscopy venograms and 3D PET images would guide the electrophysiologist to successfully place the LV leads into the target venous site.

The first tool-kit was developed in 2014 to reconstruct 3D LV venous anatomy from dual-view fluoroscopic venograms and to fuse it with LV epicardial surface on GMPS; it was suggested that the 3D fusion method is both technically accurate and clinically applicable.[130] The findings also encourage us to start the second part of the study soon which its objective is to optimize the interventricular delay in CRT patients. However the acquisition time, once the effect of several pacing modes (programming the interventricular delay) is desired to measure and the cost, once several episodes of FDG-PET/CT imaging is required for the CRT optimization and follow-up are the two major concerns in the discourse. The reduction in acquisition time would increase the image noise while longer acquisition time increases motion artifacts due to patient movements. Also, the acquisition time might have an impact on the quality of final MD parameters derived by phase analysis of the PET/CT imaging. Hence, before the first part of the studies, the effect of PET/CT acquisition time on LV MD was studied as a prerequisite. In fact, the scanner allows for the selection of a subset of list-mode data to perform the image reconstruction based on the chosen acquisition time. Therefore, using different acquisition time points of 1, 3, 5, 10, and 15 minutes (as a gold standard) in 41 HF patients with coronary artery disease, the intra-class correlation coefficient (ICC) indicated the lower-level confidence limit > 0.75 (excellent reliability) only at 10 min acquisition for all the functional and MD parameters. Therefore, 10 min acquisition would allow us to measure the effects of 5 to 6 pacing modes in about an hour. Concerning the cost of imaging for the CRT patient selection and follow-up process and also the radiation burden with the serial

scans, it is worthwhile to mention that the benefits may outweigh the risk in the end-stage HF patients for whom being a CRT responder would be the only chance for surviving.

In summary, the findings of the current thesis show that the phase analysis of both GBPS and GMPS clearly and automatically identify the extent and pattern of ventricular MD under dobutamine stress infusion, in a clinical range, either in normal or HF subjects. The MHI_4MPI software with useful indices and methodologies provided the evidence on the superiority of thickening over displacement approach on reliable MD assessments. Different levels of functional stress induced significant changes in hemodynamic and MD parameters in all of the experimental models used. Also, intrinsic physiologic effects of stress resulted in a more accurate MD assessment with lesser variability in subjects underwent pacing. Based on the reliable stress-MD assessments with GMPS, BiV with LV pre-activation more resembled the intrinsic ventricular activation at higher levels of stress and it was the preferred site of stimulation rather than single site pacing in the AV block model with normal function.

Bibliography

1. Healey JS, Merchant R, Simpson C et al. Canadian Cardiovascular Society/Canadian Anesthesiologists' Society/Canadian Heart Rhythm Society joint position statement on the perioperative management of patients with implanted pacemakers, defibrillators, and neurostimulating devices. Canadian Journal of Cardiology 2012;28:141-51.
2. Beck H, Boden WE, Patibandla S et al. 50th Anniversary of the first successful permanent pacemaker implantation in the United States: historical review and future directions. American Journal of Cardiology 2010;106:810-8.
3. Epstein A, DiMarco J, Ellenbogen K et al. Heart Rhythm Society 2012 ACCF/AHA/HRS focused update incorporated into the ACCF/AHA/HRS 2008 guidelines for device-based therapy of cardiac rhythm abnormalities: a report of the American College of Cardiology Foundation/American Heart Association Task Force on Practice Guidelines and the Heart Rhythm Society. Circulation 2013;127:e283-e352.
4. Heart&Stroke-Foundation. 2016 Report on the health of Canadians. (2016), Retrieved from http://www.heartandstroke.com/atf/cf/%7B99452d8b-e7f1-4bd6-a57d-b136ce6c95bf%7D/2016-HEART-REPORT.PDF.
5. Mozaffarian D, Benjamin EJ, Go AS et al. Executive Summary: Heart Disease and Stroke Statistics-2016 Update: A Report From the American Heart Association. Circulation 2016;133:447.
6. Kirk JA, Kass DA. Electromechanical dyssynchrony and resynchronization of the failing heart. Circulation Research 2013;113:765-776.
7. Ellenbogen KA, Wilkoff BL, Kay GN, Lau CP. Clinical Cardiac Pacing, Defibrillation and Resynchronization Therapy E-Book: Expert Consult Premium: Elsevier Health Sciences, 2011.
8. Lilly S. Pathophysiology of Heart Disease. 6th ed: Philadelphia: Wolters Kluwer, 2015.

9. Franz MR, Bargheer K, Rafflenbeul W, Haverich A, Lichtlen PR. Monophasic action potential mapping in human subjects with normal electrocardiograms: direct evidence for the genesis of the T wave. Circulation 1987;75:379-386.
10. Durrer D, Van Dam RT, Freud G, Janse M, Meijler F, Arzbaecher R. Total excitation of the isolated human heart. Circulation 1970;41:899-912.
11. Yu C-M, Hayes DL, Auricchio A. Cardiac resynchronization therapy: John Wiley & Sons, 2009.
12. Arenas IA, Jacobson J, Lamas GA. Routine Use of Biventricular Pacing Is Not Warranted for Patients With Heart Block. Circulation: Arrhythmia and Electrophysiology 2015;8:730-738.
13. Tops LF, Schalij MJ, Bax JJ. The effects of right ventricular apical pacing on ventricular function and dyssynchrony: implications for therapy. Journal of the American College of Cardiology 2009;54:764-776.
14. Nahlawi M, Waligora M, Spies SM, Bonow RO, Kadish AH, Goldberger JJ. Left ventricular function during and after right ventricular pacing. Journal of the American College of Cardiology 2004;44:1883-1888.
15. Karpawich PP, Rabah R, Haas JE. Altered cardiac histology following apical right ventricular pacing in patients with congenital atrioventricular block. Pacing and Clinical Electrophysiology 1999;22:1372-1377.
16. Kass DA. An epidemic of dyssynchrony: but what does it mean? Journal of the American College of Cardiology 2008;51:12-17.
17. Abraham WT, Fisher WG, Smith AL et al. Cardiac resynchronization in chronic heart failure. New England Journal of Medicine 2002;346:1845-1853.
18. Cazeau S, Leclercq C, Lavergne T et al. Effects of multisite biventricular pacing in patients with heart failure and intraventricular conduction delay. New England Journal of Medicine 2001;344:873-880.
19. Auricchio A, Stellbrink C, Sack S et al. Long-term clinical effect of hemodynamically optimized cardiac resynchronization therapy in patients with heart failure and ventricular conduction delay. Journal of the American College of Cardiology 2002;39:2026-2033.

20. Abraham WT, Hayes DL. Cardiac resynchronization therapy for heart failure. Circulation 2003;108:2596-2603.
21. YU CM, WING-HONG FUNG J, Zhang Q, Sanderson JE. Understanding nonresponders of cardiac resynchronization therapy—current and future perspectives. Journal of Cardiovascular Electrophysiology 2005;16:1117-1124.
22. Nelson GS, Curry CW, Wyman BT et al. Predictors of systolic augmentation from left ventricular preexcitation in patients with dilated cardiomyopathy and intraventricular conduction delay. Circulation 2000;101:2703-2709.
23. Yu C-M, Fung W-H, Lin H, Zhang Q, Sanderson JE, Lau C-P. Predictors of left ventricular reverse remodeling after cardiac resynchronization therapy for heart failure secondary to idiopathic dilated or ischemic cardiomyopathy. American Journal of Cardiology 2003;91:684-688.
24. Bax JJ, Bleeker GB, Marwick TH et al. Left ventricular dyssynchrony predicts response and prognosis after cardiac resynchronization therapy. Journal of the American College of Cardiology 2004;44:1834-1840.
25. Bader H, Garrigue S, Lafitte S et al. Intra-left ventricular electromechanical asynchrony. A new independent predictor of severe cardiac events in heart failure patients. Journal of the American College of Cardiology 2004;43:248-56.
26. Cho G-Y, Song J-K, Park W-J et al. Mechanical dyssynchrony assessed by tissue Doppler imaging is a powerful predictor of mortality in congestive heart failure with normal QRS duration. Journal of the American College of Cardiology 2005;46:2237-2243.
27. Haghjoo M, Bagherzadeh A, Fazelifar AF et al. Prevalence of mechanical dyssynchrony in heart failure patients with different QRS durations. Pacing and Clinical Electrophysiology 2007;30:616-622.
28. Yu C, Lin H, Zhang Q, Sanderson J. High prevalence of left ventricular systolic and diastolic asynchrony in patients with congestive heart failure and normal QRS duration. Heart 2003;89:54-60.
29. Cazeau SJ, Daubert J, Tavazzi L, Frohlig G, Paul V. Responders to cardiac resynchronization therapy with narrow or intermediate QRS complexes identified by

simple echocardiographic indices of dyssynchrony: the DESIRE study. European Journal of Heart Failure 2008;10:273-280.

30. Ruschitzka F, Abraham WT, Singh JP et al. Cardiac-resynchronization therapy in heart failure with a narrow QRS complex. New England Journal of Medicine 2013;369:1395-1405.
31. Shah AM, Solomon SD. Mechanical dyssynchrony: a risk factor but not a target. European Heart Journal 2015:ehv458.
32. Wiegerinck R, Schreurs R, Prinzen F. Pathophysiology of dyssynchrony: of squirrels and broken bones. Netherlands Heart Journal 2016;24:4-10.
33. Friehling M, Chen J, Saba S et al. A prospective pilot study to evaluate the relationship between acute change in left ventricular synchrony after cardiac resynchronization therapy and patient outcome using a single-injection gated SPECT protocol. Circulation: Cardiovascular Imaging 2011;4:532-539.
34. Chandraprakasam S, Mentzer GG. Recent advances in the optimization of cardiac resynchronization therapy. Current Heart Failure Reports 2015;12:48-60.
35. Patel CD, Mukherjee A. Assessment of left ventricular mechanical dyssynchrony in coronary artery disease. Journal of Nuclear Cardiology 2015:1-4.
36. AlJaroudi W, Alraies MC, Hachamovitch R et al. Association of left ventricular mechanical dyssynchrony with survival benefit from revascularization: A study of gated positron emission tomography in patients with ischemic LV dysfunction and narrow QRS. European Journal of Nuclear Medicine and Molecular Imaging 2012;39:1581-1591.
37. Goldberg AS, Alraies MC, Cerqueira MD, Jaber WA, AlJaroudi WA. Prognostic value of left ventricular mechanical dyssynchrony by phase analysis in patients with non-ischemic cardiomyopathy with ejection fraction 35-50% and QRS< 150 ms. Journal of Nuclear Cardiology 2014;21:57-66.
38. AlJaroudi WA, Hage FG, Hermann D et al. Relation of left-ventricular dyssynchrony by phase analysis of gated SPECT images and cardiovascular events in patients with implantable cardiac defibrillators. Journal of Nuclear Cardiology 2010;17:398-404.
39. AlJaroudi W, Aggarwal H, Venkataraman R, Heo J, Iskandrian AE, Hage FG. Impact of left ventricular dyssynchrony by phase analysis on cardiovascular outcomes in

patients with end-stage renal disease. Journal of Nuclear Cardiology 2010;17:1058-1064.

40. Aggarwal H, AlJaroudi WA, Mehta S et al. The prognostic value of left ventricular mechanical dyssynchrony using gated myocardial perfusion imaging in patients with end-stage renal disease. Journal of Nuclear Cardiology 2014;21:739-746.
41. Sharma RK, Volpe G, Rosen BD et al. Prognostic Implications of Left Ventricular Dyssynchrony for Major Adverse Cardiovascular Events in Asymptomatic Women and Men: The Multi-Ethnic Study of Atherosclerosis. Journal of the American Heart Association 2014;3:e000975.
42. Tavares A, Peclat T, Lima RSL. Prevalence and predictors of left intraventricular dyssynchrony determined by phase analysis in patients undergoing gatedSPECT myocardial perfusion imaging. The International Journal of Cardiovascular Imaging 2016:1-8.
43. Rosen BD, Fernandes VR, Nasir K et al. Age, Increased Left Ventricular Mass, and Lower Regional Myocardial Perfusion Are Related to Greater Extent of Myocardial Dyssynchrony in Asymptomatic Individuals The Multi-Ethnic Study of Atherosclerosis. Circulation 2009;120:859-866.
44. Lancellotti P, Moonen M. Left ventricular dyssynchrony: a dynamic condition. Heart Failure Reviews 2012;17:747-753.
45. Parsai C, Baltabaeva A, Anderson L, Chaparro M, Bijnens B, Sutherland GR. Low-dose dobutamine stress echo to quantify the degree of remodelling after cardiac resynchronization therapy. European Heart Journal 2009;30:950-958.
46. Lafitte S, Bordachar P, Lafitte M et al. Dynamic ventricular dyssynchrony: an exercise-echocardiography study. Journal of the American College of Cardiology 2006;47:2253-2259.
47. Bordachar P, Lafitte S, Reuter S et al. Echocardiographic assessment during exercise of heart failure patients with cardiac resynchronization therapy. American Journal of Cardiology 2006;97:1622-1625.
48. Rocchi G, Bertini M, Biffi M et al. Exercise stress echocardiography is superior to rest echocardiography in predicting left ventricular reverse remodelling and functional

improvement after cardiac resynchronization therapy. European Heart Journal 2009;30:89-97.

49. Zhang Q, Yu CM. Is mechanical dyssynchrony still a major determinant for responses after cardiac resynchronization therapy? Journal of Cardiology 2011;57:239-248.
50. D'andrea A, Mele D, Nistri S et al. The prognostic impact of dynamic ventricular dyssynchrony in patients with idiopathic dilated cardiomyopathy and narrow QRS. European Heart Journal-Cardiovascular Imaging 2013;14:183-189.
51. Germano G, Van Kriekinge SD. Measuring mechanical cardiac dyssynchrony in the 3-D era. Journal of Nuclear Cardiology 2015:1-4.
52. van Everdingen WM, Schipper JC, van 't Sant J, Ramdat Misier K, Meine M, Cramer MJ. Echocardiography and cardiac resynchronisation therapy, friends or foes? Netherlands Heart Journal 2016;24:25-38.
53. De Boeck BW, Teske AJ, Meine M et al. Septal rebound stretch reflects the functional substrate to cardiac resynchronization therapy and predicts volumetric and neurohormonal response. European Journal of Heart Failure 2009;11:863-871.
54. Ghani A, Delnoy PPH, Ottervanger JP et al. Apical rocking is predictive of response to cardiac resynchronization therapy. The International Journal of Cardiovascular Imaging 2015;31:717-725.
55. Chung ES, Leon AR, Tavazzi L et al. Results of the Predictors of Response to CRT (PROSPECT) trial. Circulation 2008;117:2608-2616.
56. Zheng J. Assessment of myocardial oxygenation with MRI. Quantitative Imaging in Medicine and Surgery 2013;3:67.
57. Helm RH, Lardo AC. Cardiac magnetic resonance assessment of mechanical dyssynchrony. Current Opinion in Cardiology 2008;23:440-446.
58. Henneman MM, Chen J, Dibbets-Schneider P et al. Can LV dyssynchrony as assessed with phase analysis on gated myocardial perfusion SPECT predict response to CRT? Journal of Nuclear Medicine 2007;48:1104-1111.
59. Links JM, Douglass KH, Wagner Jr HN. Patterns of ventricular emptying by Fourier analysis of gated blood-pool studies. Journal of Nuclear Medicine 1980;21:978-982.

60. Lalonde M, Birnie D, Ruddy TD, Wassenaar RW. SPECT blood pool phase analysis can accurately and reproducibly quantify mechanical dyssynchrony. Journal of Nuclear Cardiology 2010;17:803-810.
61. Tournoux F, Chequer R, Sroussi M et al. Value of mechanical dyssynchrony as assessed by radionuclide ventriculography to predict the cardiac resynchronization therapy response. European Heart Journal-Cardiovascular Imaging 2015:jev286.
62. Bleeker GB, Kaandorp TA, Lamb HJ et al. Effect of posterolateral scar tissue on clinical and echocardiographic improvement after cardiac resynchronization therapy. Circulation 2006;113:969-976.
63. Zhou W, Garcia EV. Nuclear Image-Guided Approaches for Cardiac Resynchronization Therapy (CRT). Current Cardiology Reports 2016;18:1-11.
64. Chen J, Garcia EV, Folks RD et al. Onset of left ventricular mechanical contraction as determined by phase analysis of ECG-gated myocardial perfusion SPECT imaging: development of a diagnostic tool for assessment of cardiac mechanical dyssynchrony. Journal of Nuclear Cardiology 2005;12:687-695.
65. Van Kriekinge SD, Nishina H, Ohba M, Berman DS, Germano G. Automatic global and regional phase analysis from gated myocardial perfusion SPECT imaging: application to the characterization of ventricular contraction in patients with left bundle branch block. Journal of Nuclear Medicine 2008;49:1790-1797.
66. Trimble MA, Velazquez EJ, Adams GL et al. Repeatability and reproducibility of phase analysis of gated single-photon emission computed tomography myocardial perfusion imaging used to quantify cardiac dyssynchrony. Nuclear medicine communications 2008;29:374.
67. Garcia EV, Faber TL, Cooke CD, Folks RD, Chen J, Santana C. The increasing role of quantification in clinical nuclear cardiology: the Emory approach. Journal of Nuclear Cardiology 2007;14:420-432.
68. Ziessman HA, O'Malley JP, Thrall JH. Nuclear medicine: the requisites: Elsevier Health Sciences, 2013.
69. Cherry SR, Sorenson JA, Phelps ME. Physics in nuclear medicine: Elsevier Health Sciences, 2012.
70. Germano G, Berman DS. Clinical gated cardiac SPECT: John Wiley & Sons, 2008.

71. Lyra M, Ploussi A. Filtering in SPECT image reconstruction. Journal of Biomedical Imaging 2011;2011:10.
72. Alessio A, Kinahan P. PET image reconstruction. Nuclear Medicine 2006;2.
73. Yusoff MS, Zakaria A. Determination of the optimum filter for qualitative and quantitative 99mTc myocardial SPECT imaging. Iranian Journal of Radiation Research 2009;6:173-181.
74. Germano G, Kiat H, Kavanagh PB et al. Automatic quantification of ejection fraction from gated myocardial perfusion SPECT. Journal of Nuclear Medicine 1995;36:2138.
75. Khaliq M. (2009, Aug 17). Dip Image Segmentation. PowerPoint slides. Retrieved from http://www.slideshare.net/supermubbasher/dip-image-segmentation?next_slideshow=1.
76. Gonzalez RC, Woods RE. Digital image processing. 3rd ed. Upper Saddle River, N.J.: Prentice Hall, 2008.
77. Robb RA. Biomedical imaging, visualization, and analysis. New York: Wiley-Liss, 2000.
78. Quantitative Gated SPECT (QGS). (2016) Cedars-Sinai. Retrieved 25/03/2016 from http://cedars-sinai.edu/Patients/Programs-and-Services/Medicine Department/Artificial-Intelligence-in-Medicine-AIM/Projects/Quantitative-Gated-SPECT-QGS.aspx.
79. O'Connell JW, Schreck C, Moles M et al. A unique method by which to quantitate synchrony with equilibrium radionuclide angiography. Journal of Nuclear Cardiology 2005;12:441-450.
80. Salimian S, Thibault B, Finnerty V, Grégoire J, Harel F. The effects of dobutamine stress on cardiac mechanical synchrony determined by phase analysis of gated SPECT myocardial perfusion imaging in a canine model. Journal of Nuclear Cardiology 2014;21:375-383.
81. Harel F, Finnerty V, Grégoire J, Thibault B, Khairy P. Comparison of left ventricular contraction homogeneity index using SPECT gated blood pool imaging and planar phase analysis. Journal of Nuclear Cardiology 2008;15:80-85.
82. Attali D, Chanussot J, Areste R, Guyonic S. 3D snakes for the segmentation of buried mines in 3D acoustic images. Oceans 2005-Europe: IEEE, 2005:442-446.

83. Azad K. An Interactive Guide To The Fourier Transform. (20 Dec 2012), Retrieved 20/03/2016 from http://betterexplained.com/articles/an-interactive-guide-to-the-fourier-transform/.

84. Riffle S. Understanding the Fourier transform. (2012, Apr 22), Retrieved from https://web.archive.org/web/20120418231513/http://www.altdevblogaday.com/2011/05/17/understanding-the-fourier-transform/.

85. Lalonde M. (2013). Novel SPECT RNA quantification of mechanical dyssynchrony for the prediction of CRT response. (Doctoral dissertation). Carleton University, Ottawa, Canada

86. Chen J, Faber TL, Cooke CD, Garcia EV. Temporal resolution of multiharmonic phase analysis of ECG-gated myocardial perfusion SPECT studies. Journal of Nuclear Cardiology 2008;15:383-91.

87. Trimble MA, Borges-Neto S, Smallheiser S et al. Evaluation of left ventricular mechanical dyssynchrony as determined by phase analysis of ECG-gated SPECT myocardial perfusion imaging in patients with left ventricular dysfunction and conduction disturbances. Journal of Nuclear Cardiology 2007;14:298-307.

88. Atchley AE, Trimble MA, Samad Z et al. Use of phase analysis of gated SPECT perfusion imaging to quantify dyssynchrony in patients with mild-to-moderate left ventricular dysfunction. Journal of Nuclear Cardiology 2009;16:888-894.

89. Chen J, Kalogeropoulos AP, Verdes L, Butler J, Garcia EV. Left-ventricular systolic and diastolic dyssynchrony as assessed by multi-harmonic phase analysis of gated SPECT myocardial perfusion imaging in patients with end-stage renal disease and normal LVEF. Journal of Nuclear Cardiology 2011;18:299-308.

90. Romero-Farina G, Aguadé-Bruix S, Candell-Riera J, Pizzi MN, García-Dorado D. Cut-off values of myocardial perfusion gated-SPECT phase analysis parameters of normal subjects, and conduction and mechanical cardiac diseases. Journal of Nuclear Cardiology 2015;22:1247-1258.

91. Cerqueira MD. Pharmacologic stress versus maximal-exercise stress for perfusion imaging: Which, when, and why? Journal of Nuclear Cardiology 1996;3:S10-S14.

92. Armstrong WF, Zoghbi WA. Stress echocardiography: current methodology and clinical applications. Journal of the American College of Cardiology 2005;45:1739-1747.
93. Rallidis L, Cokkinos P, Tousoulis D, Nihoyannopoulos P. Comparison of dobutamine and treadmill exercise echocardiography in inducing ischemia in patients with coronary artery disease. Journal of the American College of Cardiology 1997;30:1660-1668.
94. RUFFOLO Jr RR. The pharmacology of dobutamine. The American Journal of the Medical Sciences 1987;294:244-248.
95. Cohen JL, Ottenweller JE, George AK, Duvvuri S. Comparison of dobutamine and exercise echocardiography for detecting coronary artery disease. The American Journal of Cardiology 1993;72:1226-1231.
96. Salustri A, Fioretti P, Pozzoli M, McNeill A, Roelandt J. Dobutamine stress echocardiography: its role in the diagnosis of coronary artery disease. European Heart Journal 1992;13:70-77.
97. Previtali M, Lanzarini L, Fetiveau R et al. Comparison of dobutamine stress echocardiography, dipyridamole stress echocardiography and exercise stress testing for diagnosis of coronary artery disease. American Journal of Cardiology 1993;72:865-870.
98. Lanzer P, Topol EJ. Pan vascular medicine: integrated clinical management: Springer, 2013.
99. Cigarroa C, Brickner M, Alvarez L, Wait M, Grayburn P. Dobutamine stress echocardiography identifies hibernating myocardium and predicts recovery of left ventricular function after coronary revascularization. Circulation 1993;88:430-436.
100. Mehrotra P, Labib SB, Schick EC. Differential effects of dobutamine versus treadmill exercise on left ventricular volume and wall stress. Journal of the American Society of Echocardiography 2012;25:911-918.
101. Chattopadhyay S, Alamgir MF, Nikitin NP, Fraser AG, Clark AL, Cleland JG. The effect of pharmacological stress on intraventricular dyssynchrony in left ventricular systolic dysfunction. European Journal of Heart Failure 2008;10:412-20.

102. Lancellotti P, Stainier P-Y, Lebois F, Piérard LA. Effect of dynamic left ventricular dyssynchrony on dynamic mitral regurgitation in patients with heart failure due to coronary artery disease. American Journal of Cardiology 2005;96:1304-1307.
103. Kang S-J, Lim H-S, Choi B-J et al. The impact of exercise-induced changes in intraventricular dyssynchrony on functional improvement in patients with nonischemic cardiomyopathy. Journal of the American Society of Echocardiography 2008;21:948-953.
104. Kurita T, Onishi K, Dohi K et al. Impact of heart rate on mechanical dyssynchrony and left ventricular contractility in patients with heart failure and normal QRS duration. European Journal of Heart Failure 2007;9:637-643.
105. Valli N, Gobinet A, Bordenave L. Review of 10 years of the clinical use of brain natriuretic peptide in cardiology. Journal of Laboratory and Clinical Medicine 1999;134:437-444.
106. D'Andrea A, Caso P, Cuomo S et al. Effect of dynamic myocardial dyssynchrony on mitral regurgitation during supine bicycle exercise stress echocardiography in patients with idiopathic dilated cardiomyopathy and 'narrow'QRS. European Heart Journal 2007.
107. Izumo M, Lancellotti P, Suzuki K et al. Three-dimensional echocardiographic assessments of exercise-induced changes in left ventricular shape and dyssynchrony in patients with dynamic functional mitral regurgitation. European Heart Journal-Cardiovascular Imaging 2009;10:961-967.
108. Yagishita-Tagawa Y, Abe Y, Arai K et al. Low-dose dobutamine induces left ventricular mechanical dyssynchrony in patients with dilated cardiomyopathy and a narrow QRS: A study using real-time three-dimensional echocardiography. Journal of Cardiology 2013;61:275-280.
109. Power TP, Kramer CM, Shaffer AL et al. Breath-hold dobutamine magnetic resonance myocardial tagging: normal left ventricular response. The American journal of cardiology 1997;80:1203-1207.
110. Scott CH, Sutton MSJ, Gusani N et al. Effect of dobutamine on regional left ventricular function measured by tagged magnetic resonance imaging in normal subjects. The American journal of cardiology 1999;83:412-417.

111. Daire J-L, Jacob J-P, Hyacinthe J-N et al. Cine and tagged cardiovascular magnetic resonance imaging in normal rat at 1.5 T: a rest and stress study. Journal of Cardiovascular Magnetic Resonance 2008;10:1.
112. Cowan JC, Hilton CJ, Griffiths CJ et al. Sequence of epicardial repolarisation and configuration of the T wave. British heart journal 1988;60:424-433.
113. Opthof T, Coronel R, Janse MJ. Is there a significant transmural gradient in repolarization time in the intact heart? Repolarization gradients in the intact heart. Circulation: Arrhythmia and Electrophysiology 2009;2:89-96.
114. Opthof T, Janse MJ, Meijborg VM, Cinca J, Rosen MR, Coronel R. Dispersion in ventricular repolarization in the human, canine and porcine heart. Progress in biophysics and molecular biology 2016;120:222-235.
115. John RM, Taggart PI, Sutton PM, Ell PJ, Swanton H. Direct effect of dobutamine on action potential duration in ischemic compared with normal areas in the human ventricle. Journal of the American College of Cardiology 1992;20:896-903.
116. Callaghan F, Vollmann W, Livingston A, Boveja B, Abels D. The ventricular depolarization gradient: Effects of exercise, pacing rate, epinephrine, and intrinsic heart rate control on the right ventricular evoked response. Pacing and Clinical Electrophysiology 1989;12:1115-1130.
117. Burgess MJ, Green LS, Millar K, Wyatt R, Abildskov J. The sequence of normal ventricular recovery. American heart journal 1972;84:660-669.
118. Jackson T, Claridge S, Behar J et al. Narrow QRS systolic heart failure: is there a target for cardiac resynchronization? Expert review of cardiovascular therapy 2015;13:783-797.
119. Drake-Holland A, Noble M, Pieterse M et al. Cardiac action potential duration and contractility in the intact dog heart. The Journal of physiology 1983;345:75.
120. Bach DS, Beanlands RS, Schwaiger M, Armstrong WF. Heterogeneity of ventricular function and myocardial oxidative metabolism in nonischemic dilated cardiomyopathy. Journal of the American College of Cardiology 1995;25:1258-1262.
121. Beshai JF, Grimm RA, Nagueh SF et al. Cardiac-resynchronization therapy in heart failure with narrow QRS complexes. New England Journal of Medicine 2007;357:2461-2471.

122. Wyman BT, Hunter WC, Prinzen FW, Faris OP, McVeigh ER. Effects of single-and biventricular pacing on temporal and spatial dynamics of ventricular contraction. American Journal of Physiology-Heart and Circulatory Physiology 2002;282:H372-H379.

123. Frias PA, Corvera JS, Schmarkey L, Strieper M, Campbell RM, VINTEN-JOHANSEN J. Evaluation of Myocardial Performance with Conventional Single-Site Ventricular Pacing and Biventricular Pacing in a Canine Model of Atrioventricular Block. Journal of cardiovascular electrophysiology 2003;14:996-1000.

124. Cojoc A, Reeves JG, Schmarkey L et al. Effects of Single-Site Versus Biventricular Epicardial Pacing on Myocardial Performance in an Immature Animal Model of Atrioventricular Block. Journal of cardiovascular electrophysiology 2006;17:884-889.

125. Yu C-M, Chan JY-S, Zhang Q et al. Biventricular pacing in patients with bradycardia and normal ejection fraction. New England Journal of Medicine 2009;361:2123-2134.

126. Chan JY-S, Fang F, Zhang Q et al. Biventricular pacing is superior to right ventricular pacing in bradycardia patients with preserved systolic function: 2-year results of the PACE trial. European Heart Journal 2011:ehr336.

127. Lehner S, Uebleis C, Schüßler F et al. The amount of viable and dyssynchronous myocardium is associated with response to cardiac resynchronization therapy: initial clinical results using multiparametric ECG-gated [18F] FDG PET. European Journal of Nuclear Medicine and Molecular Imaging 2013;40:1876-1883.

128. Boogers MJ, Chen J, van Bommel RJ et al. Optimal left ventricular lead position assessed with phase analysis on gated myocardial perfusion SPECT. European Journal of Nuclear Medicine and Molecular Imaging 2011;38:230-238.

129. Uebleis C, Ulbrich M, Tegtmeyer R et al. Electrocardiogram-gated 18F-FDG PET/CT hybrid imaging in patients with unsatisfactory response to cardiac resynchronization therapy: initial clinical results. Journal of Nuclear Medicine 2011;52:67-71.

130. Zhou W, Hou X, Piccinelli M et al. 3D fusion of LV venous anatomy on fluoroscopy venograms with epicardial surface on SPECT myocardial perfusion images for guiding CRT LV lead placement. JACC: Cardiovascular Imaging 2014;7:1239-1248.